MEASUREMENT AND ANALYSIS OF METHANE EMISSIONS FROM THE CANADIAN OIL AND GAS INDUSTRY

by

© Katlyn Elizabeth MacKay

A dissertation submitted to the School of Graduate Studies
in partial fulfillment of the requirements for the degree of

Doctor of Philosophy
Oil and Gas Engineering
Faculty of Engineering and Applied Science
Memorial University of Newfoundland

May 2023

St. John's Newfoundland

Abstract

Reducing methane (CH_4) emissions from anthropogenic activities is one of the fastest ways to slow the rate of global warming. The oil and gas (O&G) industry is one of the largest contributors to global CH_4 emissions. Since CH_4 is the main constituent of valuable natural gas, reducing O&G CH_4 emissions has both economic and environmental benefits. On top of that, most of these emissions can be reduced using technologies that exist commercially today.

Although the benefits of CH_4 reduction are clear, barriers for acting remain. Despite being a significant source of the global carbon budget, an in-depth understanding of O&G CH_4 emissions are lacking. National CH_4 inventories, which are used to track emissions over time, are also uncertain, partly due to a lack of knowledge and measurements of individual sources. Along with other major O&G producing countries, Canada has committed to significant reductions of CH_4 emissions from the O&G sector. While such commitments are promising, without accurate estimates of the baseline, and an understanding of spatial and temporal patterns, achieving these reductions will be a significant challenge.

The overarching goal of this thesis and the individual studies within is to improve current understanding of CH_4 emissions from Canada's O&G sector, and to ultimately aid in reducing these emissions. This thesis includes a synthesis and analysis of nearly 10,000 site-level CH_4 emission measurements, spanning across geographies that make up most of the country's onshore O&G production. These data were used to examine CH_4 emission patterns and levels in producing regions that vary in production style, infrastructure, and geography. Production-weighted emission intensities and a total inventory for Alberta were calculated. The measurement-based inventory revealed that CH_4 emissions from the onshore O&G sector are likely underestimated by 50%. Further, a sensitivity analysis of modelled CH_4 emission inventories was performed using available measurement data and infrastructural/production characteristics. The major sources of uncertainty in inventory estimates were assessed using a Monte Carlo analysis. The final component of the thesis is the collection and analysis of the first CH_4 measurements for Canada's offshore industry, which were collected using an aircraft measurement system. Measurements revealed that unlike the onshore sector, offshore CH_4 emissions are in line with current reported estimates.

The primary contributions of this work include the first regionally nuanced estimate of Canadian O&G CH_4 emissions (on and offshore production), including production-weighted emission intensities by development. These new measurement-based estimates fill important knowledge gaps for onshore emission patterns and magnitudes, as well as Canadian offshore CH_4 emissions which have not been previously measured. Additionally, a framework for using site-level measurements to estimate CH_4 inventories was developed, and the key sources of uncertainty in current official inventories were evaluated. This work also produced a publicly available database of O&G methane emission measurements in Canada, which can be used for future research and policy development. Overall, the outcomes of this thesis will help steer CH_4 reduction efforts across the O&G sector and inform future regulations that are expected as the world collectively moves toward a low-carbon future.

Acknowledgements

First, I would like to thank my supervisors Dave Risk and Lesley James, who have kindly guided me throughout the past several years. I will be forever grateful to have had such knowledgeable, patient, and supportive mentors. Also, thank you to my thesis committee member Debra Wunch who has provided valuable feedback and support throughout this process. It has been an honour and a pleasure to work with each of you and I look forward to staying connected in the future.

Thank you to all the past and present members of the StFX FluxLab who I had the pleasure of working with and learning from over the past several years. I feel very lucky to have been part of this supportive group and am especially grateful for those who helped me with the research presented in this thesis.

I would also like to express thanks to those who provided financial support of this research, including the Petroleum Technology Alliance of Canada, Environment and Climate Change Canada, Natural Sciences and Engineering Research Council, and the Atlantic Canada Opportunities Agency.

Finally, sincere thanks to all my family and friends who have supported me throughout this process. Your support and words of encouragement were extremely helpful in keeping me motivated throughout this process.

Co-Authorship Statement

I, Katlyn Elizabeth MacKay, hold a principal author status for all the manuscript chapters (Chapter 2 – 5) in this dissertation. However, each manuscript is co-authored by my supervisor and co-researchers, whose contributions have facilitated the development of this work as described below.

- Paper 1 in Chapter 2: MacKay, K., Lavoie, M., Bourlon, E., Atherton, E., O'Connell, E., Baillie, J., Fougère, C., Risk, D., 2021. Methane emissions from upstream oil and gas production in Canada are underestimated. *Scientific Reports*, 11, 8041. https://doi.org/10.1038/s41598-021-87610-3.

  I (KM) am the primary author; KM, EA, EO, JB, CF, DR contributed to the acquisition of data; KM, ML, DR, EB, EA, CF contributed to the analysis and interpretation of data; DR contributed to conception and design; all authors contributed to refinement of the final manuscript.

- Paper 2 in Chapter 3: MacKay, K. Lavoie, M., Risk, D. A community data resource of recent methane emission measurements from upstream oil and gas sites in Canada. *Under review at Atmospheric Environment: X*.

  I (KM) am the primary author; KM, ML contributed to the analysis and interpretation of data; DR contributed to the conception and design; all authors contributed to the refinement of the final manuscript.

- Paper 3 in Chapter 4: *To be submitted.*
- Paper 4 in Chapter 5: *To be submitted.*

04/2023

Katlyn Elizabeth MacKay — Date

Table of Contents

List of Tables

List of Figures

List of Abbreviations, Symbols, and Constants

Abbreviations

Abbreviation	Description
AB	Alberta

ADP	Air data probe
AER	Alberta Energy Regulator
AI	Artificial Intelligence
atm	Atmosphere
BC	British Columbia
btu	British thermal units
C-NLOPB	Canada-Newfoundland & Labrador Offshore Petroleum Board
C_2H_6	Ethane
CAPP	Canadian association of petroleum producers
cf	cubic feet
CH_4	Methane
CHOPS	Cold Heavy Oil Production with Sand
CI	Confidence interval
CO_2	Carbon dioxide
CO_2e	Carbon dioxide equivalent
CPM	Central processing module
e	excess
E^3	1000
ECCC	Environment and Climate Change Canada
EF	Emission factor
EOR	Enhanced oil recovery
EPA	Environmental Protection Agency
ESG	Environmental, Social, and Governance
FPSO	Floating, Production, Storage and Off-Loading vessel
g	grams
GDM	Gaussian dispersion model
GHG	Greenhouse gas
GHGI	Greenhouse gas inventory
GHGRP	Greenhouse gas reporting program
GPS	Geographic positioning system
GWP	Global warming potential
H_2S	Hydrogen sulfide
Hz	Hertz
IPCC	Intergovernmental Panel on Climate Change
K	Kelvin
kg	kilogram
km	kilometer
Kpa	kilopascal
LDAR	Leak Detection and Repair

m	meter
MDL	Minimum detection limit
MJ	megajoule
MMbbl	million barrels of oil
NDCs	Nationally determined contributions
NGO	non-governmental organization
NIR	National inventory report
NL	Newfoundland and Labrador
O&G	Oil and gas
OGI	Optical gas imaging
OVA	Organic vapor analyzers
PDF	Probability density function
ppb	parts per billion
ppm	parts per million
SD	Standard deviation
SK	Saskatchewan
SLPM	Standard liters per minute
TR	Type-Region
UOG	Upstream oil and gas
V	Volts

Symbols

Symbol	**Description**	**Units**
C	CH_4 concentration enhancement downwind	ppm
h_m	Measurement height	m
h_s	Emission source height	m
σ_y and σ_z	Dispersion coefficients	unitless
Q	emission rate of point source	$m^3\ day^{-1}$
u	prevailing wind speed	m/s
U_N	Uncertainty for parameter N	%
U_{total}	Total uncertainty	%

Constants

Description	**Constant**

CH_4 GWP	25
CH_4 density (15°C, 1 atm)	678 g/m^3
Energy content of 1 m^3 CH_4	37,300 MJ
Energy content of 1 m^3 light crude oil	38,510 MJ
Energy content of 1 m^3 heavy crude oil	40,900 MJ

1. Introduction

Methane (CH_4) is a powerful greenhouse gas (GHG) that is responsible for 30% of global warming. Although atmospheric concentrations are low compared to carbon dioxide (CO_2), CH_4 is significantly better at trapping heat in the atmosphere (Roscioli et al. 2018). CH_4 also has a short atmospheric lifetime relative to CO_2 (~12 years), meaning that reducing CH_4 emissions will drastically slow the rate of global warming in the near term (Alvarez et al. 2018). While reducing global CO_2 emissions is undoubtably critical, reducing CH_4 emissions from anthropogenic activities can buy us the much-needed time to address the main cause of warming that is CO_2.

Canada's second most abundant anthropogenic GHG is CH_4, making up 13% of Canada's total GHG emissions (ECCC 2021). In 2019, ~40% of Canada's anthropogenic CH_4 emissions were from oil and gas (O&G) systems (ECCC 2021). The major sources of O&G CH_4 emissions are from activities that occur during upstream production, which include venting (intentional releases; ~48%), incomplete combustion during flaring (~1.4%), and fugitive emissions (unintentional releases from faulty equipment, or drilling; ~43%) (ECCC 2021). In 2016, Canada's federal government committed to reducing CH_4 emissions by 40-45% from the O&G sector below 2012 levels, by 2025 (ECCC 2018). This commitment is one of Canada's nationally determined contributions (NDCs) under the Paris Agreement. In October 2021, ahead of the COP26 meeting in Glasgow, the federal government made further commitments to reduce O&G CH_4 emissions by 75% by 2030 (Government of Canada 2021). At COP26, Canada also joined

the “Global Methane Pledge” along with over 100 other countries, which aims at reducing global CH_4 emissions by 30% over the coming decade.

Following the original 2016 commitment, the federal government drafted regulations to achieve the 45% reduction (ECCC 2018), but shortly after, provincial governments in Alberta, Saskatchewan, and British Columbia proposed their own regulations to achieve equivalent reduction goals, which have since received approval to replace the original federal regulations (Alberta Energy Regulator 2018, Province of British Columbia 2018, Saskatchewan Ministry of Economy 2019). The new provincial regulations officially came into effect in 2020.

While these commitments are promising, Canada’s CH_4 reduction targets are based on federally reported inventory estimates, which rely partly on industry self-estimation and self-reporting. Recent measurement studies in Canada and the United States (described in detail in the Section 1.1.2) have shown that actual emissions range from equivalent to substantially higher than what is shown in reported inventories (Atherton et al. 2017, Alvarez et al. 2018, Johnson et al. 2017, Roscioli et al. 2018, Zavala-Araiza et al. 2015, Zavala-Araiza et al. 2018). But a national understanding of these discrepancies is lacking because most measurement studies in Canada consist of region-specific sample populations that may not be extensible to other regions as there is variability in extractive techniques, geology, and geochemical properties. Different measurement techniques and technologies, applied at varying scales, require standardization for meaningful comparisons, which is not always a straightforward task.

Without a better understanding of CH_4 emissions, reducing them will be challenging. Accurate, defensible estimates of CH_4 emissions will ultimately be required to monitor regulation-driven emissions reductions in the coming years. Current CH_4 inventories are not well understood and have high uncertainties that are difficult to quantify. On top of that, regulators currently lack tools and data needed to validate emission inventories and industry-reported estimates. Such work will become increasingly important on provincial and national scales, as the O&G (and other carbon-intensive) sectors will need to start extensively tracking emissions reductions with incoming regulations and other climate-related commitments.

1.1 Background

There has been recent progress made towards filling the knowledge gap on CH_4 emissions from upstream O&G production. In Canada, there are published measurement studies that cover regions in British Columbia (Montney), Alberta (Lloydminster, Red Deer, Grande Prairie, Peace River, Medicine Hat), and Saskatchewan (Weyburn-Midale, Bakken). There are also several measurement studies that have been conducted across the United States (e.g. Alvarez et al. 2018, Brandt et al. 2016, Omara et al. 2018). O&G CH4 measurements outside of the U.S. and Canada are limited, though there have been recent studies conducted in Mexico (Zavala-Araiza et al. 2021) and Europe (France et al. 2021, Riddick et al. 2019, Yacovitch et al. 2018). These studies use a variety of methodologies to measure CH_4 emissions from O&G facilities, ranging from handheld devices to

aircraft-based measurements. An overview of frequently used measurement techniques used to measure O&G CH_4 emissions is in Section 1.1.1 below, followed by a review of the main findings from the previous literature.

1.1.1 Measurement techniques

1.1.1.1 Optical Gas Imaging (OGI) and Hi-Flow

OGI cameras are the current regulatory standard (in Canada and the U.S.) for O&G CH_4 emissions monitoring. These measurements require site access and adequate (i.e., unobstructed) line of sight between the camera and source of interest. Emissions are identified visually using the OGI camera, and then subsequently quantified using a Hi-Flow sampler (Greenpath Energy 2017, Ravikumar et al. 2020). In some cases, direct quantification a via Hi-Flow sampler is not possible (due to potential safety or access issues), and emission rates are estimated using expert judgement, emission factors from literature, and/or equipment manufacturer data (discussed further in Section 3.4.5) (Greenpath Energy 2017, Ravikumar et al. 2020). Depending on the quantification method, uncertainties range from 5% (Hi-Flow sampler) to orders of magnitude (estimation) (Greenpath Energy 2017). A significant advantage of OGI is that it provides component-level (e.g., valve, compressor seal) source attribution, which is ultimately required for repairs and mitigation.

1.1.1.2 Vehicle-based transects coupled with inverse Gaussian dispersion modelling

Many recent studies (in Canada and the U.S.) have been using vehicle-based measurement systems coupled with inverse Gaussian dispersion modelling to measure

O&G CH_4, which has gained popularity due to its measurement efficiency. For instance, authors of some studies have been able to measure 100 sites per day using this method (Baillie et al. 2019, O'Connell et al. 2019), which is >10 times more sites than what is covered during a traditional OGI survey. The method typically involves a vehicle equipped with high-precision analyzers that measure gas concentrations, geolocation, and meteorological data continuously while driving. Transects of CH_4 plumes are measured by driving downwind of O&G sites, which are then used to compute a site-level emission rate using inverse Gaussian dispersion principles. Reported uncertainties for this method vary significantly (50-350%) and depend on measurement conditions such as wind and distance from source (Caulton et al. 2017, O'Connell et al. 2019).

1.1.1.3 Vehicle-based tracer flux

The tracer flux method involves releasing one or more tracer gases (e.g. N_2O) of known flow rate in close proximity to the source of interest (i.e. O&G site). This method has been used to measure CH_4 emissions from industrial facilities for over 20 years (Roscioli et al. 2018). Gas concentrations (of CH_4 and the tracer gases), and meteorological data are measured continuously at some distance downwind, to capture downwind plume concentration profiles. Given that there is a direct linear relationship between downwind concentrations and emission rates, the site-level CH_4 emission rate is calculated by comparing the ratios of downwind concentration enhancements and the known release rate of the tracer gas (Roscioli et al. 2018, Zavala-Araiza et al. 2018). Measurement uncertainties for the tracer flux method range from 20-50% (Caulton et al. 2017, Omara et al. 2018).

1.1.1.4 Aircraft-based measurements

Aircraft-based measurements are another useful methodology for measuring CH_4 emissions. This method involves flying multiple transects or orbits upwind and downwind of the source or area of interest. Some aircraft measurements involve the use of atmospheric gas analyzers and other meteorological equipment (similar to vehicle-based systems) and estimate emissions for a defined area (e.g. Johnson et al. 2017) or point-source (e.g. Conley et al. 2017) using mass balance or inverse dispersion models. Others use imaging spectrometers to derive column averaged CH_4 concentrations which can then be used to estimate fluxes from individual sources (Sherwin et al. 2021, Thorpe et al. 2020). Aircraft-based measurements typically have coarser resolution compared to ground-based techniques but have significant spatial coverage and are not usually limited by surface characteristics. Aircraft measurements have been used to study a range of CH_4 sources such as flares (e.g. Plant et al. 2022), facilities (Baray et al. 2018), as well as to derive large regional level CH_4 fluxes (Johnson et al. 2017). Uncertainties for aircraft-based measurements vary depending on instrumentation and measurement conditions, but are typically in the range of 25-50% (Cambaliza et al. 2014, Fox et al. 2019).

1.1.1.5 Satellite measurements

Satellite-based measurements of CH_4 have advanced significantly over the past decade and have superior spatial coverage compared to other measurement technologies (Fox et al. 2019). These instruments measure backscattered solar radiation in the shortwave infrared (SWIR) to retrieve atmospheric CH_4 column concentrations (Jacob et

al. 2022). To date, there are numerous satellites orbiting the earth with the capability to measure regional (e.g. TROPOMI) and point-source (e.g. GHGSat) CH_4 emissions, albeit with coarser resolution and higher detection limits compared to aircraft and ground-based technologies. While these limitations currently present challenges for facility-level emission estimates, continued advancements in satellite-based CH_4 sensing suggests that these issues will be overcome in the near future.

1.1.2 Region-specific patterns (onshore)

Atherton et al. (2017) describes the first extensive measurement campaign conducted in the Montney region, an unconventional natural gas development in British Columbia (BC). Using a truck equipped with high precision gas analyzers and meteorological equipment, the authors measured more than 1600 well pads and facilities in the summer of 2015 and found that 47% of active wells were emitting CH_4 (Atherton et al. 2017). Extrapolating results across all of BC, they estimated that the measured sources emit more than 111,800 tonnes CH_4/year (Atherton et al. 2017). Although this study provides useful insights on emission sources and frequencies in the Montney region, the authors did not quantify emission rates from each source, but instead used an estimated minimum detection limit (MDL) for the annual emission estimate. Consequently, the uncertainty with the estimate is likely higher than if actual emission rates from measured sites were quantified and summed. However, this method of extrapolation is more likely to compute a conservative annual estimate (since some emission sources would be emitting at rates higher than the MDL), which means that the true inventory may be even higher than

Atherton et al. (2017)'s annual estimate, which was estimated to be 1.43 times higher than the reported estimate for the entire province (Atherton et al. 2017). A second BC-based measurement study was published in 2021, which included 167 site-level CH_4 measurements collected using an aircraft equipped with LiDAR technology (Tyner and Johnson 2021). Results from these aerial measurements showed that 28% of surveyed sites had measurable CH_4 emissions, with average emission rates of individual sources varying by three orders of magnitude (0.5 to 399 kg/hour) (Tyner and Johnson 2021). Notably, more than half of measured emissions originated from three sources: tanks (24%), reciprocating compressors (15%), and unlit flares (13%) (Tyner and Johnson 2021).

In 2016 and 2017, CH_4 measurements of 36 sites on the Alberta side of the Montney basin were collected using optical gas imaging (OGI) and Hi-Flow samplers (Ravikumar et al. 2020). While the main purpose of this study was to measure the effectiveness of leak detection and repair (LDAR) surveys (which operators are required to conduct for regulatory compliance) in terms of reducing emissions long-term, the study also highlighted emission patterns as a function of source type. Similar to Tyner and Johnson (2021), this study also found tanks to be a major contributor (64%) to total emissions (Ravikumar et al. 2020).

Also in 2016, another vehicle-based measurement campaign was completed, which focused on three prominent O&G developments in Alberta: Lloydminster (heavy oil), Peace River (heavy oil/bitumen), and Medicine Hat (conventional gas) (O'Connell et

al. 2019). 1299 well pads were sampled in triplicate across the three regions. The results showed that emissions were highest in Lloydminster, with 40.2% of sites emitting at a rate that exceeded the current regulatory threshold of 110 m^3/day (O'Connell et al. 2019). Similar conclusions about large emissions in Lloydminster were observed in an aircraft mass balance study by Johnson et al. (2017). In that study, the authors took aircraft measurements in two Alberta O&G regions, Lloydminster and Red Deer. These "top-down" emissions estimates revealed methane emissions of 24.5 ± 5.9 tonnes CH_4/hour and 3.05 ± 1.1 tonnes CH_4/hour for Lloydminster and Red Deer, respectively (Johnson et al. 2017). Shortly after the aircraft study was published, Zavala-Araiza et al. (2018) published ground-based CH_4 emission measurements in Red Deer. Although there was not perfect overlap between measured sites across the Johnson et al. (2017) and Zavala-Araiza et al. (2018) studies, an extrapolation analysis by Zavala-Araiza et al. (2018) found that their emission rates agree (within confidence intervals) with the Johnson et al. (2017) study.

In addition to the Johnson et al. (2017) and O'Connell et al. (2019) studies, another study by Roscioli et al. (2018) focused specifically on emissions in Lloydminster, making it one of the most frequently measured regions (with respect to O&G CH_4) in all of Canada. Authors in this study used the tracer release method to measure CH_4 emissions from five cold heavy oil production with sand (CHOPS) facilities. Their measurements revealed significant temporal variability in CH_4 emissions, with one facility exhibiting fluctuations of a factor of 10 across only a few minutes (Roscioli et al. 2018). Due to the

small sample size (n=5), the authors did not extrapolate results to determine a regional emissions estimate.

In Saskatchewan, two CH_4 measurement studies were recently published in 2019, and both use similar vehicle-based techniques as O'Connell et al. (2019). One study by MacKay et al. (2019) focused specifically on the Weyburn Enhanced Oil Recovery (EOR) oilfield, where the operator continuously injects CO_2 into the reservoir to enhance oil production (MacKay et al. 2019). This field is also unique because measurements revealed that there are very low levels of CH_4 emissions from sites within this operation, likely due to the closed-loop nature of the infrastructure network, and strict regulations around venting due to the reservoirs hydrogen sulfide (H_2S) content (H_2S is a serious health risk as it is fatal at 1000 ppm) (MacKay et al. 2019). The other Saskatchewan based study, by Baillie et al. (2019), compared CH_4 emissions from conventional (Weyburn-Midale) and unconventional (Bakken) production. The authors measured 645 conventional and 289 unconventional sites and found that conventional and unconventional sites were emitting CH_4 at similar frequencies (Baillie et al. 2019), but emissions from both development types were on the lower end when compared to other measurement studies in Canada and the US.

From a broader perspective, all the aforementioned studies conducted in Canada have limited spatial coverage when considering the vastness of the Canadian O&G sector. Canada's upstream O&G infrastructure is extremely complex (consisting of hundreds of thousands of emission sources) and spans across thousands of square kilometres.

Although these region-specific studies offer valuable insights to their respective areas, we as a country are still lacking a reliable national understanding of emission patterns and inventories. Findings from these studies also confirm that CH_4 emissions (occurrence and magnitude) can be vastly different depending on the geographic area and production styles used for extraction, reinforcing the need for more measurements and research on this topic.

1.1.3 Heavy-tailed distributions

Notably, many of the Canadian measurement studies have found CH_4 emissions to follow a "heavy-tailed" distribution, meaning that the majority of emissions are originating from only a small fraction of sources (often referred to as "super emitters") (Baillie et al. 2019, Johnson and Tyner 2021, O'Connell et al. 2019, Ravikumar et al. 2020, Zavala-Araiza et al. 2018). This trend has also been well documented in the U.S. (Alvarez et al. 2018, Brandt et al. 2016, Caulton et al. 2019, Omara et al. 2018, Robertson et al. 2020, Zavala-Araiza et al. 2015). Notably, a US-centric data synthesis study by Brandt et al. (2016) found heavy-tailed distributions in all 18 datasets used in their country-wide analysis. This is an important, policy-relevant finding, as it means that most emissions can be reduced by taking mitigation action at only a small fraction of sites. It can also have implications on measurement technology economics: if a heavy-tail distribution is present, then fast, spatially extensive measurement technologies (e.g. vehicles, aircraft) are likely the most cost-effective approach to reductions (as opposed to handheld devices that can only measure emissions from a few sites per day).

1.1.4 Current government reported inventories are underestimating actual emissions

Under the United Nations Framework Convention on Climate Change (UNFCCC), Canada's federal government is required to submit national inventories of greenhouse gases every year. Environment and Climate Change Canada (ECCC), the entity responsible for publishing the report, develop emission inventories using the "2006 Guidelines for National GHG Inventories" by the Intergovernmental Panel on Climate Change (IPCC) (ECCC 2021).

For Canada's national inventory report (NIR) estimates, CH_4 emissions from the upstream O&G sector are typically defined as either fugitive or vented emissions. Vented emissions are estimated in the NIR using industry-reported data at the facility level. In some cases, these emissions are measured directly by the producers, but often industry relies on estimating these values using emission factors and production data. Whether measured or estimated, vented emissions are self-reported, meaning that producers who own each facility are responsible for reporting their own venting rates. Producers are required to report their venting rates for all active facilities on a monthly basis through the Petrinex reporting system, using unique facility identifiers to distinguish between individual sources. The total vented emissions, as shown in the NIR, are found by summing all the reported values from all active facilities.

Currently, fugitive emissions estimates from the upstream O&G industry are estimated using two industry-led studies: the Canadian Association of Petroleum Producers' (CAPP) study titled "A National Inventory of Greenhouse Gas (GHG), Criteria Air Contaminant (CAC) and Hydrogen Sulphide (H_2S) Emissions by the Upstream Oil and Gas Industry (CAPP 2005), and an update to this inventory which was completed in 2014 for ECCC by Clearstone Engineering Ltd. (Clearstone 2014) (ECCC 2021). Methodologies for both studies follow the guidelines stated in the IPCC Tier 3 bottom-up assessment, where emission factors are estimated at the individual facility and process level, and then aggregated to produce total estimates by facility type and geographic area (ECCC 2021). It is worth mentioning that the CAPP study estimates emissions for the year 2000, and the Clearstone study similarly estimates emissions for the years 2005 and 2011. Estimates for all other years are determined by interpolating these "base" years using annual production and activity data (ECCC 2021). Within these studies, emission factors for individual emitting components were determined using published reports, equipment manufacturers data, observed industry values, measured vent rates, simulation programs and other industry studies (ECCC 2021). The results (i.e., emission factors) from the Clearstone (2014) study conducted in 2011 are used to estimate annual inventories from 2012 onwards (Clearstone 2014, ECCC 2021).

Recent measurement studies have revealed that inventories estimated using this bottom-up approach often result in underestimation of total emissions. For example, Chan et al. (2020) found that measured CH_4 emissions in Alberta and Saskatchewan were 85% higher than reported emissions, Johnson et al. (2017) found that emissions in

Lloydminster, Alberta were 3.6 times higher than reported, and Tyner and Johnson (2021) found that emissions in BC were 1.6-2.2 times higher than the current federal estimate. Several studies in the United States show similar results (e.g. Alvarez et. al 2018, Zavala-Araiza et al. 2015, Zhang et al. 2020). Some explanations for this consistent underestimation have been noted in the U.S. based literature, including the heavy-tailed nature of O&G CH_4 emissions (Brandt et al. 2016), the fact that the inventory does not include emissions from abnormal operating conditions (Alvarez et al. 2018), and the outdated nature of the underlying data sources (Rutherford et al. 2021).

Despite the growing consensus that the current national inventory methods for upstream O&G CH_4 emissions accounting are inaccurate, there is a lack of research dedicated to improving estimation methods for official upstream O&G inventories. In Canada's NIR, the foreword states that "The reporting guidelines also commit Parties to improve the quality of emission and removal of estimates on an ongoing basis" (ECCC 2021). With this statement in mind, and recent agreement in published literature across Canada and the US that current inventories are underestimated, a logical next step would be for federal governments to revise their protocols, and ideally find a way to incorporate these recent revelations into future annual inventory estimates. With the Paris agreement, the Global Methane Pledge, and new regulations put in place to limit CH_4 emissions from the O&G industry in Canada, accurate inventories are more important than ever, as they provide the means of tracking reductions to ensure international commitments are met.

1.1.5 Offshore emissions patterns

Compared to onshore production, research on emissions from offshore O&G production is scarce, likely in part due to the assumption that offshore platforms have low emissions because of increased safety protocols (e.g. no routine venting, increased leak detection surveys, 24/7 operator presence). In efforts to fill this gap, offshore O&G platforms in other parts of the world have recently been measured, like Gulf of Mexico and North Sea, and these studies have found variable results. Gorchov Negron et al. (2020) (Gulf of Mexico) and Riddick et al. (2019) (North Sea) both found that measured CH_4 emissions were higher than reported estimates, while Zavala-Araiza et al. (2021) found that measured emissions for Mexico's offshore production were more than an order of magnitude lower than reported estimates (Zavala-Araiza et al. 2021). However, authors note that the Mexican GHG inventory uses a non-Mexican specific emission factors in their calculations, which could be the reason for the observed discrepancy (Zavala-Araiza et a. 2021).

Similar work has yet to be done in Canada's offshore. However, considering these new findings from studies in other offshore regions, and Canada's commitment to reducing the carbon footprint of our O&G industry, in situ measurements of Canada's offshore CH_4 emissions are both important and necessary.

1.2 Motivation and Outline

1.2.1 Motivation

The research presented in this thesis is an extensive, worthwhile effort focused on improving knowledge on Canadian O&G CH_4 emissions and inventories. Recent contributions to this research area in Canada have mainly consisted of measurement studies concentrated in specific O&G production regions. To date, no one has undertaken the task of aggregating existing data in Canada to infer broader patterns and spatially resolved, provincial-wide inventory estimates. To my knowledge, there has also been no recent independent review on the reliability of Canada's current method of estimating the national CH_4 inventories for the O&G sector. And finally, there has never been any published direct measurements of emissions from Canada's offshore oil industry, which itself presents a potentially significant source of uncertainty with respect to our understanding of Canada's major CH_4 sources. This thesis aims to address these gaps, which are critical for reduction efforts going forward. Ultimately, improving understanding of this important GHG will help with reduction efforts in this sector and beyond, which is an essential component of our collective fight against climate change.

1.2.2 Thesis organization

This thesis follows a manuscript-style format and consists of four separate manuscripts along with introductory and conclusion chapters. There are six chapters in total, which are as follows: **Chapter 1** presents the introduction of the research, a review of previous literature, the motivation of the study, and the thesis structure. **Chapter 2** (manuscript) has been published in Scientific Reports and presents an analysis of more than 6600 site-

level CH_4 measurements in six major O&G producing regions across British Columbia, Alberta, and Saskatchewan. Absolute emissions, and emission intensities were examined and compared across geographies. This chapter also includes a measurement-based CH_4 inventory estimate for Alberta using a Monte Carlo model framework, which is also used (and improved on) in Chapter 4. **Chapter 3** (manuscript) has been resubmitted (revised after review of the initial submission in August 2021) to Atmospheric Environment: X. This chapter presents a synthesis and analysis of all CH_4 datasets collected in Canada between 2015 and 2020, which includes published and unpublished datasets obtained from industry and regulators. We conduct a statistical comparison of emissions measured using different methodologies and investigate emissions patterns and characteristics of all major Canadian onshore developments. All data from this chapter has been made publicly available via St. Francis Xavier University's Dataverse repository. **Chapter 4** (manuscript, not yet submitted) investigates the sensitivity of modelled CH_4 emission inventories to a variety of factors, building on the model used in Chapter 2. We assess how modelled CH_4 emissions from upstream O&G sources differ by incorporating different criteria. The major sources of uncertainties are discussed along with recommendations for improving current estimation methods. **Chapter 5** (manuscript, not yet submitted) presents the first-ever direct measurements of CH_4 emissions from Canada's offshore oil industry. Details on the aircraft-based measurement methodology are described, and a Gaussian plume model is used to estimate emission rates from different platforms. Measured emissions are compared to federally reported estimates to determine if any discrepancies exist. Finally, the thesis is summarized and concluded in **Chapter 6**.

References

Alberta Energy Regulator (AER), 2018. Directive 060. Retrieved from: https://www.aer.ca/documents/directives/Directive060_2020.pdf

Alvarez, R. A., Zavala-Araiza, D., Lyon, D. R., Allen, D. T., Barkley, Z. R., Brandt, A. R., Davis, K. J., Herndon, S. C., Jacob, D. J., Karion, A., Kort, E. A., Lamb, B. K., Lauvaux, T., Maasakkers, J. D., Marchese, A. J., Omara, M., Pacala, S. W., Peischl, J., Robinson, A. L., Shepson, P. B., Sweeney, C., Townsend-Small, A., Wofsy, S. C., Hamburg, S. P., 2018. Assessment of methane emissions from the U.S. oil and gas supply chain. *Science* 361, 186-188. DOI: 10.1126/science.aar7204

Atherton, E., Risk, D., Fougère, C., Lavoie, M., Marshall, A., Werring, J., Williams, J.P., Minions, C., 2017. Mobile measurement of methane emissions from natural gas developments in northeastern British Columbia, Canada. *Atmospheric Chemistry and Physics,* 17 (20): 12405–12420. DOI: 10.5194/acp-17-12405-2017

Baillie, J., Risk, D., Atherton, E., O'Connell, E., Fougère, C., Bourlon, E., MacKay, K., 2019. Methane emissions from conventional and unconventional oil and gas production sites in southeastern Saskatchewan, Canada. *Environmental Research Communications* 1, 011003. DOI: 10.1088/2515-7620/ab01f2.

Baray, S., Darlington, A., Gordon, M., Hayden, K. L., Leithead, A., Li, S.-M., Liu, P. S. K., Mittermeier, R. L., Moussa, S. G., O'Brien, J., Staebler, R., Wolde, M., Worthy, D., and McLaren, R., 2018. Quantification of methane sources in the Athabasca Oil Sands Region of Alberta by aircraft mass balance. *Atmospheric Chemistry and Physics* 18, 7361–7378, DOI: https://doi.org/10.5194/acp-18- 7361-2018

Brandt, A. R., Heath, G. A., Cooley, D., 2016. Methane leaks from natural gas systems follow extreme distributions. *Environmental Science and Technology* 50, 22, 12512-12520. DOI: https://doi.org/10.1021/acs.est.6b04303

Cambaliza, M. O. L., Shepson, P. B., Caulton, D. R., Stirm, B., Samarov, D., Gurney, K. R., Turnbull, J., Davis, K. J., Possolo, A., Karion, A., Sweeney, C., Moser, B., Hendricks, A., Lauvaux, T., Mays, K., Whetstone, J., Huang, J., Razlivanov, I., Miles, N. L., Richardson, S. J., 2014. Assessment of uncertainties of an aircraft-based mass balance approach for quantifying urban greenhouse gas emissions. *Atmospheric Chemistry and Physics* 14, 9029-9050. DOI: https://doi.org/10.5194/acp-14-9029-2014

Canadian Association of Petroleum Producers (CAPP), 2005. A National Inventory of Greenhouse Gas (GHG), Criteria Air Contaminant (CAC) and Hydrogen Sulphide (H_2S) Emissions by the Upstream Oil and Gas Industry, Vols. 1–5. Retrieved from: https://www.capp.ca/wp-

content/uploads/2019/11/A_National_Inventory_of_GHG_CAC_and_H2S_Emissions_Volume_1-86220.pdf

Caulton, D. R., Lu, J. M., Lane, H. M., Bucholz, B., Fitts, J. P., Golston, L. M., Guo, X., Li, Q., McSpiritt, J., Pan, D., Wendt, L., Bou-Zeid, E., Zondlo, M. A., 2019. Importance of Superemitter Natural Gas Well Pads in the Marcellus Shale. *Environmental Science and Technology* 53, 4747−4754. DOI: 10.1021/acs.est.8b06965

Caulton, D. R., Li, Q., Bou-Zeid, E., Lu, J., Lane, H. M., Fitts, J. P., Buchholz, B., Golston, L. M., Guo, X., McSpiritt, J., Pan, D., Wendt, L., Zondlo, M. A., 2017. Improving Mobile Platform Gaussian-Derived Emission Estimates Using Hierarchical Sampling and Large Eddy Simulation. *Atmospheric Chemistry and Physics Discussions*, 1–39.

Chan, E., Worthy, D. E. J., Chan, D., Ishizawa, M., Moran, M. D., Delcloo, A., Vogel, F., 2020. Eight-Year Estimates of Methane Emissions from Oil and Gas Operations in Western Canada Are Nearly Twice Those Reported in Inventories. *Environmental Science and Technology* 54, 23, 14899-14909. DOI: https://doi.org/10.1021/acs.est.0c04117

Clearstone Engineering Ltd., 2014. Technical Report on Canada's Upstream Oil and Gas Industry. Vols. 1–4. Prepared for Environment Canada. Calgary (AB)

Conley, S., Faloona, I., Mehrotra, S., Suard, M., Lenschow, D. H., Sweeney, C., Herndon, S., Schwietzke, S., Pétron, G., Pifer, J., Kort, E. A., Schnell, R., 2017. Application of Gauss's theorem to quantify localized surface emissions from airborne measurements of wind and trace gases. *Atmospheric Measurement Techniques* 10, 3345– 3358. DOI: https://doi.org/10.5194/amt-10-3345-2017

Environment and Climate Change Canada (ECCC), 2021. National Inventory Report 1990–2019: Greenhouse Gas Sources and Sinks in Canada. Retrieved from: http://www.publications.gc.ca/site/eng/9.506002/publication.html

Environment and Climate Change Canada (ECCC), 2018. Technical Backgrounder: Federal methane regulations for the upstream oil and gas sector. Retrieved from: https://www.canada.ca/en/environment-climate-change/news/2018/04/federal-methane- regulations-for-the-upstream-oil-and-gas-sector.html

Fox, T. A., Barchyn, T. E., Risk, D., Ravikumar, A. P., Hugenholtz, C. H., 2019. A review of close-range and screening technologies for mitigating fugitive methane emissions in upstream oil and gas, *Environment Research Letters,* 14, 053002. DOI: https://doi.org/10.1088/1748-9326/ab20f1

France, J.L., Bateson, P., Dominutti, P., Allen, G., Andrews, S., Bauguitte, S., Coleman,

M., Lachlan-Cope, T., Fisher, R.E., Huang, L., Jones, A.E., Lee, J., Lowry, D., Pitt, J., Purvis, R., Pyle, J., Shaw, J., Warwick, N., Weiss, A., Wilde, S., Witherstone, J., Young, S., 2021. Facility level measurement of offshore oil and gas installations from a medium-sized airborne platform: method development for quantification and source identification of methane emissions. *Atmospheric Measurement Techniques*, 14, 71–88. DOI: https://doi.org/10.5194/amt-14-71-2021

Gorchov Negron, A. M., Kort, E. A., Conley, S. A., Smith, M., 2020. Airborne Assessment of Methane Emissions from Offshore Platforms in the U.S. Gulf of Mexico, *Environmental Science and Technology,* 54, 5112-5120. DOI: https://dx.doi.org/10.1021/acs.est.0c00179

Government of Canada, 2021.News Release: Canada confirms its support for the Global Methane Pledge and announces ambitious domestic actions to slash methane emissions. Retrieved from: https://www.canada.ca/en/environment-climate-change/news/2021/10/canada-confirms-its-support-for-the-global-methane-pledge-and-announces-ambitious-domestic-actions-to-slash-methane-emissions.html

Greenpath Energy, 2017. Historical Canadian fugitive emissions management program assessment. Prepared for PTAC. Retrieved from: https://greenpathenergy.com/wp-content/uploads/2019/10/Historical-Canadian-Fugitive-Emissions-Management-Program-Assessment.pdf

Jacob, D. J., Varon, D. J., Cusworth, D. H., Dennison, P. E., Frankenberg, C., Gautam, R., Guanter, L., Kelley, J., McKeever, J., Ott, L. E., Poulter, B., Qu, Z., Thorpe, A. K., Worden, J. R., and Duren, R. M., 2022. Quantifying methane emissions from the global scale down to point sources using satellite observations of atmospheric methane. *Atmospheric Chemistry and Physics* 22, 9617–9646. DOI: https://doi.org/10.5194/acp-22-9617-2022

Johnson, M., Tyner, D., Conley, S., Schwietzke, S. and Zavala-Araiza, D. 2017. Comparisons of Airborne Measurements and Inventory Estimates of Methane Emissions in the Alberta Upstream Oil and Gas Sector. *Environmental Science and Technology* 51(21): 13008–13017. DOI: https://doi.org/10.1021/acs.est.7b03525

MacKay, K., Risk, D., Atherton, E., Fougere, C., Bourlon, E., O'Connell, E., Baillie, J., 2019. Fugitive and vented methane emissions surveying on the Weyburn CO_2-EOR field in southeastern Saskatchewan, Canada. *International Journal of Greenhouse Gas Control* 88, 118-123. DOI: https://doi.org/10.1016/j.ijggc.2019.05.032

O'Connell, E., Risk, D., Atherton, E., Bourlon, E., Fougère, C., Baillie, J., Lowry, D., Johnson, J., 2019. Methane emissions from contrasting production regions within Alberta, Canada: Implications under incoming federal methane regulations. *Elementa Science of the Anthropocene* 7. DOI: 10.1525/elementa.341.

Omara, M., Zimmerman, N., Sullivan, M. R., Li, X., Ellis, A., Cesa, R., Subramanian, R., Presto, A. A., Robinson, A. L., 2018. Methane Emissions from Natural Gas Production Sites in the United States: Data Synthesis and National Estimate. *Environmenal Science and Technology* 52, 12915−12925. DOI: 10.1021/acs.est.8b03535

Petrinex, Alberta Public Data. Public data archives. Retrieved from: https://www.petrinex.ca/PD/Pages/APD.aspx

Plant, G., Kort, E. A., Brandt, A. R., Chen, Y., Fordice, G., Gorchov Negron, A. M., Schwietzke, S., Smith, M., Zavala-Araiza, D., 2022. Inefficient and unlit natural gas flares both emit large quantities of methane. *Science* 377, 6614, 1566-1571. DOI: https://www.science.org/doi/10.1126/science.abq0385

Province of British Columbia, 2018. Oil and Gas Activities Act. Retrieved from: http:// www.bclaws.ca/civix/document/id/regulationbulletin/regulationbulletin/Reg286_2018

Ravikumar, A. P., Roda-Stuart, D., Liu, R., Bradley, A., Bergerson, J., Nie, Y., Zhang, S., Bi, X., Brandt, A. R., 2020. Repeated leak detection and repair surveys reduce methane emissions over a scale of years. *Environmental Research Letters* 15, 034029. DOI: https://iopscience.iop.org/article/10.1088/1748-9326/ab6ae1

Riddick, S. N., Mauzerall, D. L., Celia, M., Harris, N. R. P., Allen, G., Pitt, J., Staunton-Sykes, J., Forster, G. L., Kang, M., Lowry, D., Nisbet, E. G., Manning, A. J., 2019. Methane emissions from oil and gas platforms in the North Sea, *Atmospheric Chemistry and Physics* 19, 9787-9796. DOI: https://doi.org/10.5194/acp-19-9787-2019

Robertson, A. M., Edie, R., Field, R. A., Lyon, D., McVay, R., Omara, M., Zavala-Araiza, D., Murphy, S. M., 2020. New Mexico Permian Basin Measured Well Pad Methane Emissions Are a Factor of 5–9 Times Higher Than U.S. EPA Estimates. *Environmental Science and Technology,* 54 (21), 13926-13934. DOI: 10.1021/acs.est.0c02927

Roscioli, J. R., Herndon, S. C., Yacovitch, T. I., Knighton, W. B., Zavala-Araiza, D., Johnson, M. R., and Tyner, D. R., 2018. Characterization of methane emissions from five cold heavy oil production with sands (CHOPS) facilities. *Journal of Air and Waste Management Association* 68 (7): 671−684. DOI: https://doi.org/10.1080/10962247.2018.1436096

Rogelj, J., Shindell, D., Jiang, K., Fifita, S., Forster, P., Ginzburg, V., Handa, C., Kheshgi, H., Kobayashi, S., Kriegler, E., Mundaca, L., Séférian, R., Vilariño, M. V., 2018. Mitigation Pathways Compatible with 1.5°C in the Context of Sustainable Development. Retrieved from: https://www.ipcc.ch/sr15/chapter/chapter-2/

Rutherford, J. S., Sherwin, E. D., Ravikumar, A. P., Heath, G. A., Englander, J., Cooley,

S., Lyon, D., Omara, M., Langfitt, Q., Brandt, A. R, 2021. Closing the methane gap in US oil and natural gas production emissions inventories. *Nature Communications* 12, 1–12. DOI: https://doi.org/10.1038/s41467-021-25017-4

Saskatchewan Ministry of Economy, 2019. The Oil and Gas Emissions Management Regulations: Chapter O-2 Reg 7. Retrieved from: https://www.canlii.org/en/sk/laws/regu/rrs-c-o-2-reg-7/latest/rrs-c-o-2-reg-7.html

Sherwin, E. D., Chen, Y., Ravikumar, A. P., Brandt, A. R., 2021. Single-blind test of airplane-based hyperspectral methane detection via controlled releases. *Elementa: Science of the Anthropocene* 9 (1): 00063. DOI: https://doi.org/10.1525/elementa.2021.00063

Thorpe, A. K., Duren, R. M., Conley, S., Prasad, K. R., Bue, B. D., Yadav, V., Foster, K. T., Rafiq, T., Hopkins, F. M., Smith, M. L., 2020. Methane emissions from underground gas storage in California. *Environmental Research Letters* 15, 045005. DOI: https://iopscience.iop.org/article/10.1088/1748-9326/ab751d

Tyner, D. R., and Johnson, M. R., 2021. Where the Methane is – Insights from Novel Airborne LiDAR Measurements Combined with Ground Survey Data. *Environmental Science and Technology,* 55, 14, 9773-9783, DOI: https://doi.org/10.1021/acs.est.1c01572

Yacovitch, T. I., Neininger, B., Herndon, S. C., van der Gon, H. D., Jonkers., S., Hulskotte, J., Roscioli, J. R., Zavala-Araiza, D., 2018. Methane emissions in the Netherlands: The Groningen field. *Elementa: Science of the Anthropocene* 6: 57. https://doi.org/10.1525/elementa.308

Zavala-Araiza, D., Lyon, D. R., Alvarez, R. A., Davis, K. J., Harriss, R., Herndon, S. C., Karion, A., Kort, E. A., Lamb, B. K., Lan, X., Marchese, A. J., Pacala, S. W., Robinson, A. L., Shepson, P. B., Sweeney, C., Talbot, R., Townsend-Small, A., Yacovitch, T. I., Zimmerle, D. J., Hamburg, S. P., 2015. Reconciling divergent estimates of oil and gas methane emissions. *Proceedings of the National Academy of Sciences*, 112(51): 15597–15602. DOI: https:// doi.org/10.1073/pnas.1522126112

Zavala-Araiza, D., Herndon, S. C., Roscioli, J. R., Yacovitch, T. I., Johnson, M. R., Tyner, D. R., Omara, M., Knighton, B., 2018. Methane emissions from oil and gas production sites in Alberta, Canada. *Elementa Science of the Anthropocene* 6(1): 27. DOI: https://doi.org/10.1525/ elementa.284

Zavala-Araiza, D., Omara, M., Gautam, R., Smith, M. L., Pandey, S., Aben, I., Almanza-Veloz, V., Conley, S., Houweling, S., Kort, E. A., Maasakkers, J. D., Molina, L. T., Pusuluri, A., Scarpelli, T., Schwietzke, S., Shen, L., Zavala, M., Hamburg, S., 2021. A tale of two regions: methane emissions from oil and gas production in

offshore/onshore Mexico. *Environmental Research Letters* 16, 024019. DOI: https://doi.org/10.1088/1748-9326/abceeb

Zhang, Y., Gautam, R., Pandey, S., Omara, M., Maasakkers, J. D., Sadavarte, P., Lyon, D., Nesser, H., Sulprizio, M. P., Varon, D. J., Zhang, R., Houweling, S., Zavala-Araiza, D., Alvarez, R. A., Lorente, A., Hamburg, S. P. Aben, I., Jacob, D. J., 2020. Quantifying methane emissions from the largest oil-producing basin in the United States from space. *Science Advances*, 6, 17, eaaz5120. DOI: 10.1126/sciadv.aaz5120

2. Methane emissions from upstream oil and gas production in Canada

2.1 Preface

A version of this chapter has been published in *Scientific Reports* (Nature). I am the primary author, and co-authors are Martin Lavoie, Evelise Bourlon, Emmaline Atherton, Elizabeth O'Connell, Jennifer Baillie, Chelsea Fougère, and David Risk. I led the writing and analysis included in this chapter, and all authors, revised, edited, and provided valuable feedback that was used to refine the published paper.

2.2 Abstract

Methane emissions were measured at 6650 sites across six major oil and gas producing regions in Canada to examine regional emission trends, and to derive an inventory estimate for Canada's upstream oil and gas sector. Emissions varied by fluid type and geographic region, with the heavy oil region of Lloydminster ranking highest on both absolute and intensity-based scales. Emission intensities varied widely for natural gas production, where older, low-producing developments such as Medicine Hat, Alberta showed high emission intensities, and newer developments in Montney, British Columbia

showed emission intensities that are amongst the lowest in North America. Overall, we estimate that the Canadian upstream oil and gas methane inventory is underestimated by a factor of 1.5, which is consistent with previous studies of individual regions.

2.3 Introduction

Reducing methane (CH_4) emissions from anthropogenic activities is a critical part of climate change mitigation efforts (Rogelj et al. 2018). Although atmospheric CH_4 concentrations are low (~1.8 ppm) (Dlugokencky 2020), the warming potential of CH_4 is 84 times higher than that of carbon dioxide over a 20-year timeframe (Myhre et al. 2013), making it an immediate target for greenhouse gas (GHG) reductions.

Canada's second most abundant GHG is CH_4, making up 13% of national GHG emissions (ECCC 2020). In 2018, 43% of Canada's anthropogenic CH_4 emissions originated from oil and gas (O&G) systems (ECCC 2020). The major sources of O&G CH_4 emissions are from activities that occur during upstream production, which include venting (intentional releases; ~52%), incomplete combustion during flaring (~1.4%), and fugitive emissions (unintentional releases from faulty equipment, or drilling; ~42%) (ECCC 2020). In response to the climate crisis, Canada's federal government committed to reducing CH_4 emissions from the O&G sector 40-45% below 2012 levels by 2025 (ECCC 2018). Although the federal government drafted regulations to achieve these reductions (ECCC 2018), provincial governments in Alberta, Saskatchewan, and British Columbia have also proposed their own regulations to achieve equivalent reduction goals, which have since received approval to replace the original federal regulations

(Saskatchewan Ministry of Economy 2019, Province of British Columbia 2018, Alberta Energy Regulator 2020).

Canada's CH_4 reduction targets are based on component-level inventory estimates reported annually in the national inventory report (NIR), which are based in part on industry self-estimation and self-reporting (ECCC 2020). Field measurement studies in Canada and the United States have shown that actual emissions range from equivalent to substantially higher than inventory estimates (Atherton et al. 2017, Alvarez et al. 2019, Baray et al. 2018, Greenpath Energy 2016, Johnson et al. 2017, Roscioli et al. 2018, Zavala-Araiza et al. 2015, Zavala-Araiza et al. 2018). But a national understanding of discrepancies is lacking because most measurement studies in Canada consist of relatively region-specific sample populations which may not be extensible to regions with varying extractive techniques, geology, and geochemical properties. Different emission measurement techniques and technologies, applied at varying scales, also make comparisons difficult.

How do upstream CH_4 emissions and intensities vary across major O&G producing regions in Canada, and how do they compare to the federal inventory? We addressed this question by aggregating site-level emission data collected during nine extensive vehicle-based measurement campaigns across six prominent O&G regions in Canada: Montney (British Columbia), Medicine Hat (Alberta), Lloydminster (Alberta & Saskatchewan), Peace River (Alberta), Red Deer (Alberta), and southeastern Saskatchewan. Measurements were collected between 2015 and 2018, with some regions

(Lloydminster, Peace River) visited on more than one occasion. These six regions (Figure 2.1) include ~20% of the non-oilsands producing sites in western Canada. Results from four of these campaigns have already been published (Baillie et al. 2019, O'Connell et al. 2019), but this is the first time the 6650 emission rate estimates have been aggregated. This study represents the most regionally nuanced estimate of upstream Canadian O&G fugitive and vented CH_4 emissions to date, and uses a much larger sample population than the ~300 site survey studies used by the Canadian industry to calibrate its upstream CH_4 inventory (Clearstone Engineering Ltd. 2018).

2.4 Materials and Methods

2.4.1 Data acquisition and processing

2.4.1.1 Overview

The methods used to collect and process data involve a four-step process: 1) Data was collected via extensive truck-based surveys of air composition measuring three or more atmospheric gases at ppb-levels, geo-located, at 1 Hz frequency. Gas concentrations (CH_4, CO_2, C_2H_6, H_2S; analyzer dependent) were measured in real time using laser spectrometers (Picarro Inc., Santa Clara, CA, USA). 2) Computational signal processing and geochemical analysis was used to distinguish O&G emissions from biogenic, naturally occurring sources, or other anthropogenic emissions. 3) A back-trajectory analysis was used to attribute CH_4 anomalies observed on-road to specific upwind O&G sites. 4) Volumetric emissions rates were estimated via a point-source Gaussian Dispersion Model (GDM). Each of these steps, and uncertainties therein are described

below, are also discussed extensively in Atherton et al. (2017) and O'Connell et al. (2019).

Table 2.1 provides basic statistics (dates, number of surveys, distance) for all measurement campaigns included in this analysis. Although some of these individual campaigns were the focus of previous peer-reviewed studies, all measurements were conducted by our research group (StFX FluxLab) using the same equipment (Picarro analyzer(s), anemometer, GPS) and survey protocols, which allowed for uniform processing and analysis of the data for this work. All data was reprocessed and combined into a single dataset to ensure consistency and fair comparisons. It should also be noted that measurements included active and suspended sites only, as emissions from abandoned infrastructure were not the focus of these studies. Short-lived emissions from intermittent activities like exploration and drilling were also not included (i.e. measured emissions represent emissions during routine production only). These data cover six contrasting regions across the three major O&G producing provinces in Canada (British Columbia, Alberta, and Saskatchewan). Figure 2.1 is a map with polygons depicting the geographical boundaries covered in this study. A total of nine vehicle-based measurement campaigns were completed between 2015 and 2018 (with some regions being surveyed more than once). All campaigns were conducted on public roads without giving notice to operators or regulators in the regions. Preplanned survey routes were driven multiple times (often on different days) and were designed to target areas with dense infrastructure. Table 2.2 describes general profiles for each region, including the type of

hydrocarbon produced, primary production styles, and approximate active well counts as of January 2020.

Table 2.1. General information for all survey campaigns included in this analysis. Each survey consisted of multi-hour vehicle-based data collection, with gas concentrations being measured every second while driving. All campaigns were conducted on public roads.

Region/Campaign	Year	Month(s)	Total surveys	Approx. km surveyed	Publication
Southeastern Saskatchewan	2015	October-November	28	4,500	Baillie et al. 2019
Montney, BC	2016	February-March	20	5,000	-
Lloydminster (AB side)	2016	October-November	15	2,684	O'Connell et al. 2019
Medicine Hat	2016	October-November	15	2,881	O'Connell et al. 2019
Peace River	2016	October-November	15	2,784	O'Connell et al. 2019
Lloydminster (AB side)	2017	October	15	2,600	-
Red Deer	2017	September	15	2,600	-
Lloydminster (AB & SK sides)	2018	July	9	2,400	-
Peace River	2018	July	3	440	-
All			165	25,889	

Table 2.2. General production information for regions included in this analysis. Polygons shown in Figure 2.1 below are used as geographic boundaries for well count estimation for each region.

Region	Main hydrocarbon produced	Primary Production style(s)	Approx. number of active wells (2020)
Southeastern Saskatchewan	Oil (sour)	Conventional drilling, hydraulic fracturing, EOR	11,698
Montney, BC	Gas (sweet)	Horizontal drilling, multi-stage hydraulic fracturing	5,382
Lloydminster	Heavy oil (sweet)	Cold Heavy Oil Production with Sand (CHOPS)	10,571
Medicine Hat	Conventional Gas (sweet), light oil	Conventional drilling	20,508
Peace River	Heavy oil/bitumen (sour)	Cold Heavy Oil Production, thermal recovery	5,874
Red Deer	Natural gas/light oil	Conventional drilling, hydraulic fracturing	5,648

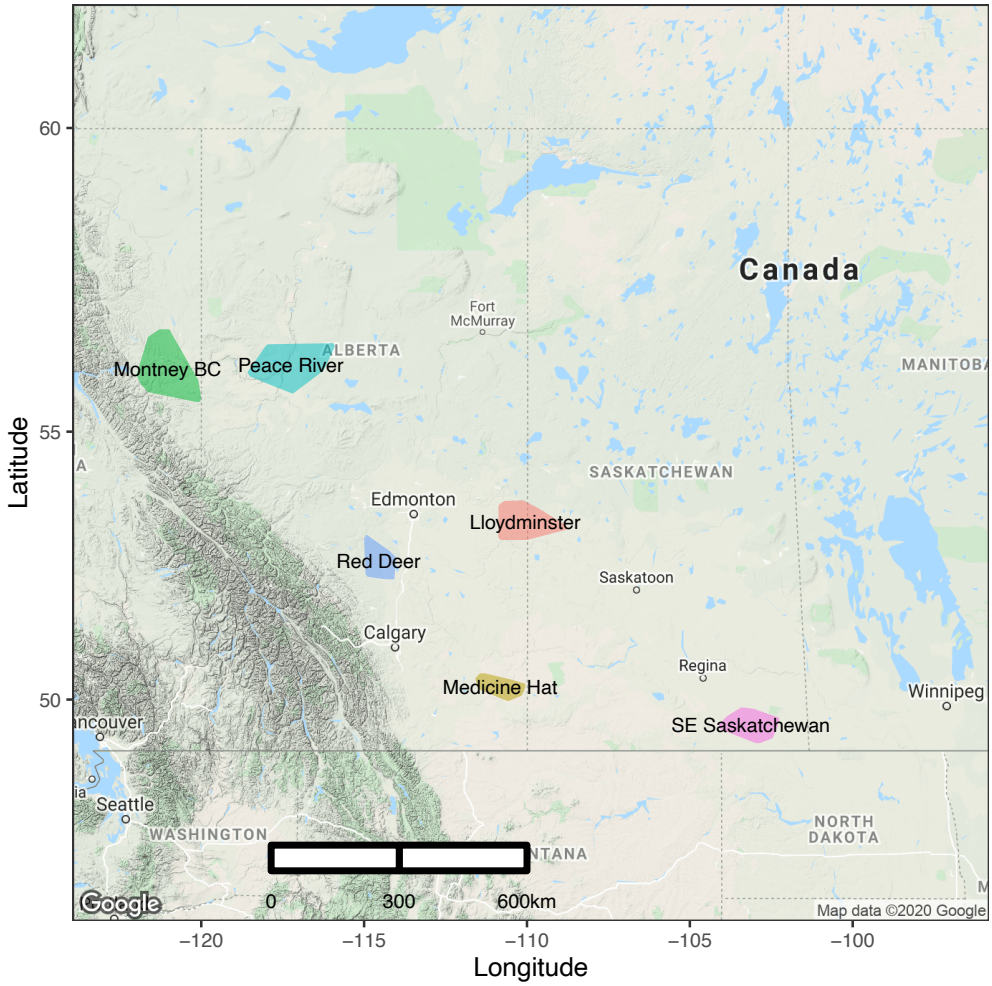

Figure 2.1. Polygons showing the geographic regions in British Columbia, Alberta, and Saskatchewan covered during vehicle-based measurement campaigns. All measured oil and gas sites for each region fall within these polygons, however not all sites within the polygons were measured during survey campaigns. Lloydminster and Peace River regions were visited more than once (across different years).

2.4.1.2 Geochemical and geospatial analysis

Ratios of super-ambient CO_2 and CH_4 concentrations were used to identify thermogenic CH_4 plumes, as opposed to raw atmospheric concentrations which are more prone to false characterization. To do this, an adaptive algorithm (Atherton et al. 2017, O'Connell et al. 2019) was used to establish background concentrations of each gas, which considers the spatiotemporal variability of ambient background concentrations often observed on multi-hour surveys. From there, background concentrations were subtracted from measured values to calculate excess concentrations of CO_2 and CH_4, which were then used to calculate excess ratios (hereafter referred to as e-ratios). These e-ratios act as a geochemical fingerprint and were used to identify plumes of CH_4-enrichment. They were also used to distinguish between different emission sources (e.g. from natural sources or engine combustion). For this analysis, an eCO_2:eCH_4 threshold of <100 was used as an indicator of thermogenic CH_4 plumes. Such measurements of CH_4-enrichment needed to persist for more than three individual measurements to be considered a thermogenic plume (i.e. if there was one measurement that fell below the e-ratio threshold, but the following measurement was above the threshold, then the first measurement was not considered to be from a plume). During surveys, time-series measurements were collected every second.

Once the CH_4 plumes were identified and geospatially located, a back-trajectory analysis was performed to attribute the plumes observed on road to upstream infrastructure sites (using up to date infrastructure databases obtained via a subscription for IHS Markit). Here, an infrastructure 'site' is defined as all pieces of infrastructure at upstream O&G production sites (wells and facilities), that exist within a 45 m radius of

each other. Sites were considered sampled when at least two sequences of measurements (i.e. "passes") were taken <500 m downwind (i.e. it was passed downwind at least twice). Sites were considered to be emitting only if a CH_4 plume was detected <500 m downwind on more than 50% of passes. If multiple sites fell within 500 m of a plume, the closest site was tagged as the emission source.

2.4.1.3 Volumetric CH_4 emission rate estimates using inverse Gaussian dispersion model

After geochemical and geospatial attribution, emission rates were estimated for all sites tagged as emitting. A point-source Gaussian Dispersion Model (GDM) was used, which incorporates both measured and estimated parameters including downwind CH_4 concentration, wind speed, measurement-to-source distance, emission source height, and Pasquill atmospheric stability. Since most sites consist of multiple pieces of infrastructure, and this methodology cannot confidently attribute plumes to a single well or facility, emission rates were estimated for all unique sources within each site, which considers variable equipment (i.e. potential leak source) heights. The median emission rate per site (i.e. the median value of all unique source emission rates) is then used for all subsequent analyses. Reasons for using the median rather than the mean is discussed further in the next section.

2.4.1.4 Measurement and modeling uncertainty

The uncertainties related to methods of plume detection, attribution, and emission rate estimation have been previously evaluated (Atherton et al. 2017, Baillie et al. 2019, O'Connell et al. 2019). Plume detection uncertainty (i.e. the probability of detecting false

positives) is estimated to be <1%, whereas attribution (i.e. assigning the plume to the proper site) uncertainty ranges from 7.5-33% (depending on infrastructure density) (Atherton et al. 2017). Emission rate estimates (calculated using the GDM) represent the largest source of uncertainty, which is described extensively in O'Connell et al. (2019)'s Supplemental Material. O'Connell et al. (2019) documented an emission rate estimate uncertainty (standard error) of ± 63%, which was calculated using controlled release experiments conducted over five days, under a range of atmospheric conditions (O'Connell et al. 2019). Results from these experiments also revealed an upward bias of 30% for mean emission rates measured by three passes, but the median value was found to be less skewed (O'Connell et al. 2019). For these reasons (as noted above), the median emission rate for each site was used in my analysis, to ensure a more conservative, unbiased estimate. These emission rate uncertainties are comparable to those documented in other transect-based Gaussian dispersion model studies (e.g. Day et al. 2015, Fietz et al. 2018).

2.4.1.5 Fluid type classification

Fluid types for all measured sites were classified as "Oil", "Bitumen", "Gas", or "Undefined" based on their infrastructure description included in the databases used for emissions attribution. For example, a "Crude oil single well battery" site was classified as an oil site since the word oil is included in the site description. If oil, bitumen, or gas were not included in the site description, then the site was classified as "Undefined". Out of all 6651 measured sites, 1239 were classified as "Undefined."

2.4.2 Site-level Emission Factor calculations and Alberta CH_4 inventory estimate

2.4.2.1 Emission Factor calculations

We calculated site-level Emission Factors (EFs) using our measurements and applied them to all non-oilsands producing sites in Alberta to derive an overall CH_4 inventory estimate. Oil sands sites were excluded as we lacked measurements for these facilities (these sites are not ideal for vehicle-based measurement techniques). EFs were derived by calculating the mean emission rate for all unique combinations of infrastructure types and regions, which we define as Type-Region (TR) bins. For example, Single wells in Medicine Hat would represent a unique TR bin. All emission rate measurements for active sites (including those measured as 0) were included in the calculations. We used the ten Alberta Energy Regulator (AER) administrative regions (Figure 2.2) as the physical boundaries in which measurements were considered for region-specific EFs (excluding the oilsands dominant Fort McMurray region). Using the previous example, an EF for TR bin Single well-Medicine Hat is the average of all emission rates (including sites measured as non-emitting, i.e. emission rate = 0) for single well sites within the Medicine Hat region (Figure 2.2). It is important to note that while using this method, a type of infrastructure site could have multiple EFs across different regions. For example, an EF for a single well in Medicine Hat might be different than an EF for a single well in Red Deer (since they would each represent a unique TR bin). If a certain infrastructure site type was not sampled in a particular region, an EF was derived by averaging all measurements (from all regions) of that site type.

We chose to calculate EFs separately for all unique TR bins because we know from previous studies (Greenpath Energy 2016, Johnson et al. 2017, Roscioli et al. 2018, Zavala-Araiza et al. 2018, MacKay et al. 2019, O'Connell et al. 2019) that emissions can vary significantly based on these two factors. Our method lets us account for the variability that exists within the upstream sector, which in turn helps avoid scenarios of over and underestimations.

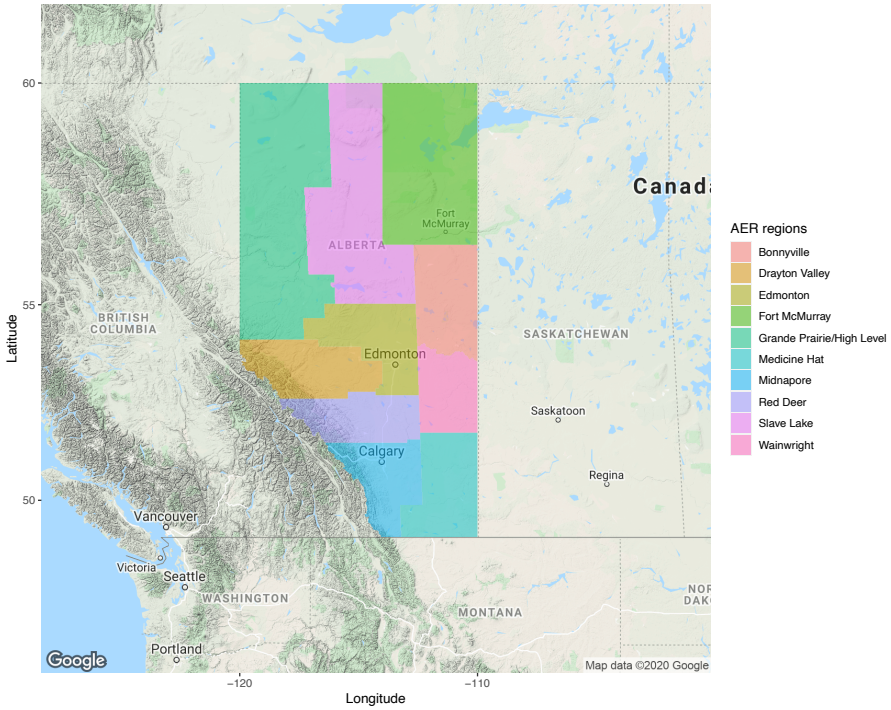

Figure 2.2. AER administrative regions for the province of Alberta. These regions (excluding the oilsands dominant region Fort McMurray) are the geographic boundaries used in emission factor calculations and the provincial inventory estimate (map created in R software version 4.0.0, https://www.r-project.org/, using publicly available shapefile from http://www1.aer.ca/ProductCatalogue/649.html).

2.4.2.2 Alberta CH_4 inventory estimate and uncertainty

To estimate an overall CH_4 inventory for Alberta upstream O&G production, we first needed to calculate the total number of O&G sites in the province (excluding oilsands). IHS databases (IHS Markit) were used to determine site counts. Since infrastructure data in IHS databases are not aggregated to site-level, we grouped individual wells and facilities that fell within a 45 m radius of one another to determine total site counts. This step is required because our EFs correspond to a site-level estimate. Then, we subset our infrastructure dataset to only include sites that were either producing, venting, or flaring hydrocarbons during the 2018 production year (according to publicly available Petrinex reporting data). Finally, this dataset was used to calculate individual site counts for each TR bin.

From there, we used a Monte Carlo analysis to estimate the total Alberta inventory and 95% confidence interval (CI). For each TR bin, we created a probability density function (pdf) with a lognormal distribution (mean=EF, n=10,000, SD=±63%). A lognormal fit was chosen as previous studies have shown emissions to follow this distribution (Zavala-Araiza et al. 2015, Zavala-Araiza et al. 2018, Alvarez et al. 2018, O'Connell et al. 2019, Baillie et al. 2019, Zavala-Araiza et al. 2017). Then, a random value from each pdf is sampled, and multiplied by the corresponding TR bin site count, resulting in a total emission estimate for each TR bin. Totals from all TR bins are then summed to compute a total provincial inventory. This process was repeated 10,000 times across all TR bins, resulting in a distribution of total inventory estimates (n=10,000). Using this method, we were able to incorporate the "heavy-tail" of the emissions

distribution, as well as our measurement uncertainty into the total estimate. We assumed infrastructure count uncertainty to be negligible.

2.4.3 Emissions intensity analysis

2.4.3.1 Calculations

Since there are no standard units to calculate emission intensities, we expressed our estimates using two ratios: 1) Average megajoule emitted per megajoule produced (MJ/MJ), and 2) grams of CO_2 equivalent emitted per megajoule produced (gCO_2e/MJ). These units were chosen based on what was typically used in other similar literature.

To calculate the amount of energy (MJ) emitted for each region, the cumulative CH_4 emission rate (in $m^3\ day^{-1}$) was calculated for each campaign (i.e. the sum of all site-level emissions that were measured over each campaign). These cumulative emissions were converted to megajoules (MJ) using a conversion of 1 m^3 CH_4 = 37.3 MJ, which is based on 1000 Btu/cf (Canada Energy Regulator 2016). We converted emissions (in $m^3\ day^{-1}$) to grams of CO_2e using a global warming potential (GWP) of 25 (over 100 years), and a density of 678 g/m^3 (15°C, 1 atm) for CH_4.

To calculate the average energy produced at the measured sites, we extracted aggregated production data for measured sites from IHS databases. Complete lists of all wells measured during each campaign were imported to IHS Markit software (AccuMap) to get specific production data for the same sites that were measured for emissions. Daily average production rates for all producing wells in the well lists were extracted, and then

summed to get a total production rate per day per region. In other words, average daily production rates for all sampled wells were summed to get a combined daily average production rate. This was done separately for both oil (m^3 day^{-1}) and gas ($E3m^3$ day^{-1}), and production data used in these calculations corresponded to the same month(s) in which the sites were measured for emissions. Consequently, production rates are based on a small subset of wells relative to total infrastructure counts in these areas (especially when many of the sampled wells were not producing), and as a result, these production values may not be representative of the entire regions. However, this method was the best way to ensure the use of site- and time-specific production values for actual wells that were measured for emissions.

From there, the combined average daily production rates for O&G were converted to megajoules (MJ). For oil production, a conversion of 1 m^3 = 38510 MJ for light oil, and 1 m^3 = 40900 MJ for heavy oil was used (Canada Energy Regulator 2016). For gas production, the same conversion rate from above was used to convert CH_4 emissions to energy units (MJ). These values were then summed to get a single value representing the average energy produced per day for all sampled sites.

Finally, daily energy (MJ) emitted and daily gCO_2e emitted values are divided by the average daily energy produced (MJ), resulting in a single emission intensity value for each measurement campaign. For regions sampled across multiple campaigns (Lloydminster and Peace River), final intensities were averaged to get a single value per region.

2.4.3.2 Emission intensity uncertainty

To quantify uncertainties in the intensity calculations, both uncertainties related to emission rate estimates and production volumes needed to be considered. As noted above, average emission rate uncertainties were estimated to be ± 63%. For production volume uncertainties, an uncertainty value of ± 25% is assumed, based on values published in Table 13 of Clearstone Engineering's inventory methodology report (same methodology used for Canada's national inventory reporting estimates) (Clearstone Engineering 2019). The overall emissions intensity uncertainty was calculated by combining the uncertainty in emission rates and production volumes using the following error propagation equation:

$$U_{total} = \sqrt{U_1^2 + U_2^2 \ldots + U_n^2} \quad (2.1)$$

Where U_1, U_2 are the percent uncertainties for each value (emission rates and production volumes). The U_{total} value was then used to determine the upper and lower bounds for each emission intensity estimate.

2.5 Results and Discussion

2.5.1 Emissions rate distributions

Site-level measurements show that CH_4 emissions vary by fluid type and geographic region (Figure 2.3). This variability has been documented in recent Canadian studies, at both regional (Johnson et al. 2017, O'Connell et al. 2019), and component-level scales (Clearstone Engineering 2018, Greenpath Energy 2016, Ravikumar et al. 2020), as a function of several determinants.

In no particular order, the first determinant is the fluid type. Extraction techniques and infrastructure can vary depending on the hydrocarbon produced, which affects emission levels. Sites producing gas had lower average emission rates compared to oil-producing sites, and the overall average emission rate for oil sites was roughly 3.6 times higher than the overall average for gas sites (71.1 m^3 day^{-1}/site vs. 19.9 m^3 day^{-1}/site) (Figure 2.3). In many oil-producing regions, CH_4 gas is routinely considered a by-product and vented because the economics of conservation are unfavorable (Johnson and Coderre 2012). Additionally, some in-situ heavy oil production processes such as Cold Heavy Oil Production with Sand (CHOPS) generally yield higher rates of routine venting (Alberta Energy Regulator 2019, Greenpath Energy 2016, Johnson et al. 2017, O'Connell et al. 2019, Roscioli et al. 2018); this is evident in Lloydminster, where CHOPS is the dominant production technique (Figure 2.3).

Regulation is another factor that influences regional variability in CH_4 emission rates. Some geographies are subject to more stringent regulations due to historical air quality violations or other health and safety concerns. For instance, special regulations were enacted in 2017 for the Peace River area because of historical air quality issues, and in recent years producers in the area have reportedly eliminated all venting (Alberta Energy Regulator 2018, O'Connell et al. 2019). Measurements showed average site-level emission rates in Peace River decreased nearly three-fold from 2016 (31.5 m^3 day^{-1}/site) to 2018 (11.1 m^3 day^{-1}/site) (Table 2.3), which suggests that these new regulations are resulting in significant mitigation success in this area. Sour (H_2S-bearing) fields are another example of regulatory success; since H_2S is a serious health risk, sour

developments like SE Saskatchewan have more restrictions on venting, which inadvertently aids in CH_4 mitigation since the gases are co-emitted (Baillie et al. 2019, MacKay et al. 2019). SE Saskatchewan had the lowest average site-level emission rate out of all regions included in this analysis (Figure 2.3, Table 2.3). Effective mitigation depends on an understanding of these determinants.

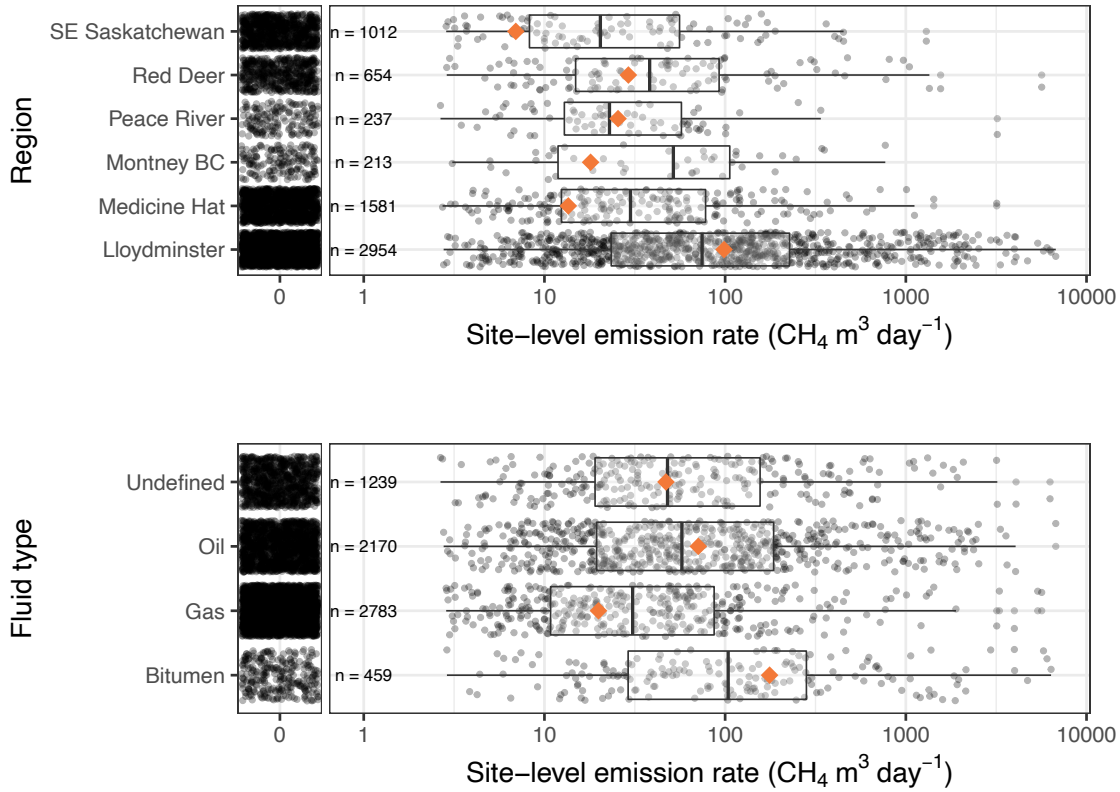

Figure 2.3. Distributions of measured emission rates (logarithmic scale) by region (top) and by fluid type (bottom). Black dots represent individual site-level emission rates, and the orange diamond is the sub-population mean. For better visualization of the emission rate distributions, the plots are broken down to show non-emitting sites (left panels, emission rate = 0), and emitting sites (right panels). The mean

values (orange diamond) are based on all measurements in both panels for each sub-population.

2.5.2 Current component-level inventory is underestimated

Various authors have pointed out systematic biases in the component-level inventory process (as used in federal reporting), especially the propensity to miss rare large emitters (Alvarez et al. 2019, Brandt et al. 2014, Zavala-Araiza et al. 2017). To estimate the degree to which the current Canadian upstream CH_4 inventory is underestimated, we calculated site-level Emission Factors (EFs) from our measurements and applied them to all non-oilsands producing sites in Alberta. Site-level EFs are different than component-level EFs in that they represent an average of aggregate emissions for an oil/gas site (multiple pieces of infrastructure), whereas component-level EFs are average emissions for specific leaking components (e.g. valves, hatches).

To capture the variability in emissions across sites and regions, site-level EFs were calculated for every unique combination of site type and region. Then, we used a Monte Carlo analysis to estimate a total inventory for Alberta. Alberta was chosen for this exercise because most of our measurements were collected in this province, and because it represents 80% and 67% of total Canadian O&G production, respectively (Johnson and Tyner 2020).

Our measurement-based inventory indicates that the non-oilsands upstream O&G sector in Alberta emitted 5,074,449 m^3 CH_4/day in 2018 (2.5 percentile = 3,741,309 m^3

day^{-1}; 97.5 percentile = 7,453,798 m^3 day^{-1}), which is about 1.5 times the most recent component-level inventory of 3,408,534 m^3 CH_4/day, derived by Environment and Climate Change Canada (ECCC) for Alberta in 2018 (ECCC 2020). Our findings are consistent with previous CH_4 emission studies within Canadian developments; no studies have yet identified a Canadian O&G producing region with emissions lower than the inventory estimate. In previous studies, factors of 1-15 have been estimated, with most being in the range of 1.5-3.0 (Atherton et al. 2017, Baray et al. 2018, Johnson et al. 2017, Roscioli et al. 2018, Zavala-Araiza et al. 2018). This implies that CH_4 abatement costs could be lower per ton of CO_2 equivalent than previously reported, due to higher volumes of CH_4 (i.e. profitable natural gas) present at O&G sites (Tyner and Johnson 2018).

2.5.3 Emission intensities

Average emissions intensities across regions vary significantly, ranging from 0.0004 ± 0.0003 (Peace River) to 0.0706 ± 0.0479 (Lloydminster) (Figure 2.4, Table 2.4). Lloydminster heavy oil ranks highest in intensity, with roughly 7% of the energy produced being lost via fugitives and vents. This finding was somewhat expected, given the high average emission rates in this region (Figure 2.4, Table 2.4). Interestingly, however, Medicine Hat ranked second highest in intensity (0.0243 ± 0.0165), despite having a relatively low average emission rate per site (Tables 2.3, 2.4). The high intensities in Medicine Hat are a result of low production rates in this region. Although Medicine Hat has the highest density of wells in Alberta (Table 2.2), the region only accounts for a small portion (~7%) of the province's gas production (Greenpath Energy 2016). Such findings are important, because aggregate production, transmission, and

distribution leaks here (and potentially in other old and low-producing developments) could conceivably approach overall leak rates of 3.2% - where natural gas is estimated to approach the climate warming impact of coal (Alvarez et al. 2012). If so, these developments could become increasingly exposed to market or investment barriers, as investors and consumers move towards fuels with less embodied carbon.

Our estimated emissions intensities (in gCO2e/MJ) for each region can be readily compared with those recently published in Masnadi et al. (2018). In that study, authors calculated full life-cycle (well-to-refinery) emissions intensities for hundreds of oilfields around the world. Using the best available data and the OPGEE model, Masnadi et al. (2018) found a global carbon intensity life-cycle average of 10.3 gCO_2e/MJ (+ 6.7, − 1.7, 95% CI), of which 2.6 gCO_2e/MJ was exclusively derived from CH_4 emissions. For 84 Canadian oilfields in the study, the overall average carbon intensity was 17.6 gCO_2e/MJ (Masnadi et al. 2018). With the exception of Lloydminster, all of our intensity estimates are lower than their average for Canadian oilfields (Figure 2.4), which was expected since our estimates only consider the CH_4 emissions component of total life-cycle carbon. However, our Lloydminster and Medicine Hat CH_4-only intensities exceeded Masnadi et al. (2018)'s global average for total carbon life-cycle emissions (Figure 2.4). In these regions, full life-cycle emissions may significantly outstrip the global average. On the other hand, we also found that the Montney BC and Peace River regions have extremely low CH_4 emission intensities that fall well below the global and Canadian averages, suggesting that these regions produce oil and gas more efficiently with respect to CH_4 leakage. Additionally, emission intensities for all producing regions in Canada, except for

Lloydminster and Medicine Hat, were lower than the US average of 2.3% (of gross production) recently reported by Alvarez et al. (2018).

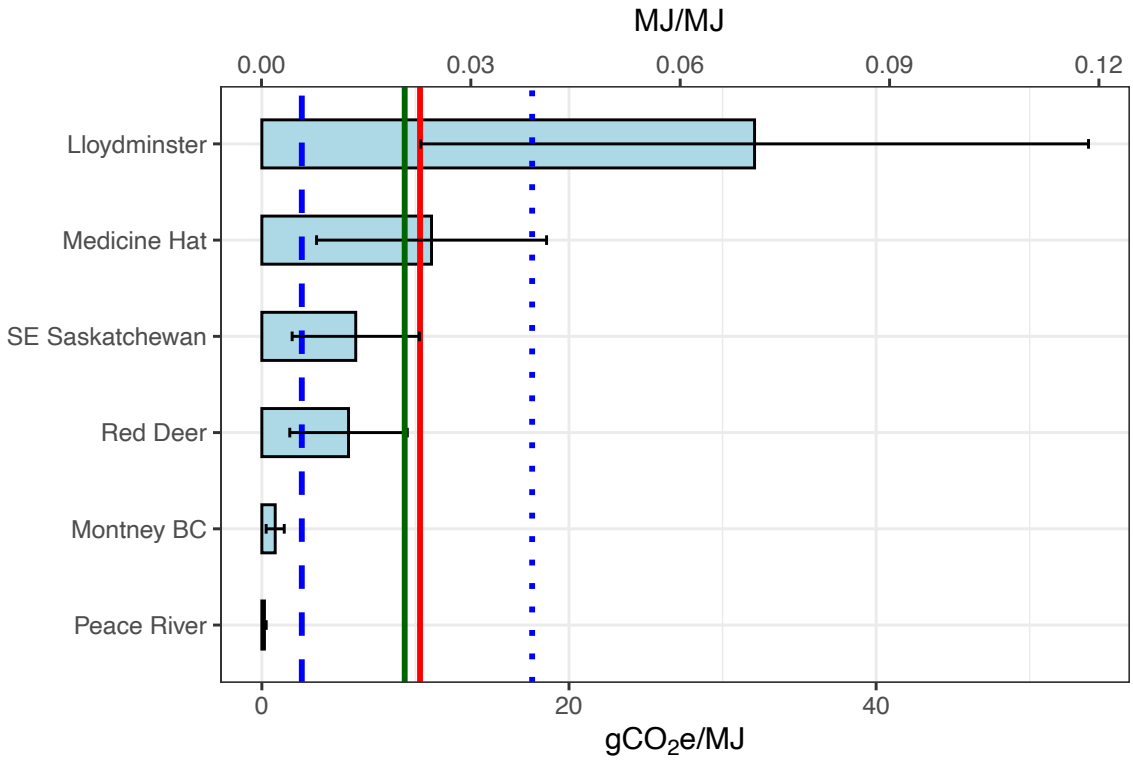

Figure 2.4. Emission intensities for each region included in this study (horizontal grey bars). The top axis shows intensities as a function of megajoule emitted per megajoule produced (MJ/MJ), and the bottom axis displays intensities as a function of grams of CO_2 equivalent emitted per megajoule produced (gCO_2e/MJ). Emission intensity uncertainty ranges are represented via the black error bars. The solid green vertical line is the overall average from this study, the solid vertical red line is the global average reported in Masnadi et al. (2018), the dotted blue line shows their estimate for Canada (based on data from 84 oil fields), and the blue dashed line is their global average intensity for CH_4 only (Masnadi et al. 2018).

Table 2.3. Average site-level CH_4 emission rates, cumulative CH_4 emission rates and average production volumes for sites sampled during each campaign. Production averages correspond to the monthly average in which the campaign took place.

Campaign/ Region	Year	Avg. CH_4 emission rate (m^3 day^{-1}/site)	Cumulative CH_4 emission rate (m^3 day^{-1}/region)	Avg. oil production (m^3 day^{-1})	Avg. gas production ($E3m^3$ day^{-1})
SE Saskatchewan	2015	6.94	7025.73	168.09	348.58
Montney BC	2016	18.01	3835.27	0.00	2006.74
Lloydminster	2016	74.89	83731.58	866.84	139.40
Medicine Hat	2016	13.56	21434.65	312.22	559.16
Peace River	2016	31.47	5286.66	843.52	272.09
Lloydminster	2017	71.62	80076.48	992.53	175.86
Red Deer	2017	29.14	19060.41	279.33	1245.96
Lloydminster	2018	168.45	120778.38	1378.32	174.45
Peace River	2018	11.13	768.00	1478.26	452.00

Table 2.4. Emission intensities in MJ/MJ and gCO2e/MJ by region. A GWP = 25 and density = 0.678 kg/m^3 (15°C, 1 atm) for CH_4 was used for the gCO_2e calculation.

Region	MJ/MJ	gCO_2e/MJ
Montney BC	0.0019 ± 0.0013	0.869 ± 0.589
SE Saskatchewan	0.0135 ± 0.0091	6.115 ± 4.145
Lloydminster	0.0706 ± 0.0479	32.084 ± 21.746
Medicine Hat	0.0243 ± 0.0165	11.050 ± 7.489
Peace River	0.0004 ± 0.0003	0.168 ± 0.114

Red Deer	0.0124 ± 0.0084	5.645 ± 3.826

2.6 Summary

In conclusion, there is noteworthy variability in absolute CH_4 emissions and emission intensities across major O&G regions in Canada. As seen in previous studies, Lloydminster is an area characteristic of high CH_4 emissions. Fortunately, new regulations should address some of these prominent emission sources (especially vented emissions), and future work in this area could verify regulation-driven reductions. Our emissions intensity analysis revealed that low producing regions like Medicine Hat have high intensities, which has both environmental and economic implications that should be considered as we move towards a low-carbon future. In contrast, Montney BC and Peace River regions showed extremely low emission intensities, making natural gas produced here an attractive investment for companies with Environment, Social, and Governance (ESG) standards. Lastly, CH_4 emissions from the O&G sector in Canada likely exceed inventories by a factor of 1.5. Because conserved CH_4 is saleable, this implies that reduction costs per ton could be less than previously estimated (Tyner and Johnson 2018). Increased measurement and reporting requirements as a result of new regulations should be used to inform future inventory estimates, to ensure annual reductions are accurately estimated.

References

Alberta Energy Regulator (AER), 2018. Directive 084. Retrieved from: https://aer.ca/documents/directives/Directive084.pdf.

Alberta Energy Regulator (AER), 2019. Upstream petroleum industry flaring and venting report: Industry performance for year ending December 31, 2018. Retrieved from: https://www.aer.ca/documents/sts/ST60B-2019.pdf

Alberta Energy Regulator (AER), 2020. Directive 060. Retrieved from: https://www.aer.ca/documents/directives/Directive060_2020.pdf

Alvarez, R. A., Pacala, S. W., Winebrake, J. J., Chameides, W. L., Hamburg, S. P., 2012. Greater focus needed on methane leakage from natural gas infrastructure. *Proceedings of the National Academy of Sciences* 109 (17), 6435-6440. DOI: https://doi.org/10.1073/pnas.1202407109

Alvarez, R. A., Zavala-Araiza, D., Lyon, D. R., Allen, D. T., Barkley, Z. R., Brandt, A. R., Davis, K. J., Herndon, S. C., Jacob, D. J., Karion, A., Kort, E. A., Lamb, B. K., Lauvaux, T., Maasakkers, J. D., Marchese, A. J., Omara, M., Pacala, S. W., Peischl, J., Robinson, A. L., Shepson, P. B., Sweeney, C., Townsend-Small, A., Wofsy, S. C., Hamburg, S. P., 2018. Assessment of methane emissions from the U.S. oil and gas supply chain. *Science* 361, 186-188. DOI: 10.1126/science.aar7204

Atherton, E., Risk, D., Fougère, C., Lavoie, M., Marshall, A., Werring, J., Williams, J.P., Minions, C., 2017. Mobile measurement of methane emissions from natural gas developments in northeastern British Columbia, Canada. *Atmospheric Chemistry and Physics* 17(20): 12405–12420. DOI: 10.5194/acp-17-12405-2017

Baillie, J., Risk, D., Atherton, E., O'Connell, E., Fougère, C., Bourlon, E., MacKay, K., 2019. Methane emissions from conventional and unconventional oil and gas production sites in southeastern Saskatchewan, Canada. *Environmental Research Communications* DOI: 10.1088/2515-7620/ab01f2.

Baray, S., Darlington, A., Gordon, M., Hayden, K. L., Leithead, A., Li, S-M., Liu, P. S. K., Mittermeier, R. L., Moussa, S. G., O'Brien, J., Staebler, R., Wolde, M., Worthy, D., McLaren, R., 2018. Quantification of methane sources in the Athabasca Oil Sands Region of Alberta by aircraft mass balance, *Atmospheric Chemistry and Physics* 18, 7361-7378. DOI: https://doi.org/10.5194/acp-18-7361-2018

Brandt, A. R., Heath, G. A., Kort, E. A., O'Sullivan, F., Petron, G., Jordaan, S. M., Tans, P., Wilcox, J., Gopstein, A. M., Arent, D., Wofsy, S., Brown, N. J., Bradley, R., Stucky, G. D., Eardley, D., Harriss, R., 2014. Methane Leaks from North American Natural Gas Systems, *Science,* 343, 6172. DOI: https://www.jstor.org/stable/24743002

Canada Energy Regulator, 2016. Energy conversion tables. Retrieved from: https://apps.cer-rec.gc.ca/Conversion/conversion-tables.aspx?GoCTemplateCulture=en-CA.

Clearstone Engineering Ltd., 2018. Update of equipment, component and fugitive

emission factors for Alberta upstream oil and gas. Retrieved from: https://www.aer.ca/documents/UpdateofEquipmentComponentandFugitiveEmissionFactorsforAlber-1.pdf.

Clearstone Engineering Ltd., 2019. 2018 Alberta upstream oil & gas methane emissions inventory and methodology. Retrieved from: https://www.aer.ca/documents/ab-uog-emissions-inventory-methodology.pdf

Day, S., Dell'Amico, M., Fry, R., Javanmard Tousi, H., 2014. Field measurements of fugitive emissions from equipment and well casings in Australian coal seam gas production facilities. Report to the Department of the Environment, CSIRO. Retrieved from: https://publications.industry.gov.au/publications/climate-change/system/files/resources/57e/csg-fugitive-emissions-2014.pdf

Dlugokencky, E., 2020. Trends in Atmospheric Methane. NOAA/ESRL Retrieved from: esrl.noaa.gov/gmd/ccgg/trends_ch4/.

Environment and Climate Change Canada (ECCC), 2020. National Inventory Report 1990–2018: Greenhouse Gas Sources and Sinks in Canada. Retrieved from: http://www.publications.gc.ca/site/eng/9.506002/publication.html

Environment and Climate Change Canada (ECCC), 2018. Technical Backgrounder: Federal methane regulations for the upstream oil and gas sector. Retrieved from: https://www.canada.ca/en/environment-climate-change/news/2018/04/federal-methane- regulations-for-the-upstream-oil-and-gas-sector.html

Feitz, A., Schroder, I., Phillips, F., Coates, T., Neghandhi, K., Day, S., Luhar, A., Bhatia, S., Edwards, G., Hrabar, S., Hernandez, E., Wood, B., Naylor, T., Kennedy, M., Hamilton, M., Malos, J., Kochanek, M., Reid, P., Wilson, J., Deutscher, N., Zegelin, S., Vincent, R., White, S., Ong, C., George, S., Maas, P., Towner, S., Wokker, N., Griffith, D., 2018. The Ginninderra CH_4 and CO_2 release experiment: An evaluation of gas detection and quantification techniques. *International Journal of Greenhouse Gas Control* 70, 202-224. DOI: https://doi.org/10.1016/j.ijggc.2017.11.018

Greenpath Energy Ltd., 2016. Alberta Fugitive and Vented Emissions Inventory Study. Retrieved from: http://www.greenpathenergy.com/wp-content/uploads/2017/03/GreenPath- AER-Field-Survey-Results_March8_Final_JG.pdf

Johnson, M. R., Coderre, A. R., 2012. Opportunities for CO_2 equivalent emissions reductions via flare and vent mitigation: A case study for Alberta, Canada. *International Journal of Greenhouse Gas Control* 8, 121–131. DOI: https://doi.org/10.1016/j.ijggc.2012.02.004

Johnson, M. R., and Tyner, D. R., 2020. A case study in competing methane regulations:

Will Canada's and Alberta's contrasting regulations achieve equivalent reductions? *Elementa Science of the Anthropocene*, 8: 7. DOI: https://doi.org/10.1525/elementa.403

Johnson, M., Tyner, D., Conley, S., Schwietzke, S. and Zavala-Araiza, D. 2017. Comparisons of Airborne Measurements and Inventory Estimates of Methane Emissions in the Alberta Upstream Oil and Gas Sector. *Environmental Science and Technology* 51(21): 13008–13017. DOI: https://doi.org/10.1021/acs.est.7b03525

Masnadi, M. S., El-Houjeiri, H. M., Schunack, D., Li, Y., Englander, J. G., Badahdah, A., Monfort, J. C., Anderson, J. E., Wallington, T. J., Bergerson, J. A., Gordon, D., Koomey, J., Przesmitzki, S., Azevedo, I. L., Bi, X. T., Duffy, J. E., Heath, G. A., Keoleian, G. A., McGlade, C., Meehan, D. N., Yeh, S., FeYou, F., Wang, M., Brandt, A. R., 2018. Global carbon intensity of crude oil production, *Science, 361 (6405), 851-853.* DOI: 10.1126/science.aar6859

Myhre, G., Shindell, D., Breon, F. M., Collins, W., Fuglestvedt, J., Huang, J., Koch, D., Lamarque, J. F., Lee, D., Mendoza, B., Nakajima, T., Robock, A., Stephens, G., Takemura, T., Zhang, H., 2013. Anthropogenic and Natural Radiative Forcing, Chapter in Climate Change 2013: The Physical Science Basis. Contribution of Working Group I to the Fifth Assessment Report of the Intergovernmental Panel on Climate Change. Retrieved from: http://www.climatechange2013.org/images/report/WG1AR5_Chapter08_FINAL.pdf

O'Connell, E., Risk, D., Atherton, E., Bourlon, E., Fougère, C., Baillie, J., Lowry, D., Johnson, J., 2019. Methane emissions from contrasting production regions within Alberta, Canada: Implications under incoming federal methane regulations. *Elementa Science of the Anthropocene,* 7. DOI: 10.1525/elementa.341.

Petrinex, Alberta Public Data. Public data archives. Retrieved from: https://www.petrinex.ca/PD/Pages/APD.aspx

Province of British Columbia, 2018. Oil and Gas Activities Act. Retrieved from: https://www.bclaws.gov.bc.ca/civix/document/id/regulationbulletin/regulationbulletin/r0286_2018

Ravikumar, A. P., Roda-Stuart, D., Liu, R., Bradley, A., Bergerson, J., Nie, Y., Zhang, S., Bi, X., Brandt, A. R., 2020. Repeated leak detection and repair surveys reduce methane emissions over a scale of years. *Environmental Research Letters* 15, 034029. DOI: https://iopscience.iop.org/article/10.1088/1748-9326/ab6ae1

Rogelj, J., Shindell, D., Jiang, K., Fifita, S., Forster, P., Ginzburg, V., Handa, C.,

Kheshgi, H., Kobayashi, S., Kriegler, E., Mundaca, L., Séférian, R., Vilariño, M. V., 2018. Mitigation Pathways Compatible with 1.5°C in the Context of Sustainable Development. Retrieved from: https://www.ipcc.ch/sr15/chapter/chapter-2/

Roscioli, J. R., Herndon, S. C., Yacovitch, T. I., Knighton, W. B., Zavala-Araiza, D., Johnson, M. R., and Tyner, D. R., 2018. Characterization of methane emissions from five cold heavy oil production with sands (CHOPS) facilities. *Journal of Air and Waste Management Association* 68 (7): 671−684. DOI: https://doi.org/10.1080/10962247.2018.1436096

Saskatchewan Ministry of Economy, 2019. The Oil and Gas Emissions Management Regulations: Chapter O-2 Reg 7. Retrieved from: https://www.canlii.org/en/sk/laws/regu/rrs-c-o-2-reg-7/latest/rrs-c-o-2-reg-7.html

Tyner, D. R., and Johnson, M. R., 2018. A Techno-Economic Analysis of Methane Mitigation Potential from Reported Venting at Oil Production Sites in Alberta, *Environmental Science and Technology* 52, 21, 12877-12885. DOI: https://doi.org/10.1021/acs.est.8b01345

Zavala-Araiza, D., Lyon, D. R., Alvarez, R. A., Davis, K. J., Harriss, R., Herndon, S. C., Karion, A., Kort, E. A., Lamb, B. K., Lan, X., Marchese, A. J., Pacala, S. W., Robinson, A. L., Shepson, P. B., Sweeney, C., Talbot, R., Townsend-Small, A., Yacovitch, T. I., Zimmerle, D. J., Hamburg, S. P., 2015. Reconciling divergent estimates of oil and gas methane emissions. *Proceedings of the National Academy of Sciences*, 112(51): 15597–15602. DOI: https:// doi.org/10.1073/pnas.1522126112

Zavala-Araiza, D., Alvarez, R. A., Lyon, D. R., Allen, D. T., Marchese, A. J., Zimmerle, D. J., Hamburg, S. P., 2017. Super-emitters in natural gas infrastructure are caused by abnormal process conditions. *Nature Communications* 8, 14012. DOI: 10.1038/ncomms14012

Zavala-Araiza, D., Herndon, S. C., Roscioli, J. R., Yacovitch, T. I., Johnson, M. R., Tyner, D. R., Omara, M., Knighton, B., 2018. Methane emissions from oil and gas production sites in Alberta, Canada. *Elementa Science of the Anthropocene* 6(1): 27. DOI: https://doi.org/10.1525/ elementa.284

3. A community data resource of recent methane emission measurements from upstream oil and gas sites in Canada

3.1 Preface

A version of this chapter is currently under review at *Atmospheric Environment: X*

(Elsevier). It has already gone through one round of review at the same journal (revised

version was submitted in December 2021). I am the primary author, and co-authors are Martin Lavoie and David Risk. I led the writing and analysis included in this chapter, and all authors, revised, edited, and provided valuable feedback that was used to refine the published paper.

3.2 Abstract

In response to the need for measurements to better understand methane emission levels at Canadian oil and gas sites, we pooled 9540 site-level methane (CH_4) measurements, from 13 oil and gas producing regions, across three provinces in western Canada. Measurements were contributed from academia, industry, regulators, and non-governmental organizations, which we made available in a public data repository for those working on methane measurement and mitigation. Our analysis of the aggregated measurements revealed that all production regions are characterized by a heavy-tailed distribution, where more than 50% of measured emissions originate from 10% of measured sites. This trend has been observed elsewhere in Canada and in the United States and suggests that, for many producers, a focus on mitigation at higher-emitting sites may provide an efficient pathway to meet governmental reduction targets. We also compared average site-level estimates acquired using five different measurement methodologies (one "top-down" and four "bottom-up") and found no significant differences, though more research is needed to confirm this result. This study emphasizes the value of a public data archive for oil and gas methane emission measurements, as this resource can improve the efficiency and cost-effectiveness of oil and gas methane reductions.

3.3 Introduction

Oil and gas (O&G) production is one of the largest sources of methane (CH_4) globally, which needs to be reduced to meet climate goals outlined in the Paris Agreement (Intergovernmental Panel on Climate Change 2018). CH_4 emissions released during the production, transmission, and distribution of O&G account for nearly half (43%) of the Canada's total CH_4 emissions (Environment and Climate Change Canada 2020). Also, since CH_4 is the primary constituent of natural gas, conserving O&G related CH_4 emissions has both economic and environmental benefits. In 2020, new regulations were introduced for the Canadian O&G industry with the aim of reducing CH_4 emissions from upstream sources by 40-45% below 2012 levels by 2025 (ECCC 2020).

In situ measurements of CH_4 emissions play an important role in mitigation efforts. Historically, measurements of O&G CH_4 emissions followed the United States Environmental Protection Agency's (US EPA) Method 21 regulatory guideline, in which handheld concentration analyzers (e.g. flame ionization, catalytic oxidation) are used to detect CH_4 from individual components (EPA 2017, Fox et al. 2019). Optical gas imaging (OGI) cameras, which offer visual CH_4 emission detection using infrared imaging, were approved as an alternative to Method 21 in 2008 (Fox et al. 2019). Since they are time-tested and have been in North American regulation for over a decade, OGI cameras coupled with Hi-Flow samplers (for quantification) are still consistently used for O&G CH_4 measurement in Canada (e.g. CapOp Energy 2019, Clearstone Engineering 2019).

However, in the past five years there has been a growing number of measurements collected using so-called "alternative techniques" that couple high-precision CH_4 sensors with mobile vessels such as vehicles, aircrafts, and satellites (Atherton et al. 2017, Johnson et al. 2017, Sheng et al. 2017, Zavala-Araiza et al. 2018). These alternatives often have significant spatial coverage, which is a noteworthy advantage over the time and labor-intensive OGI and US EPA's Method 21 techniques.

Regardless of the methodology, CH_4 measurements of all types are valuable and can provide information on emission patterns and sources, that in turn guide CH_4 emission reduction efforts. Considering the short timeframe we have to meet our CH_4 reduction goals, aggregating measurements to produce an extensive, spatially resolved analysis has significant value. Similar synthesis work has been done in the United States (US) (Brandt et al. 2016, Littlefield et al. 2017, Omara et al. 2018), which have revealed important insights that cannot be discovered through small scale studies in specific geographic regions. In aggregation studies, one problem is that differences amongst the methodologies such as sensor limits of detection, spatial scales of measurement, measurement units, and descriptive vocabulary used to characterize the infrastructure being measured, can present challenges for meta-analysis. To our knowledge, no one has undertaken a large-scale synthesis of Canadian O&G CH_4 emissions data, despite the growing need for greater data accessibility and transparency.

In this study, we aggregated site-level CH_4 measurements from several sources, covering 13 O&G producing regions across three provinces in western Canada (British

Columbia, Alberta, Saskatchewan). These regions cover over 90% of the country's total O&G production. In total, we obtained measurements from 9540 O&G sites that were collected between 2009 and 2020. Measurements were obtained from academia, industry, regulators, and non-governmental organizations, and were aggregated into an open data repository that ties emissions to infrastructure and/or component type, region, and measurement methodology. The primary purpose of this work was to build an easy to use, publicly accessible database of existing CH_4 emission measurements for use by stakeholders as part of CH_4 reduction efforts. The second purpose of our initiative was to use aggregated measurements to examine emission levels and patterns across Canada, with particular emphasis on examining the distribution profile of emissions within different producing regions.

3.4 Methods

3.4.1 Data aggregation

Methane measurements included in this study came from many different groups, who collected measurements for different reasons (e.g. research, regulatory compliance, routine leak surveys), using different measurement tools (e.g. laser spectrometers coupled with a mobile platform, optical gas imaging, handheld devices), at various spatial scales (0.01 to 600 km^2). A description of each measurement methodology is below, and we encourage readers to consult original research papers (listed in Table 3.1) for additional methodological information and related uncertainties. Fox et al. (2019) also provides a comprehensive review on the suite of CH_4 measurement methodologies used here. Due to

the nature of the measurement techniques, all measurements included in our analysis were collected during short time intervals, therefore these data do not take temporal variability of site-level emissions into account, which can occur during changes in operations, as noted in other studies such as Lavoie et al. (2017).

In total, we aggregated measurements from ten individual datasets, covering 13 regions in western Canada (Table 3.1, Figure 3.1). Roughly 71% of the acquired site-level measurements originate from recently published measurement studies (Baillie et al. 2019, Johnson et al. 2017, MacKay et al. 2019, MacKay et al. 2021, O'Connell et al. 2019, Ravikumar et al. 2020, Roscioli et al. 2018, Zavala-Araiza et al. 2018), whereas the other 29% were from non-academic partners or unpublished studies.

Measurement data were often in different formats (spreadsheets, pdf, etc.), and had significant inconsistencies in terms of infrastructure names, measurement units, and timestamps. To address these inconsistencies, we used a semi-automated process to unify and anonymize the measurements into a single, consistently formatted dataset, so all measurements could be readily analyzed and compared. First, each dataset went through a manual review to ensure the minimum required variables were included, which were a unique site identifier, CH_4 emission rate (and units), measurement method, and geolocation (exact or approximate). Additional information (e.g. site/component type, measurement date) was included if provided. Second, measurements were aggregated or de-aggregated to site-level since many measurements were made at that scale and because it was straightforward to aggregate component-level measurements (or to de-aggregate

regional measurements) to the site scale. Next, all site-level emission rates were converted into common units of cubic metres per day (m^3 day^{-1} at 101.325 kPa and 15°C) because a majority of contributed measurements were already recorded in this Canadian-standard unit. Finally, all measurements were combined into a single anonymized dataset, and all sensitive information was removed. Discussion on assumptions and limitations with respect to aggregated measurements can be found in Section 3.4.5.

Table 3.1: Summary of different measurement techniques used to collect CH_4 measurements that are included in this study. Individual sites that were sampled on different dates (i.e. months, years) were considered as independent (i.e. unique) measurements.

Dataset ID	Measurement Method	Number of sites measured	Approx. distance from source (m)	Approx. detection limits (m^3 CH_4 day^{-1}) [a]	Source
1	Vehicle-based transect (Gaussian dispersion)	6651	50-500	1-25	MacKay et al. 2021 [b]
2	Optical gas imaging/Hi-Flow	192	<10	<1	Non-academic partner
3	Optical gas imaging/Hi-Flow	21	<10	<1	Non-academic partner
4	Optical gas imaging/Hi-Flow	1342	<10	<1	Non-academic partner
5	Vehicle-based transect (tracer flux and Gaussian dispersion)	60	>20	1-25	Zavala-Araiza et al. 2018

6	Aircraft (mass balance)	2[c]	150-1000	>50	Johnson et al. 2017
7	Vehicle-based tracer flux	5	>20	1-25	Roscioli et al. 2018
8	Optical gas imaging/Hi-Flow	44	<10	<1	Ravikumar et al. 2020
9	Vehicle-based transect (Gaussian dispersion)	3	10-25	1-25	MacKay et al. 2019
10	Vehicle-based transect (Gaussian dispersion)	1220	50-500	1-25	Vogt et al. *(manuscript under review)*

[a] Detection limits can vary significantly depending on several factors (e.g. measurement distance, sensor, meteorology); these are estimates based on published literature

[b] Includes data from Baillie et al. (2019), O'Connell et al. (2019), and Lavoie et al. (2021)

[c] Site-level averages are based on two regional-scale measurements.

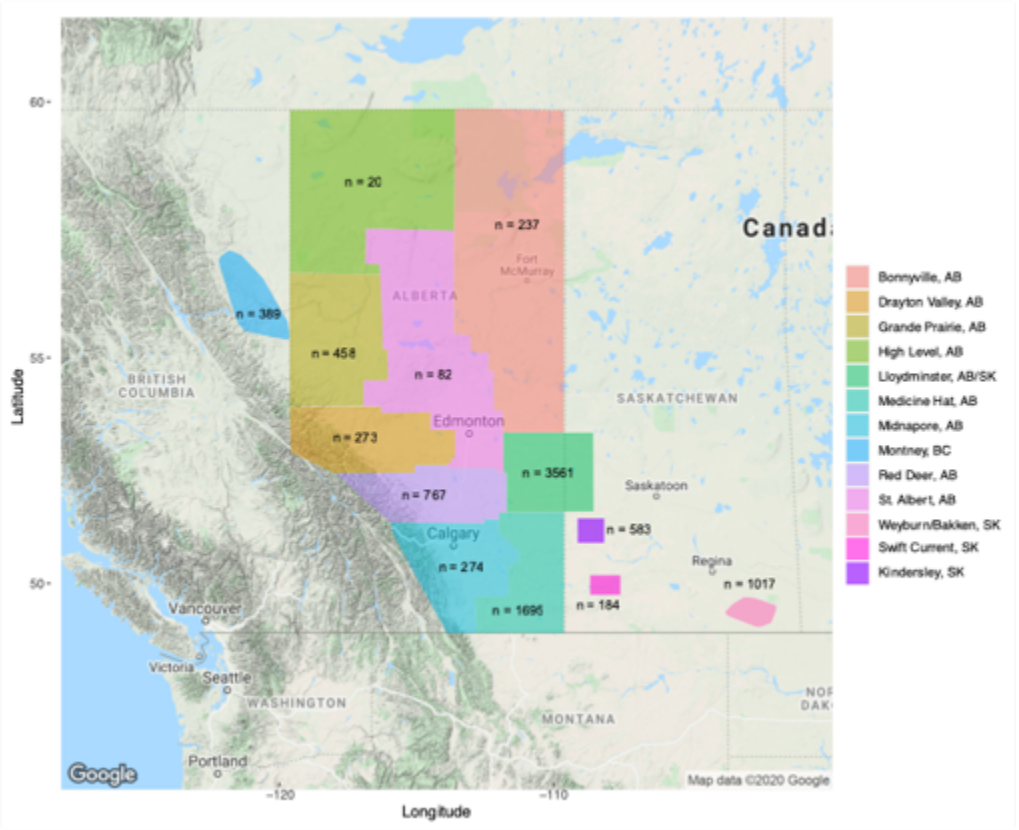

Figure 3.1. Map of 13 regions from which measurements were collected in British Columbia, Alberta, and Saskatchewan. n values correspond to the number of unique site-level measurements for each region. Note that this map shows general area boundaries only, and exact locations of measured sites within each area are not shown.

3.4.2 Measurement methodologies

3.4.2.1 Optical Gas Imaging (OGI) and Hi-Flow

OGI cameras are the current regulatory standard for O&G CH_4 emissions monitoring. These measurements require site access and adequate (i.e. unobstructed) line of sight between the camera and source of interest. Emissions are identified visually using the

OGI camera, and then subsequently quantified using a Hi-Flow sampler (Greenpath Energy 2017, Ravikumar et al. 2020). In some cases, direct quantification a via Hi-Flow sampler is not possible (due to potential safety or access issues), and actual emission rates are estimated using expert judgement, emission factors from literature, and/or equipment manufacturer data (discussed further in Section 3.4.5) (Greenpath Energy 2017, Ravikumar et al. 2020). Depending on the quantification method, uncertainties range from 5% (Hi-Flow sampler) to orders of magnitude (estimation) (Greenpath Energy 2017). OGI/Hi Flow measurements are collected at the component-level (e.g. thief hatch, valve), thus site-level emissions are calculated by summing the emission rates from all components using a common site identifier. Approximately 16% of all site-level measurements included in this analysis were collected using this method.

3.4.2.2 Vehicle-based transects coupled with inverse Gaussian dispersion modelling

Many recent studies (in Canada and the US) have been using vehicle-based measurement systems coupled with inverse Gaussian dispersion modelling to measure O&G CH_4, which has gained popularity due to its measurement efficiency. For instance, authors of some studies have been able to measure 100 sites per day using this method (Baillie et al. 2019, O'Connell et al. 2019), which is >10 times more sites than what is covered during a traditional OGI survey. The method typically involves a vehicle equipped with high-precision analyzers that measure gas concentrations, geolocation, and meteorological data continuously while driving. Transects of CH_4 plumes are measured by driving downwind of O&G sites, which are then used to compute a site-level emission rate using inverse Gaussian dispersion principles. Reported uncertainties for this method vary significantly,

ranging from 50-350% (Caulton et al. 2017, O'Connell et al. 2019). Roughly 83% of site-level measurements included in this study were collected using this method.

3.4.2.3 Vehicle-based tracer flux

The tracer flux method involves releasing one or more tracer gases (e.g. N_2O) of known flow rate in close proximity to the source of interest (i.e. O&G site). This method has been used to measure CH_4 emissions from industrial facilities for over 20 years (Roscioli et al. 2018). Gas concentrations (of CH_4 and the tracer gases), and meteorological data are measured continuously at some distance downwind, to capture downwind plume concentration profiles. Given that there is a direct linear relationship between downwind concentrations and emission rates, the site-level CH_4 emission rate is calculated by comparing the ratios of downwind concentration enhancements and the known release rate of the tracer gas (Roscioli et al. 2018, Zavala-Araiza et al. 2018). Measurement uncertainties for the tracer flux method range from 20-50% (Caulton et al. 2017, Omara et al. 2018). Less than 1% of data in this study was collected using this method (30 site-level measurements).

3.4.2.4 Aircraft mass balance

Aircraft-based measurements are another useful methodology for measuring CH_4 emissions. This method involves flying multiple transects upwind and downwind of the source of interest using an aircraft equipped with atmospheric gas analyzers and other meteorological equipment. Emissions are estimated for a defined area using the in-situ measurements and the well-established mass balance method. Aircraft mass balance

measurements typically have coarse resolution and are unable to estimate emission rates at the site-level. The aircraft study included in this analysis (the only one conducted in Canada outside of the oilsands region) estimated two regional-level emission rates for Lloydminster and Red Deer. Measurement uncertainties (95% confidence intervals) were ±24% and ±36% for Lloydminster and Red Deer, respectively (Johnson et al. 2017). For our site-level analysis, we used the same approach described in O'Connell et al. (2019), where the regional emission rates were divided by the total number of sites (n=4394 for Lloydminster and n=4166 for Red Deer) within the defined area to compute a site-level average. Site counts for each region were obtained using IHS infrastructure databases (IHS Markit) and the geographic limits reported in the original study (Johnson et al. 2017).

3.4.3 Methodological comparison

We compared site-level CH_4 emission rates measured using different techniques to assess whether there were significant differences in measured emissions. For this comparison, we looked at site-level measurements specifically in the Red Deer region, as this was the only region that included measurements from all methodologies. Since site overlap was not perfect in the measurement dataset, we had to assume for our comparison that the sites with similar infrastructure and production characteristics in the region were emitting at similar rates. We tested for homogeneity of variances across measurement methods (for those with sample sizes greater than 1) using Levene's test, and Welch's analysis of variance (ANOVA) test was used to determine whether there is a statistical difference between population means of the different measurement methods.

In this study, vehicle-based Gaussian dispersion measurements collected in the Red Deer region came from two different contributors, and are further denoted as method A (Zavala-Araiza et al. 2018) or B (MacKay et al. 2021) in the methodological comparison below. We chose to distinguish between the two because we determined that the data processing and sampling methods of each dataset were different enough to be considered separate measurement techniques. For instance, Vehicle-based Gaussian Dispersion A involved single, slow transects of sites known to be emitting CH_4, while vehicle-based Gaussian Dispersion B involved multiple downwind transects of sites at different times, and a "detection threshold", where the site was only considered to be emitting if CH_4 was detected on >50% of downwind transects. The processing of raw data and Gaussian model parameter estimations and assumptions (e.g. source height) also differed across the two methods, further warranting a distinction between the two.

3.4.4 Data accessibility and user information

The final anonymized dataset, consisting of 22,748 individual CH_4 measurements from 9540 unique sites, was deposited in St. Francis Xavier University's Dataverse repository (https://doi.org/10.5683/SP2/I0436P), where it can be downloaded for free. The dataset exists in csv format, with a single row for every unique measurement, along with several columns with important information on each measurement, including the dataset ID number, the site and/or component type, the number of measured components per site, the measurement method, the measurement date, and the general area where the site is located. Both site-level and component-level (when available) CH_4 emission rates are

included (in m^3 day^{-1} and SCFM units). A metadata file is also published alongside the dataset, which includes other relevant information such as links to where published data came from (also shown in Table 3.1), the original measurement units used in each dataset, etc. We encourage users to download both data files when using these measurements for future analysis and interpretation. Additionally, anyone who is interested in contributing measurements to this resource may do so by contacting the corresponding author, who will continue to update the data archive on a regular basis.

When using this dataset for future analysis, we recommend that users should have a basic understanding of O&G infrastructure terminology, and an understanding of the measurement methodologies used to collect data. Measurement methodology information is described above, and more details are available in other recent publications such as Fox et al. (2019) and the original studies listed in Table 3.1. Information on O&G infrastructure (site types, component types, production styles) is widely available online (e.g. CEPA 2017, CapOp Energy 2019, Clearstone Engineering 2019).

The format of the dataset allows users to easily conduct a meta-analysis (analysis of all data) or to partition the dataset based on their own personal needs or interests. For example, users can also subset data based on CH_4 emission thresholds, site type, component type, measurement methodology, measurement year, dataset source (published vs unpublished), as well as combinations of any of these variables.

3.4.5 Data assumptions and limitations

There are several limitations that were discovered throughout this study that need to be mentioned. Future work should focus on addressing these limitations, as they can have significant impact on the overall quality of this type of analysis. First, the lack of consistency related to data records was substantial, especially for infrastructure/site descriptions. For example, Gas well, Gas single, Gas single well battery, and Gas battery were all names used in datasets, and it is unclear whether all of these are essentially the same type of site, or if they are different (e.g. do they consist of one well and one battery, or just one well, etc.). Without additional infrastructural information, it becomes difficult to establish accurate common site names that would be useful for analyzing emissions as a function of infrastructure characteristics. For these reasons, we did not put a large focus on infrastructure characteristics during our analysis. Fortunately, it is likely that this issue will be improved as new regulations require more strict, comprehensive emissions reporting.

The second limitation is specific to the measurement methodology comparison. Due to the limited locational data available for acquired data, it was impossible to determine if there were specific sites measured by each of the different measurement methodologies. Consequently, we assumed that the sites measured by each methodology in Red Deer (the only region with measurements taken using all methodologies) emit similar amounts of CH_4, given that they all have similar infrastructure and production characteristics. A more robust methodological comparison should include measurements collected at the exact same locations at relatively the same time (since emissions can vary

temporally). Nonetheless, the fact that there was regional overlap for five different methodologies and was worth examining, and we believe our results offer valuable insights on how these measurement technologies stack up to one another in a real-world setting.

The third limitation is specific to OGI data. Since OGI cameras do not quantify leaks (they are simply a visual tool), actual emission rates are usually determined via two methods: using a Hi-Flow sampler (e.g. Bacharach), or visual estimation/expert judgement. For the majority of OGI data that was obtained for this study, the quantification method for individual measurements was not specified, which is an important detail since visual estimation has much greater uncertainty than Hi-Flow measurements. In some cases, the emission rate values can be used to differentiate between estimated and measured OGI data, as Hi-Flow samplers have a maximum measurement rate of 10 cubic feet per minute (CFM) (Greenpath Energy 2017). So, one could assume that rates greater than 10 CFM were visually estimated, whereas ones less than 10 CFM were measured via Hi-Flow sampler. In our aggregated dataset, there were 23 component-level measurements, from 16 sites that exceeded the 10 CFM threshold. We assessed whether these values affected the distribution shape of the data and found that omitting these values had no significant impact on overall results. Nonetheless, this differentiator is not a definite confirmation of one method over the other and should be used with caution (e.g. some emission sources are inaccessible/unsafe for Hi-Flow measurements, and are always estimated regardless of the rate), which is why it is important to assume that all OGI data in this dataset has high uncertainty.

3.5 Results and Discussion

3.5.1 Site-level statistics

The 9540 site-level emission rate measurements spanned 13 producing regions in Alberta, British Columbia, and Saskatchewan (Figure 3.1, Table 3.2). Most measurements were collected in Alberta (the largest O&G producing province), and measurements were especially common in the Lloydminster region (n=3561) which sits on the border of Alberta and Saskatchewan. The Red Deer region in Alberta was the only region with measurements collected using all five measurement methodologies.

Table 3.2 shows statistics for site-level emission rates for each region included in this study. Average site-level emissions ranged from 6.9 m^3 day^{-1} in Weyburn/Bakken, SK, to 103 m^3 day^{-1} in Red Deer, AB (Table 3.2). The overall site-level average was 58.7 m^3 day^{-1}. In general, site-level emission measurements from previously published studies of individual regions in Canada show good agreement with our aggregated results (Baillie et al. 2019, MacKay et al. 2021, O'Connell et al. 2019, Ravikumar et al. 2020, Roscioli et al. 2018, Zavala-Araiza et al. 2018). Our regional site-level averages are also comparable to those reported in US studies, such as Bell et al. 2017, Caulton et al. 2019, and Robertson et al. 2020.

Table 3.2: Summary statistics of site-level CH_4 emissions included in this study, broken down by region.

Region	No. of site-level measure ments	Incidence (fraction of sites emitting)	Mean emission rate (m^3 day^{-1}/site)	Max. emission rate (m^3 day^{-1}/site)	Standard Deviation
Bonnyville, AB	237	93%	58.9	3780.8	298.5
Drayton Valley, AB	273	51%	47.9	1177.2	131.3
Grande Prairie, AB	458	66%	82.7	3208.2	264.6
High Level, AB	20	90%	83.8	486.1	145.7
Lloydminster, AB/SK	3561	33%	86.8	6758.6	407.7
Medicine Hat, AB	1695	18%	14.1	3186.6	102.7
Midnapore, AB	274	99%	38.6	397.2	70.2
Red Deer, AB	767	41%	103.0	8454.6	558.1
Weyburn/Bakk en, SK	1017	10%	6.9	1298.5	53.0
St. Albert, AB	82	51%	92.4	2344.2	309.2
Montney, BC	389	50%	55.8	769.8	115.2
Kindersley, SK	583	32%	54.2	4719.4	289.2
Swift Current, SK	184	4%	15.2	1700.1	140.7

3.5.2 Methodological comparison

Figure 3.2 shows boxplots of site-level emission rates from Red Deer, with individual boxplots representing unique measurement methodologies. Note that there are two distributions of vehicle-based (Gaussian dispersion) measurements (denoted as A and B in Figure 3.2), because for each the data processing and sampling methods were notably different. As stated in the methods, OGI measurements (component-level) were summed

to site-level value, and aircraft measurements were de-aggregated to a site-level average. Looking at Figure 3.2, we can see that all boxplots overlap which suggests there is no statistical significance that can be discerned amongst the large variability. However, both vehicle-based (Gaussian dispersion) techniques (A and B) as well as OGI measurements result in higher average site-level emissions than other techniques, with mean emission rates of 283 m^3 day^{-1} (A), 209 m^3 day^{-1} (B) and 294 m^3 day^{-1} respectively. OGI measurements are higher on average presumably because of measurement proximity (<10 m from the source), and the ability to enumerate all emission sources within each site exhaustively. For other measurement methodologies, measurements are taken at distance (ranging from one meter to hundreds, depending on the technique) and it is possible that quantification is limited by obstructions in the flow path, or because emissions are below the minimum detection limits.

Using the data shown in Figure 3.2, we tested whether the average site-level emissions measured by each methodology were statistically different. Aircraft data were excluded from the statistical tests due to lack of unique observations, although it is worth mentioning that the estimated site-level emission rate from the aircraft data for Red Deer (26 ± 9.3 m^3 day^{-1}) falls squarely within the other distributions shown in Figure 3.2. After omitting the aircraft data, we tested for homogeneity of variances across measurement methods, which were determined to be unequal (using Levene's test; $p<0.05$). Since variances across methods were not equal, we used Welch's ANOVA test to determine whether there is a statistical difference between population means of the different measurement methods. According to the results, average site-level emission rates

measured by each method are not statistically different (p-value = 0.09). That said, it is important to note that our sample sizes for these comparisons are relatively small and are lacking perfect (site to site) overlap, and a more robust methodological comparison is required (which was beyond the scope of this study) to confirm this finding. Nonetheless, since we did have five different measurement techniques included in our aggregated data, we believe this comparison was worth investigating.

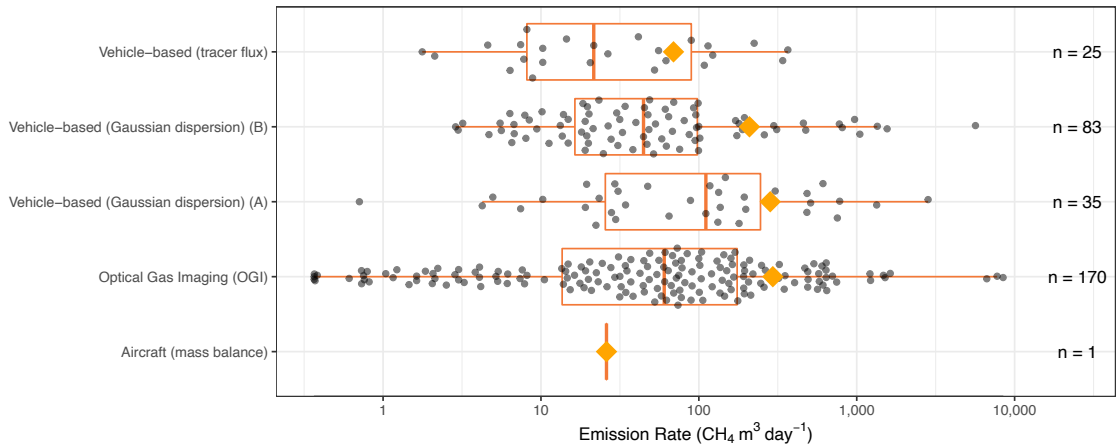

Figure 3.2. Comparison of site-level emission rates (logarithmic scale) across different measurement techniques. Vehicle-based Gaussian dispersion measurements came from two different contributors, and are further denoted as method A or B, as the data processing and sampling methods were different enough to be considered separate measurement techniques. Each point represents an individual site-level emission rate. Only measurements with a measured rate > 0 from the Red Deer region were included in the comparison, to ensure site and production characteristics were similar across measurements. The middle line in each box is the subpopulation median, and the orange diamond is the subpopulation

mean. The number of unique site-level measurements (n) collected using each method are listed on the right.

3.5.2 Heavy-tail distributions

Measurements revealed that in all regions, a small portion of infrastructure was responsible for the majority of emissions (Figure 3.3). This "heavy-tail" trend has been observed in individual Canadian measurement studies included in this analysis (Baillie et al. 2019, O'Connell et al. 2019, Zavala-Araiza et al. 2018), and similar trends have been well-documented across the US O&G industry (Alvarez et al. 2018, Brandt et al. 2016, Caulton et al. 2019, Omara et al. 2018, Robertson et al. 2020, Zavala-Araiza et al. 2015). Notably, Brandt et al. (2016) found heavy-tailed distributions in all 18 datasets used in their US country-wide analysis.

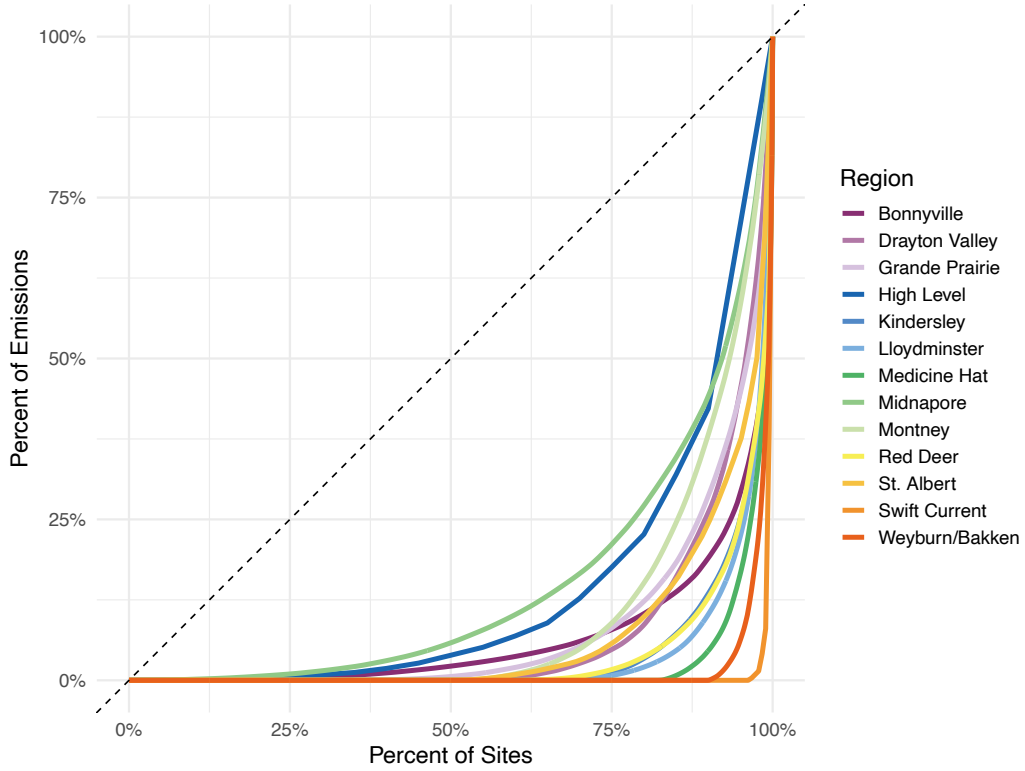

Figure 3.3. Lorenz curve for all regions with contributed CH_4 measurements, which shows the percent of emissions as a function of percent of sites. For all regions, >50% of measured emissions are from 10% measured sites.

Measured emissions in certain regions showed a more severe skewness than others, which is best shown in Figure 3.4. Figure 3.4 shows the cumulative percent of total measured emissions that are contributed by the top 2, 5, and 10% of measured sites for each region. Here we can see Swift Current (SK), Weyburn/Bakken (SK), Medicine Hat (AB) regions are the most skewed, with the top 5% of sites contributing to 100%, 94%, 83% of total emissions, respectively (Figure 3.4). Recent US-based measurement studies show similar skewness, often referred to as following the 5/50 rule, where at least 50% of emissions come from the top 5% of emitting sites. For example, Caulton et al.

(2019) found that 77% of emissions are from the top 10% of sites in the Marcellus shale (Penns.), and Zavala-Araiza et al. (2015) found that 50% of emissions originated from the top 2% of sites in the Barnett Shale region. Similarly, a synthesis study by Omara et al. (2018) reported that 57% of emissions are from the top 5% of sites. There were three regions (High Level, Montney, and Midnapore) in our study that did not align with the 5/50 rule, although emissions were still skewed, with the top 10% of emitting sites contributing over 50% of total emissions.

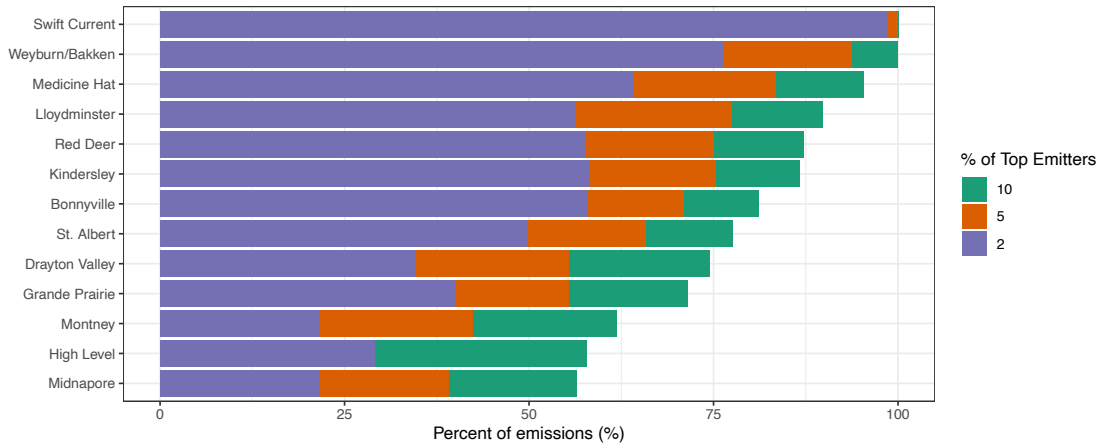

Figure 3.4. The cumulative proportion of emissions contributed by the top (i.e. highest emitting) 2, 5, and 10% of measured sites within each region.

We also looked specifically at the different site and component types are in the top 2% (i.e. CH_4 measurements that exceed the 98th percentile of all measured emission rates) to determine whether certain component and/or site types were responsible for the majority of large emissions. We found that out of the top 2% of component types (n=269), open-ended lines were the most common, representing 40% of the top emitting components (Figure 3.5). An open-ended line is a valve (e.g. compressor-unit blowdown,

supply-gas, instrument block, drain valves) that has a pipe with process fluid on one side, and is open to the atmosphere on the other (CEPA 2016, CapOp Energy 2019, Clearstone Engineering 2019). Open-ended lines are common across several equipment types, including tanks and well heads (Clearstone Engineering 2019). A BC-based measurement study similarly found open-ended lines to be a major contributor to overall emissions (CapOp Energy 2019).

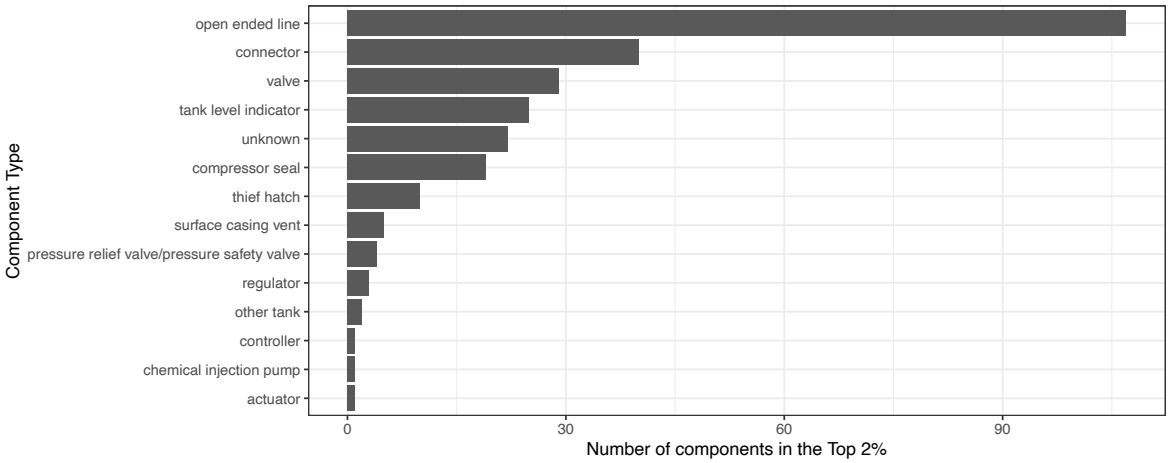

Figure 3.5. Counts of different component types in the top 2% (98th percentile) of all measured components.

For the top 2% of site types (n=191), we found that oil single well batteries were the most common, making up 22% of the top emitting sites (Figure 3.6). Other studies have also found that tank batteries are often characterized by large emissions (Tyner & Johnson 2021). Although our measurements show that there are some site and component types contributing more to the heavy-tail, it is also noting that there were several different

site and component types in the top 2%, showing that abnormally high CH_4 emissions can arise from several different site and component types.

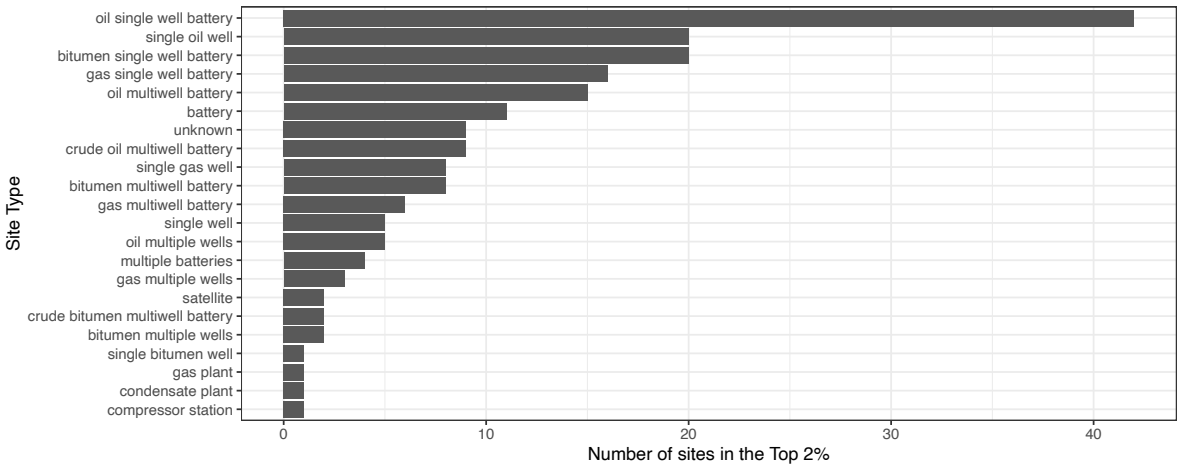

Figure 3.6. Counts of different site types in the top 2% (98th percentile of all measured sites). Oil single well battery sites make up 22% of all sites in the top 2% (n=42).

The prevalence of the heavy-tail distribution across all regions has important implications. First, it is a policy-relevant finding, as it means that the majority of emissions can be reduced by taking mitigation action at only a small number of sites. Although this presents a low-hanging fruit with respect to reduction efforts, locating these rare large emitters remains a significant challenge. To date, scholars and industry experts in this domain have generally been unsuccessful in predicting the cause and locations of these emitters. Consequently, the best way to locate these large emitters are via large-scale measurement campaigns that have significant spatial coverage (>100 sites/day). Therefore, it is important that regulations allow (and perhaps promote) the use of

alternative measurement technologies suitable for rapid screening of sites (e.g. trucks, drones, and aircrafts) in monitoring programs, rather than OGI surveys only.

Second, this trend poses implications on measurement technology innovation and economics: if a heavy-tail distribution is present, then fast, spatially extensive measurement (sometimes referred to as "screening" or "alternative") technologies are not only efficient, but are also likely the most cost-effective approach to reductions. Indeed, cost-benefit studies such as Kemp & Ravikumar (2021) and Fox et al. (2021) found that for highly skewed emissions distributions, deploying alternative technologies can result in lower costs and, in some cases, greater reductions. Although alternative measurement technologies are unable to pinpoint emission sources (i.e. to the component-level), when they are used as a first step in monitoring programs, they can screen hundreds of sites per day, and are able to identify the general locations of large emitters, from which the exact source can then be pinpointed in follow-up inspections using handheld instruments such as OGI. This tiered approach eliminates the need to conduct "blind" OGI surveys, which are not only slow (~6 sites/day), but can cost up to $600 CAD per site (Kemp & Ravikumar 2021). If mitigation at a few high-emitting sites can bring total emissions down by over 50%, its logical to put investments toward technologies that are best suited to quickly find them, rather than spending large sums of money on traditional OGI surveys.

3.6 Summary

In conclusion, recent CH_4 emissions measurements from O&G facilities yield important insights for emissions patterns across the Canadian O&G sector. Our analysis revealed that average site-level emissions vary by production region, but a heavy-tail distribution is prevalent across the entire onshore Canadian O&G industry. Infrequent large emitters represent a low hanging fruit for reduction efforts and should thus be a primary focus of regulatory monitoring programs, as well as future technology development.

We hope this work accelerates efforts related to data sharing and transparency within the Canadian O&G community. Transparency with respect to emissions and other environmental impacts is becoming a requirement for O&G sector in today's world, yet most producing countries either lack data, or do not effectively share data. Taxpayers in particular should have a right to access information of this type, especially where governments subsidize O&G production or provide tax breaks. Future work should continue to build upon the data resource that was created from this study, and we encourage anyone who is collecting emission measurements to contribute to this resource by contacting the corresponding author, who will continue to update the data archive on a regular basis. Increased accessibility to measurement data not only improves our understanding of emission patterns, but it also helps technology innovators because it helps paint an accurate picture of the detection needs and is also essential for advanced data analysis such as artificial intelligence (AI) and machine learning.

References

Alvarez, R. A., Zavala-Araiza, D., Lyon, D. R., Allen, D. T., Barkley, Z. R., Brandt, A. R., Davis, K. J., Herndon, S. C., Jacob, D. J., Karion, A., Kort, E. A., Lamb, B. K., Lauvaux, T., Maasakkers, J. D., Marchese, A. J., Omara, M., Pacala, S. W., Peischl, J., Robinson, A. L., Shepson, P. B., Sweeney, C., Townsend-Small, A., Wofsy, S. C., Hamburg, S. P., 2018 Assessment of methane emissions from the U.S. oil and gas supply chain. *Science* 361, 186-188.

Baillie, J., Risk, D., Atherton, E., O'Connell, E., Fougère, C., Bourlon, E., MacKay, K., 2019. Methane emissions from conventional and unconventional oil and gas production sites in southeastern Saskatchewan, Canada. *Environmental Research Communications* DOI: 10.1088/2515-7620/ab01f2.

Bell, C. S, Vaughn, T. L., Zimmerle, D., Herndon, S. C., Yacovitch, T. I., Heath, G. A., Petron, G., Edie, R., Field, R. A., Murphy, S. M., Robertson, A. M., Soltis, J., 2017. Comparison of methane emission estimates from multiple measurement techniques at natural gas production pads. *Elementa Science of the Anthropocene,* **5**: 79. DOI: https://doi.org/10.1525/elementa.266

Brandt, A. R., Heath, G. A., Cooley, D., 2016. Methane leaks from natural gas systems follow extreme distributions. *Environmental Science and Technology* 50, 22, 12512-12520. DOI: https://doi.org/10.1021/acs.est.6b04303

Canadian Energy Pipeline Association (CEPA), 2016. Best Management Practice: Fugitive Emissions at Natural Gas Transmission and Storage Facilities. Retrieved from: https://www.cepa.com/wp-content/uploads/2016/11/CEPA-Best-Management-Practice-Fugitive-Emissions-at-NG-Facilities.pdf

CapOp Energy, 2019. British Columbia Oil and Gas Methane Emissions Field Study. Retrieved from: https://www.bcogc.ca/files/resources/bc-cas-mefs-chapters-1-3-err2-20200224.pdf

Caulton, D. R., Lu, J. M., Lane, H. M., Bucholz, B., Fitts, J. P., Golston, L. M., Guo, X., Li, Q., McSpiritt, J., Pan, D., Wendt, L., Bou-Zeid, E., Zondlo, M. A., 2019. Importance of Superemitter Natural Gas Well Pads in the Marcellus Shale. *Environmental Science and Technology* 53, 4747−4754. DOI: 10.1021/acs.est.8b06965

Caulton, D. R., Li, Q., Bou-Zeid, E., Lu, J., Lane, H. M., Fitts, J. P., Buchholz, B., Golston, L. M., Guo, X., McSpiritt, J., Pan, D., Wendt, L., Zondlo, M. A., 2017. Improving Mobile Platform Gaussian-Derived Emission Estimates Using Hierarchical Sampling and Large Eddy Simulation. *Atmospheric Chemistry and Physics Discussions*, 1–39.

Clearstone Engineering Ltd., 2019. 2018 Alberta upstream oil & gas methane emissions

inventory and methodology. Retrieved from: https://www.aer.ca/documents/ab-uog-emissions-inventory-methodology.pdf

Environment and Climate Change Canada (ECCC), 2020. General factsheet regarding the release of methane and certain volatile organic compounds. Retrieved from: https://www.canada.ca/en/environment-climate-change/services/canadian-environmental-protection-act-registry/factsheet-general-information-regulations-reduction-methane.html

Environmental Protection Agency (EPA), 2020. Oil and Natural Gas Sector: Emission Standards for New, Reconstructed, and Modified Sources Reconsideration. Retrieved from: https://www.federalregister.gov/documents/2020/09/15/2020-18115/oil-and-natural-gas-sector-emission-standards-for-new-reconstructed-and-modified-sources

Fox, T. A., Barchyn, T. E., Risk, D., Ravikumar, A. P., Hugenholtz, C. H., 2019. A review of close-range and screening technologies for mitigating fugitive methane emissions in upstream oil and gas, *Environmental Research Letters,* 14, 053002. DOI: https://doi.org/10.1088/1748-9326/ab20f1

Fox, T. A., Hugenholtz, C. H., Barchyn, T. E., Gough, T. R., Gao, M., Staples, M., 2021. Can new mobile technologies enable fugitive methane reductions from the oil and gas industry? *Environmental Research Letters,* 16, 064077. DOI: https://iopscience.iop.org/article/10.1088/1748-9326/ac0565

Greenpath Energy, 2017. Historical Canadian fugitive emissions management program assessment. Prepared for PTAC. Retrieved from: https://greenpathenergy.com/wp-content/uploads/2019/10/Historical-Canadian-Fugitive-Emissions-Management-Program-Assessment.pdf

Intergovernmental Panel on Climate Change (IPCC), 2018. Global Warming of 1.5°C. An IPCC Special Report on the impacts of global warming of 1.5°C above pre-industrial levels and related global greenhouse gas emission pathways, in the context of strengthening the global response to the threat of climate change, sustainable development, and efforts to eradicate poverty [Masson-Delmotte, V., P. Zhai, H.-O. Pörtner, D. Roberts, J. Skea, P.R. Shukla, A. Pirani, W. Moufouma-Okia, C. Péan, R. Pidcock, S. Connors, J.B.R. Matthews, Y. Chen, X. Zhou, M.I. Gomis, E. Lonnoy, T. Maycock, M. Tignor, and T. Waterfield (eds.)]. In Press.

Johnson, M., Tyner, D., Conley, S., Schwietzke, S. and Zavala-Araiza, D. 2017. Comparisons of Airborne Measurements and Inventory Estimates of Methane Emissions in the Alberta Upstream Oil and Gas Sector. *Environmental Science and Technology* 51(21): 13008–13017. DOI: https://doi.org/10.1021/acs.est.7b03525

Kemp, C. E., and Ravikumar, A. P., 2021. New Technologies Can Cost Effectively

Reduce Oil and Gas Methane Emissions, but Policies Will Require Careful Design to Establish Mitigation Equivalence. *Environmental Science and Technology* 55, 9140-9149. DOI: https://doi.org/10.1021/acs.est.1c03071

Lavoie, M., Baillie, J., Bourlon, E., O'Connell, E., MacKay, K., Boelens, I., Risk, D., 2021. Sweet and sour, A quantitative analysis of methane emissions in contrasting Alberta, Canada, heavy oil developments. *Science of the Total Environment*, 807(Pt 2):150836. DOI: 10.1016/j.scitotenv.2021.150836

Lavoie, T. N., Shepson, P. B., Cambaliza, M. O. L., Stirm, B. H., Conley, S., Mehrotra, S., Faloona, I. C., Lyon, D., 2017. Spatiotemporal Variability of Methane Emissions at Oil and Natural Gas Operations in the Eagle Ford Basin. *Environmental Science and Technology* 51, 14, 8001-8009. DOI: https://doi.org/10.1021/acs.est.7b00814

Littlefield, J. A., Marriott, J., Schivley, G. A., Skone, T. J., 2017. Synthesis of recent ground-level methane emission measurements from the U.S. natural gas supply chain. *Journal of Cleaner Production* 148, 118-126. DOI: https://doi.org/10.1016/j.jclepro.2017.01.101

MacKay, K., Risk, D., Atherton, E., Fougere, C., Bourlon, E., O'Connell, E., Baillie, J., 2019. Fugitive and vented methane emissions surveying on the Weyburn CO_2-EOR field in southeastern Saskatchewan, Canada. *International Journal of Greenhouse Gas Control* 88, 118-123. DOI: https://doi.org/10.1016/j.ijggc.2019.05.032

MacKay, K., Lavoie, M., Bourlon, E., Atherton, E., O'Connell, E., Baillie, J., Fougère, C., Risk, D., 2021. Methane emissions from upstream oil and gas production in Canada are underestimated. *Scientific Reports* 11, 8041. DOI: https://doi.org/10.1038/s41598-021-87610-3

O'Connell, E., Risk, D., Atherton, E., Bourlon, E., Fougère, C., Baillie, J., Lowry, D., Johnson, J., 2019. Methane emissions from contrasting production regions within Alberta, Canada: Implications under incoming federal methane regulations. *Elementa Science of the Anthropocene* 7. DOI: 10.1525/elementa.341.

Omara, M., Zimmerman, N., Sullivan, M. R., Li, X., Ellis, A., Cesa, R., Subramanian, R., Presto, A. A., Robinson, A. L., 2018. Methane Emissions from Natural Gas Production Sites in the United States: Data Synthesis and National Estimate. *Environmental Science and Technology* 52 (21), 12915-12925. DOI: 10.1021/acs.est.8b03535

Ravikumar, A. P., Roda-Stuart, D., Liu, R., Bradley, A., Bergerson, J., Nie, Y., Zhang, S., Bi, X., Brandt, A. R., 2020. Repeated leak detection and repair surveys reduce methane emissions over a scale of years. *Environmental Research Letters* 15, 034029. DOI: https://iopscience.iop.org/article/10.1088/1748-9326/ab6ae1

Robertson, A. M., Edie, R., Field, R. A., Lyon, D., McVay, R., Omara, M., Zavala-

Araiza, D., Murphy, S. M., 2020. New Mexico Permian Basin Measured Well Pad Methane Emissions Are a Factor of 5–9 Times Higher Than U.S. EPA Estimates. *Environmental Science and Technology* 54 (21), 13926-13934. DOI: 10.1021/acs.est.0c02927

Roscioli, J. R., Herndon, S. C., Yacovitch, T. I., Knighton, W. B., Zavala-Araiza, D., Johnson, M. R., and Tyner, D. R., 2018. Characterization of methane emissions from five cold heavy oil production with sands (CHOPS) facilities. *Journal of Air and Waste Management Association* 68 (7): 671−684. DOI: https://doi.org/10.1080/10962247.2018.1436096

Sheng, J-X., Jacob, D. J., Maasakkers, J. D., Sulprizio, M. P., Zavala-Araiza, D., Hamburg, S. P., 2017. A high-resolution (0.1° x 0.1°) inventory of methane emissions from Canadian and Mexican oil and gas systems. *Atmospheric Environment* 158, 211-215. DOI: http://dx.doi.org/10.1016/j.atmosenv.2017.02.036

Vogt, J., LaForest, J., Argento, M., Kennedy, S., Bourlon, E., Lavoie, M., Risk, D. Methane emissions from three Canadian oil and natural gas developments. *Manuscript under review.*

Zavala-Araiza, D., Lyon, D. R., Alvarez, R. A., Davis, K. J., Harriss, R., Herndon, S. C., Karion, A., Kort, E. A., Lamb, B. K., Lan, X., Marchese, A. J., Pacala, S. W., Robinson, A. L., Shepson, P. B., Sweeney, C., Talbot, R., Townsend-Small, A., Yacovitch, T. I., Zimmerle, D. J., Hamburg, S. P., 2015. Reconciling divergent estimates of oil and gas methane emissions. *Proceedings of the National Academy of Sciences*, 112 (51): 15597–15602. DOI: https://doi.org/10.1073/pnas.1522126112

Zavala-Araiza, D., Herndon, S. C., Roscioli, J. R., Yacovitch, T. I., Johnson, M. R., Tyner, D. R., Omara, M., Knighton, B., 2018. Methane emissions from oil and gas production sites in Alberta, Canada. *Elementa Science of the Anthropocene* 6 (1): 27. DOI: https://doi.org/10.1525/ elementa.284

4. Sensitivity analysis of methane emission inventories using site-level emissions data and a Monte Carlo model framework

4.1 Preface

This chapter has not been submitted to a journal at the time of writing. I led the writing and analysis included in this chapter, and my supervisor David Risk provided feedback throughout the analysis. My colleague Martin Lavoie assisted with the developing the initial model framework used in this analysis.

4.2 Abstract

Greenhouse gas emission inventories are important for policy development and tracking emission levels and patterns over time. However, current methods for estimating oil and gas methane inventories (the second largest source of global methane emissions) have high uncertainties that are difficult to quantify. In this study, we investigate the sensitivity of oil and gas methane inventories to different factors using a Monte Carlo model framework and a measurement dataset with over 4500 site-level methane measurements. We assess how modelled methane inventories and uncertainties change under a range of scenarios. Results showed that if emission factor estimates consider variability from geography, production, and site type, the total inventory ranges from -25% to +78% when compared to reported estimates that only consider component type as an indicator of emissions variability. A goodness of fit analysis found that site-level methane emissions in Canada follow extreme distributions, and if lognormal distributions are used to represent emissions distributions in inventory models, they consistently underestimate the

heavy-tail, resulting in an overall underestimation of emissions. We also found that using skewed distributions to represent emissions significantly increases the uncertainty range of the total inventory, but are likely more representative of true emissions. The two main takeaways from this study are: 1) the importance of including super emitters in inventory estimates, and 2) the need to better understand the true distributions of oil and gas methane emissions. The latter will likely only be achieved through more measurements, which signals a need for Canada to enhance their regulatory measurement protocols.

4.3 Introduction

Greenhouse gas emission (GHG) inventories are an important tool as they inform policies and regulations that are used to achieve reduction goals. They are also helpful in identifying specific areas (sources, sectors, etc.) in which reductions are needed, and for tracking changes in global emission levels and patterns over time. Methane (CH_4), the second most abundant greenhouse gas, is one of the pollutants that individual countries are required to estimate annual inventories for in accordance with the United Nations Framework Convention on Climate Change (UNFCCC, 1992). Due to its potency and relatively short atmospheric lifetime (~12 years), reducing CH_4 has been deemed as the most effective method to slow the rate of human induced climate change in the short term. That said, accurate CH_4 inventories, especially from sectors and countries that have the capacity to achieve significant reductions, are essential in the short-term. For Canada, CH_4 emissions make up 13% of our total GHG emissions, with the largest source of CH_4 (~43%) coming from the oil and gas (O&G) sector (ECCC 2021).

In Canada, federally reported CH_4 emission inventories for the O&G sector are currently estimated using a bottom-up approach ("Tier 3") that follow guidelines created by the Intergovernmental Panel on Climate Change (IPCC) (ECCC 2021). Using this method, total emissions are estimated using the following equation:

$$Emission_b = EF_b \times A_b \tag{4.1}$$

where b represents a specific source category (e.g. component type), EF is the emission factor (representative emission rate) for b, and A is the activity factor (i.e., count) for source b. The calculation is done separately for all known sources, which are then summed to compute a total inventory. Typically, emission factors (EFs) are based on an average emission rate derived from a small sample of direct measurements and/or manufacturers specifications, however calculation methods vary across specific emission sources and industrial sectors.

Recent measurement studies have revealed that O&G CH_4 inventories estimated using this bottom-up approach often result in underestimation of total emissions. For example, Chan et al. (2020) found that measured CH_4 emissions in Alberta and Saskatchewan were 85% higher than reported emissions, and Johnson et al. (2017) found that emissions in Lloydminster and Red Deer, Alberta were 25-50% higher than reported. Several studies in the United States show similar results (e.g. Alvarez et. al 2018, Zavala-Araiza et al. 2015, Zhang et al. 2020).

Statistical modelling is one way that can improve inventory certainty. Indeed, the IPCC suggests that when models such as Monte Carlo simulations are used in inventory estimation, they do a better job of capturing the linkages between processes influencing emissions and can improve spatial and temporal resolution of estimates (IPCC 2010). However, the accuracy of such modelling requires reliable input data and a detailed understanding of model assumptions and sensitivities.

In this study, we use ~4500 site-level CH_4 emissions measurements, O&G infrastructure databases, and Monte Carlo simulations to investigate the sensitivity of Canadian O&G CH_4 inventory estimates to different factors. We expand on a Monte Carlo model framework first described in Chapter 2 (MacKay et al. 2021) by incorporating other infrastructure information and distribution types, to assess the influence of both infrastructure characteristics and observed emission distributions on total inventories and overall uncertainty. Alberta, Canada, was the focus of this work because most of Canada's O&G production occurs there, and it is also the province with the most available measurement data.

4.4 Methods

4.4.1 Theory and rationale

There are several factors that could be causing uncertainties in the current bottom-up inventory. First, individual EFs are calculated at the component-level, which assumes that

emissions variability is caused by component type only (e.g. valve, compressor seal), and other factors such as geography, production, and site types are not considered. It is possible that the total inventory could be improved by incorporating other variables besides component type. For example, if measurements show that emissions vary spatially, then it would make sense for EF calculations to incorporate this variability (i.e., by calculating separate EFs for different regions). The same can be true for other infrastructural and process related characteristics, but little is known on exactly how much CH_4 emissions variability is caused by these factors.

Second, using single values for EF's derived from a small number of direct measurements fails to capture the true distributions of emissions, which are observed to be positively skewed. Small sample sizes used to derive EFs often miss the so-called "super emitters", resulting in a low-biased EF (Brandt et al. 2016). Increasing sample size for EF calculations could help address this issue but using a single average value will still fail to capture the contribution of the largest sources. Using a more complex modelling approach is likely a better solution, as the emissions distribution (including the super emitters) can be directly incorporated into the total inventory.

Both of these factors (and many others that are beyond the scope of this study) are likely contributing to inventory uncertainty, but the relative importance (i.e., which one has the biggest effect on inventories) of these factors are not well understood. If changes to the current method are necessary, it is important to know which areas of uncertainty should be prioritized.

4.4.2 The Monte Carlo method for estimating inventories

As mentioned, the Monte Carlo method for estimating inventories and their uncertainties is one modelling approach (Tier 2) recommended by the IPCC. The method involves selecting random values from a probability density function (pdf) generated using data from each input parameter (i.e., EFs and activity data), and calculating the total emission by multiplying the two randomly selected values (as shown in Equation 1). The total value is stored, and this step is repeated many times, and the final product is a distribution of values representing the total inventory, where the mean and uncertainty (95% confidence interval) can be computed from the resulting distribution (IPCC 2001).

Though the underlying equation is the same, the Monte Carlo approach has several advantages over the simplified Tier 3 method. First, the use of probability density functions (rather than a single value) allows for the complexity of specific emission sources (and their related uncertainties) to be directly incorporated. Second, the model can handle any type of distribution, regardless of width or shape. This is especially important for O&G CH_4 inventories, as emission distributions are known to be positively skewed. Third, the iterative nature of the model allows for a more realistic quantification of overall uncertainty, especially for cases when uncertainty is asymmetrical.

The Monte Carlo inventory model used here was coded in R Software (R Core Team). The code has been generalized so that it can estimate an inventory for any area

and source(s) of interest. The model requires users to input a file containing the source categories of interest and their corresponding emission factors (EFs) and activity data (i.e., counts). It is up to the user to obtain this information for the model.

Figure 4.1 is a simplified diagram showing the model framework. As mentioned, EFs and corresponding counts are the required inputs. For our analysis, we use site-level CH_4 measurements to calculate EFs, and O&G infrastructure databases to calculate site counts (further discussed in Sections 4.4.3 and 4.4.4). Once this required information is fed into the model, it starts by creating individual probability density functions (pdfs) for all unique EFs, representing the emissions distributions for all specific source categories (i.e. bins) within the inventory boundary (Figure 4.1). Next, a value from each pdf is randomly sampled (with replacement), and multiplied by the corresponding site count to compute a total emission (i.e. bin total) per source type (Figure 4.1). This process is repeated 10,000 times, with the sum of all the products (i.e. sum of emissions from all individual bins) being stored after each iteration. The resulting output is a distribution of values representing the total emission inventory (n=10,000), which is then used to calculate a mean and 95% confidence interval of the inventory.

In addition to the advantages of Monte Carlo simulations stated above, the structure of our model also allows for individual sources to be partitioned by any infrastructural characteristic, such as site type, geography, or production. There is also no limit to the number of unique sources that can be included. Finally, the size and shape of the pdfs representing the EF distributions can be easily modified by the user.

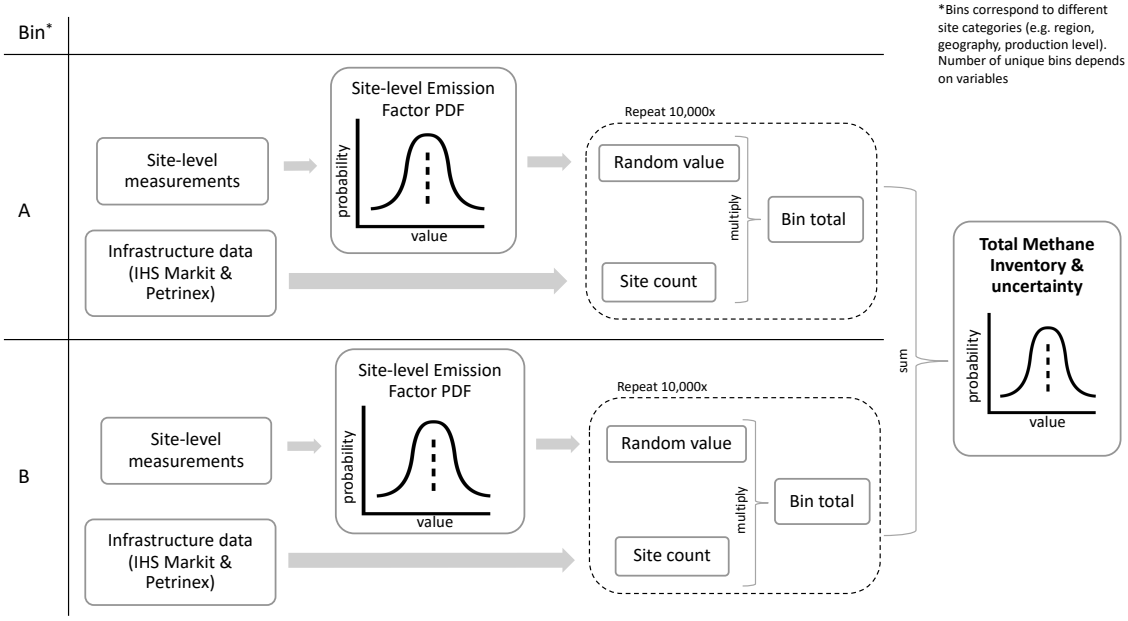

Figure 4.1. Diagram showing the Monte Carlo model framework used in our analysis. For simplicity, only two unique bins are shown, but the actual number varies and is dependent on the number of source categories included in the inventory.

4.4.3 Calculating site-level emission factors and corresponding site counts

To examine the sensitivity of the modelled inventories to EF calculation approach, we used over 4500 site-level measurements from MacKay et al. (2021) (Chapter 2) to calculate site-level EFs using one or more of the following variables: site type, geographic region, and production levels. In other words, we subdivided our measurements using these variables to compute individual EFs to use in our model.

As mentioned, the province of Alberta was chosen for this analysis because it is Canada's largest O&G producing province, and it is where most available measurements are concentrated. Alberta also has the most publicly available data in terms of production levels and infrastructural characteristics, which allows us to readily explore the variability associated with these characteristics. Note that for this analysis, the same measurement data is used for all scenarios, and the total site count for the study region (Alberta) always remains the same (i.e. we assume site count uncertainty to be negligible).

Site counts were estimated using a combination of IHS databases (IHS Markit) and publicly available Petrinex data. IHS databases include coordinates of all physical wells and facilities that exist in Alberta, but they are not aggregated to the site-level. In other words, there is no common site identifier for wells and/or facilities that are at the same location. Therefore, we grouped individual wells and facilities into "sites" using a 45 m buffer radius. This step was required because EFs are computed using measurements that represent whole site emissions (rather than individual infrastructure or components).

Once we grouped all infrastructure into physical sites, we used Petrinex monthly reporting data to extract only sites that were either producing, venting, or flaring hydrocarbons during the 2018 production year. Inactive sites were excluded from our analysis due to a lack of measurements, and 2018 was chosen as the inventory year for comparison purposes (i.e. Chapter 2 inventory estimate was for 2018). Finally, all sites were subdivided into respective bins using the same variables used to partition

measurement data for the EF calculations, to compute total site counts that correspond to each EF.

4.4.4 Region, site type, and production specific emission factor classifications

The ten Alberta Energy Regulator (AER) administrative regions (Figure 4.2) were used to represent the physical boundaries for region-specific EF calculations. Some regions are dominated by a specific production type (e.g. Wainwright is dominated by cold heavy oil production with sand, also known as CHOPS), whereas other regions include a mix of production. Our measurement dataset includes measurements in eight out of the ten AER regions, and for the two regions that lack measurements (Fort McMurray and Midnapore), EFs are derived using all measurements (i.e. provincial average). Table 4.1 lists the ten region-specific EFs and corresponding counts used in our model.

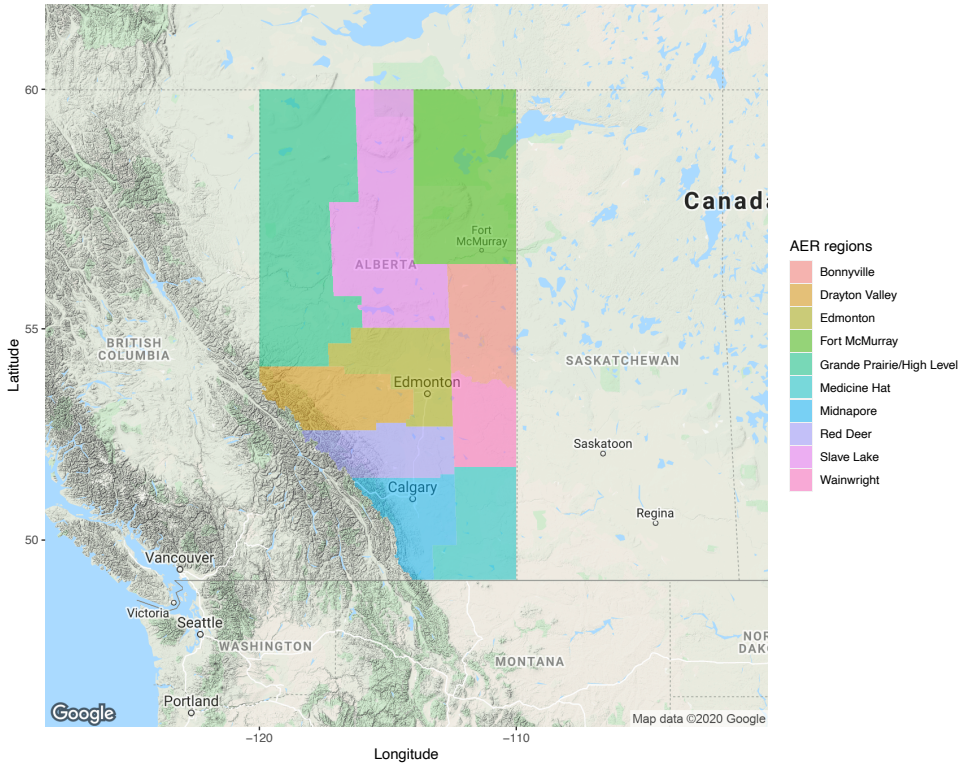

Figure 4.2. AER administrative regions for the province of Alberta. These regions are the geographic boundaries used for region-specific EF calculations.

Table 4.1: Region-specific emission factors and site counts used in our analysis. Emission factors represent the average emission rate of all measured sites in each region.

Region	Site Count	EF (m^3 day^{-1})
Bonnyville	4,881	63.46
Drayton Valley	12,158	12.8
Edmonton	5,332	20.41
Fort McMurray	169	56.05
Grande Prairie/High Level	11,230	45.9

Medicine Hat	45,305	13.69
Midnapore	9,797	56.05
Red Deer	11,608	36.17
Slave Lake	2,858	10.43
Wainwright	11,031	98.62

Individual sites were classified into 19 different types based on the description of infrastructure that make up each site. For example, if a site consisted of a single oil well, and one battery, then it was classified as an "oil single well battery." Similar to the region-specific EF calculations, if we lacked measurements for a specific site type, then the overall average is used for the EF. Table 4.2 lists the 19 site-specific EFs and corresponding counts used in our model.

Table 4.2: Site-specific emission factors and site counts used in our analysis. Emission factors represent the average emission rate of all measured sites for each site type.

Site Type	Site Count	EF (m^3 day^{-1})
bitumen multi-well battery	855	176.6
bitumen single well battery	909	206.72
commingled multi-well battery	250	103.43
complex facility	3	34.96
gas gathering system	1	34.96
gas multi-well battery	772	22.58
gas single well battery	3,539	102.79

injection plant	3	24.47
multi battery	512	43.41
multiple bitumen wells	1,887	95.54
multiple gas wells	6,509	23.45
multiple oil wells	4,140	15.5
multiple wells	198	36.95
oil multi-well battery	862	90.66
oil single well battery	4,212	64.44
single battery	4,572	68.06
single bitumen well	612	52.73
single gas well	67,421	9.39
single oil well	17,112	24.87

Finally, production tiers for sites were classified based on combined annual (2018) oil and gas production for all wells producing at each site (production values were obtained from public Petrinex files). Individual production rates for producing wells were summed to the site-level to compute a production rate per site. Sites were then partitioned into eight production classes, ranging from zero to five million m^3/year. Table 4.3 lists the eight production specific EFs and corresponding counts used in our model.

Table 4.3: Production-specific emission factors and site counts used in our analysis. Emission factors represent the average emission rate of all measured sites within each production class.

Production class (m^3/year)	Site Count	EF (m^3 day^{-1})

A (<1)	7,894	143.33
B (1-5000)	3,962	72.29
C (5000-50,000)	20,205	51.17
D (50,000-100,000)	17,510	49.68
E (100,000-500,000)	38,239	48.66
F (500,000-1,000,000)	9,831	43.59
G (1,000,000-5,000,000)	12,818	64.53
H (>5,000,000)	3,910	53.42

4.4.5 Goodness of fit and distribution selection

When using Monte Carlo simulations for inventory estimates, the probability density functions used to represent EFs should be closely aligned with the true distributions of emissions. As mentioned, many recent measurement studies found that O&G CH_4 emissions follow skewed distributions, with most literature citing lognormal distributions as the best fit. In Chapter 2, a lognormal distribution was used to represent site-level EFs, which was an assumption based on other recent studies and not a statistical goodness of fit analysis on measured emissions.

In this analysis, we examined the distributions of our measured data (n = 4544) to statistically determine whether a lognormal distribution is an appropriate choice for Canadian O&G CH_4 inventories. We also explore different distribution types and compare to empirical data to evaluate which distribution best represents measured emissions. Finally, we assess how the modelled inventory changes under different distribution types that are more positively skewed than a lognormal fit.

4.5 Results and Discussion

4.5.1 Effect of geography, infrastructure characteristics, and production on inventory estimates

Six different model simulations were run to assess how the total inventory is affected by EFs that vary by region, production, and site types. Three simulations used one variable for EF calculations (as shown in Tables 4.1, 4.2, and 4.3), and the other three simulations used a combination of variables (e.g. site type *and* region) for EF calculations. Depending on the variables used, the number of unique EFs used in each simulation ranged from 8 to 190. All EFs were represented by the same lognormal distributions for these simulations, therefore the variability shown here is solely due to the EFs. Figure 4.3 shows the distributions of the resulting six modelled inventories, with the vertical dashed line representing the estimate reported by ECCC for the same year (2018). Note that we use the reported value as a reference point when discussing variability, but we do not use it as an indicator of the "true" inventory or the accuracy of the other outputs. It should also be noted that we do not claim that any of these modelled estimates are more accurate than the other, but simply we are showing how the inventory changes under different scenarios.

When EFs are partitioned by one or more infrastructural characteristics (i.e. site type, production level) and geography, the average values of modelled inventories range from 25% lower to 78% higher than the reported estimate (Figure 4.3). The production specific EFs produced the highest inventory estimate, which is interesting since the

individual EFs (Table 4.3) were all within similar ranges to EFs used in the other simulations. However, the lowest production specific EF was 48.66 m^3 day^{-1}, while some region and site-specific EFs were less than 15 m^3 day^{-1}, which may explain some of the discrepancies.

Uncertainty ranges for each output also varied slightly, although the upper uncertainty limit was always higher than the lower. This consistent asymmetry was expected since all simulations used a lognormal distribution to represent EFs. Lower uncertainties ranged from -23% (Site Type x Production) to -40% (Production), and upper uncertainties ranged from +31% (Site Type x Production) to +60% (Production).

Our uncertainties are notably higher than the current reported uncertainty (-9% to +10.5%) for O&G CH_4 emissions, especially for the upper uncertainty limit. The reported uncertainty was calculated using a simple error propagation approach, otherwise known as the IPCC Tier 1 method (ECCC 2021). Due to the nature of the Tier 1 method, the overall uncertainty estimate is almost always symmetrical. However, we argue that the asymmetrical uncertainties shown in our modelled estimates are appropriate, as they reflect the well-documented skewed nature of O&G CH_4 emissions. This further justifies the use of Monte Carlo simulations as opposed to error propagation, as they can incorporate asymmetric uncertainties in the overall inventory.

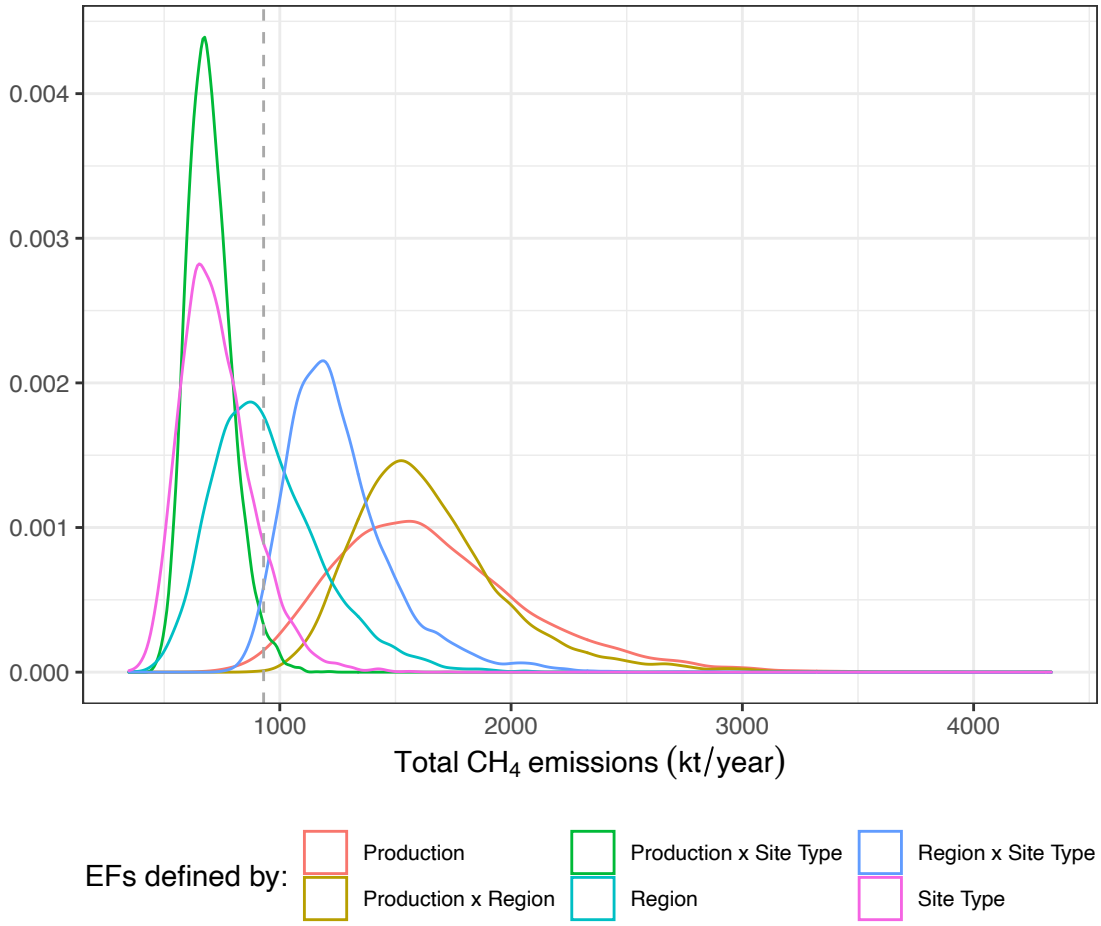

Figure 4.3. Distributions of total CH_4 emissions from six different model simulations. Each simulation uses one or more variables to define site-level emission factors. The dashed line represented the reported estimate for the same year.

4.5.2 Challenges of modelling extremely skewed distributions

Determining which distribution type was the best fit to our measurement dataset was a significant challenge. We used Kolmogorov–Smirnov (K-S) tests to compare several different types of distributions to our measurement dataset. We also used R software packages to iteratively cycle through hundreds of distributions to predict the best fit,

which indicated a pareto distribution. However, when we created new pareto distributions using parameters defined by the measurement dataset, they still failed the two-sample K-S test when compared to the measured distribution. We also experimented with different variations of lognormal distributions, and the outcome was the same. After several unsuccessful attempts, we concluded that it is unlikely that any parametric distribution is going to meet the K-S threshold for statistical significance when compared to the measured distribution. Consequently, we assessed the goodness of fit of both the pareto and lognormal distributions using combinations of visual inspection and a resampling analysis.

Figures 4.4 and 4.5 show density plots comparing different fitted distributions to the measured distributions. Figure 4.4 shows the comparison for the full measurement dataset (n=4544), and Figure 4.5 shows the comparison broken down by AER region. Four different distributions are included in this comparison: the "original" lognormal distribution (as used in Chapter 2), a new lognormal distribution, and two versions of a pareto distribution. The difference between the original and new lognormal distributions are the standard deviations used to define them. For the original lognormal distribution, the standard deviation for EFs pdfs were defined based on our estimated measurement error (±63%), which was a conservative assumption that resulted in a narrower distribution that does not reflect the range of measured emissions. The standard deviations for the new lognormal distribution were calculated directly from the measured dataset, which resulted in a wider distribution. Including this new lognormal distribution allowed us to better understand the implications of our original assumption, and to see

whether it changes the total inventory. The difference between the two pareto distributions is that pareto (2) was truncated to remove unrealistically high values. The cut off for truncating was defined by the maximum measured value for each distribution. In other words, any values that exceeded the maximum measured value were replaced with the maximum. Therefore, the two pareto distributions shown in Figures 4.4 and 4.5 are basically identical except for the right tail.

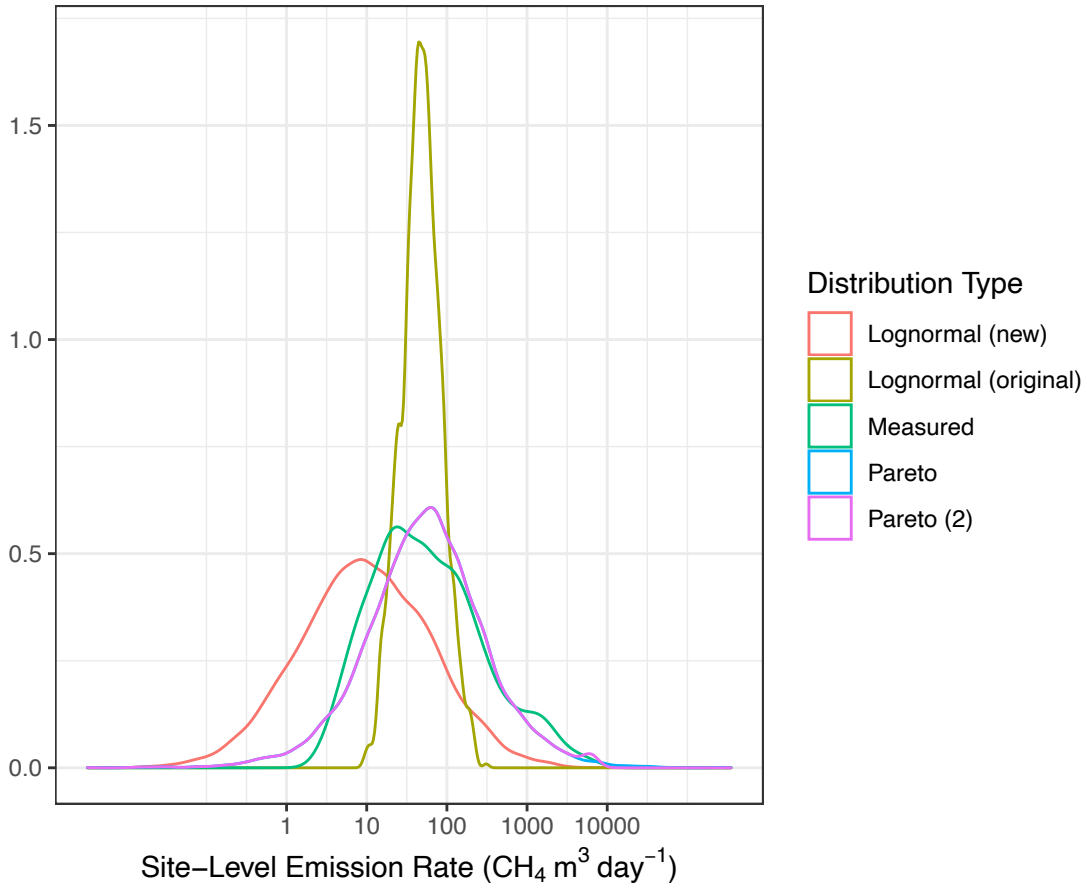

Figure 4.4. Density plots of measured and various fitted CH_4 emissions distributions. The x-axis is shown on a logarithmic scale for better visualization.

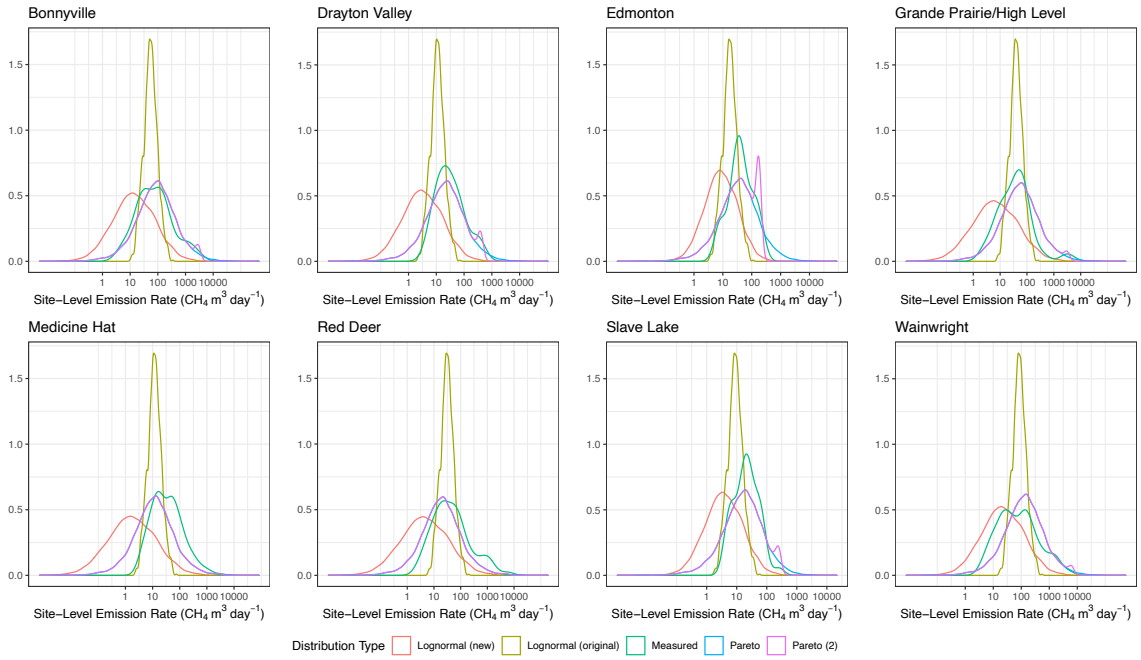

Figure 4.5. Density plots of measured and fitted CH_4 emissions distributions, broken down by AER region. The x-axis is shown on a logarithmic scale for better visualization.

A visual inspection of these plots clearly shows that the fitted pareto distributions show better alignment compared to the original lognormal distributions used in Chapter 2. The original lognormal distribution (used in Chapter 2) seems to represent the mean well, but the width is very narrow, and the tail is completely cut off (Figures 4.4 and 4.5). The new lognormal distributions all show a slight offset to the left compared to the measured distributions, which could imply that new lognormal distributions are underrepresenting the magnitude of the largest sources. Figures 4.4 and 4.5 also show that the pareto

distributions seem better at characterizing the heavy-tail compared to lognormal distributions, which rarely align with the heavy-tail of the measured distribution.

Table 4.4 shows the mean emission rates of the fitted and measured distributions shown in Figure 4.4. The percentage of the total contributed by the top 5% of values (i.e. the heavy-tail) are also listed in Table 4.4, which again shows that lognormal distributions (especially the original) are underestimating the contribution of the heavy-tail. Here we also see that the pareto distribution significantly overestimates the mean, and the truncation of unrealistically high values did not make a substantial difference (and actually reduced the contribution of the heavy-tail to a lower percentage than the new lognormal). It is also worth mentioning that even the pareto distributions still underestimate the contribution of the top 5%, by 14%.

Table 4.4: Summary statistics for measured CH_4 emissions and fitted distributions.

Distribution	n	Mean CH_4 emission rate (m^3 day^{-1})	Contribution of the top 5%
Measurement dataset	4544	56.1	84%
Lognormal (original)	10000	56.5	14%
Lognormal (new)	10000	54.2	58%
Pareto	10000	336.6	70%
Pareto (2)	10000	225.7	55%

To better understand how lognormal and pareto distributions compare with respect to representing the heavy-tail, we randomly sampled 500 values (with replacement) from

each fitted distribution type, and calculated two statistics from the sample: 1) the mean of the top 5% of values and the 2) the fraction of total contributed by the top 5%. We repeated this 500 times for each fitted distribution, resulting in 500 values of each statistic. Figure 4.6 shows the distributions of the results (red boxplots), broken down by AER region, compared to the same statistics derived from the measurement dataset (blue diamonds). Here we see that the fitted lognormal distributions consistently underestimate both the average emission rate of the top 5%, and their contribution to the total. The pareto distribution consistently overestimates the mean, and in most cases, underestimates the contribution of the top 5%. However, Figure 4.6 does show that the pareto distribution is better at representing the contribution of the heavy-tail in comparison to the lognormal distribution, but neither show perfect alignment with the measured values.

Similar results were observed in a synthesis study by Brandt et al. (2016). In that study, authors aggregated 18 CH_4 measurement datasets across the United States and found that all datasets showed severe skewness that did not align with a standard lognormal distribution. Through a similar analysis looking specifically at the top 5% of sources, Brandt et al. (2016) also found that lognormal distributions consistently underestimate the contribution of the largest sources.

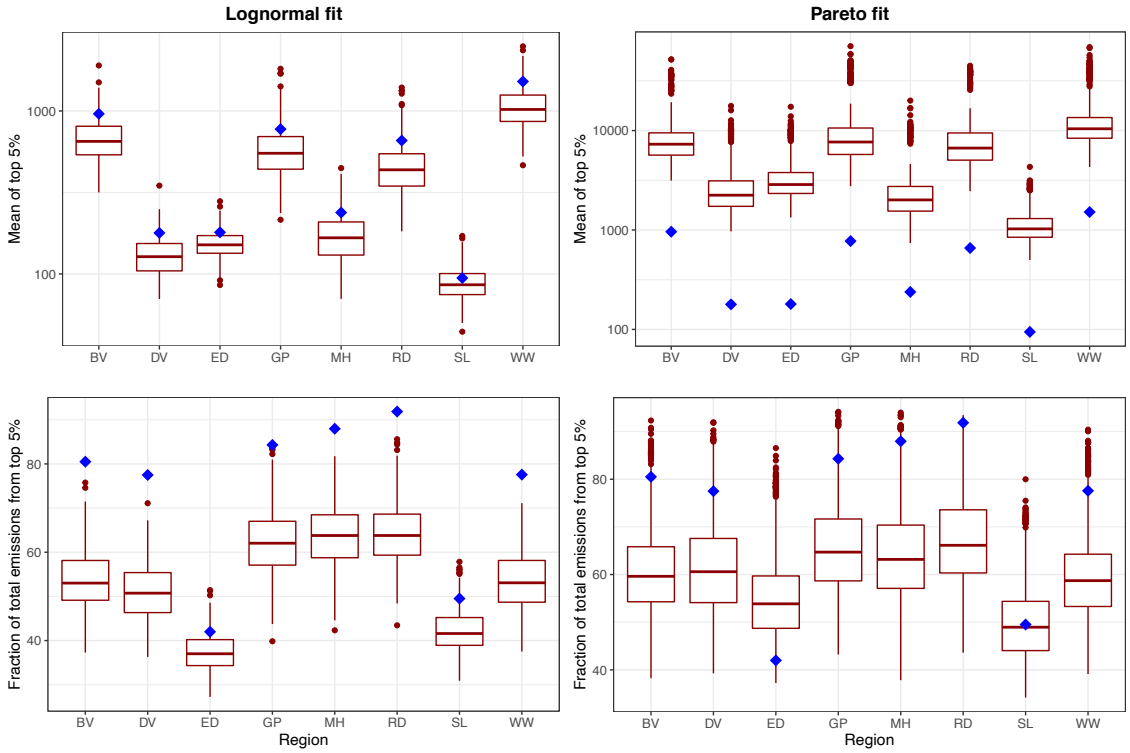

Figure 4.6. Comparison of the top 5% of values of fitted lognormal (left) and pareto (right) (red boxplots) distributions to measured emissions for each AER region with measurements (blue diamond). The top graphs show the mean of the top 5%, and bottom graphs show the percent of total emissions contributed by the top 5%. Boxplots represent distributions of individual values calculated from 500 random samples of the respective fitted distributions. For the top figures, the y-axis is a lognormal scale for better visualization.

4.5.3 Effect of distribution type on total inventory

Even though all four fitted distributions do not perfectly conform to our measured data, we still wanted to examine how the use of different distributions affect the total inventory and related uncertainty. Four different model simulations were run using the four

distributions to represent EF pdfs. Interestingly, the new lognormal distribution hardly changed the average inventory compared to the old lognormal distribution, but as expected, it did result in a wider uncertainty range. Total inventory uncertainty using the new lognormal distribution was -89% to +380%, which is significantly wider than the current reported uncertainty. Brandt et al. (2016) also found that more skewed distributions result in larger uncertainties of total emissions. Additionally, modelled inventories using truncated and untruncated pareto distributions were significantly higher (300-600% more than the reported inventory), but uncertainty ranges were comparable to those derived from the lognormal fits (-90% to +330%). Although the pareto distributions resulted in a much higher inventory compared to the reported estimate, other measurement studies have revealed similar divergences when comparing measured emissions to reported estimates. For instance, Robertson et al. (2020) estimates that CH_4 emissions in the New Mexico Permian Basin are 500-900% higher than reported estimates by the U.S. Environmental Protection Agency (EPA). Therefore, a 300-600% difference is not wholly unrealistic.

4.6 Summary

In conclusion, our analysis revealed how modelled CH_4 emission inventories are influenced by emission factor parameterization and, more importantly, the distribution chosen to represent emissions. Due to the complexity of O&G CH_4 emissions, modelling will always be a necessary component for bottom-up inventories, and as with any model, there will always be an associated uncertainty. Our results show that when using a Monte

Carlo approach, the total inventory uncertainty is strongly influenced by the distribution chosen to represent emissions. We also found that the uncertainty range increases with the use of more skewed distributions, which is important since measurements show that actual emissions show severe skewness. Since the Canadian inventory is constructed using simplified approaches, the current uncertainty range is unrealistically narrow given what we know about CH_4 emission distributions across Canada and the United States.

While our analysis certainly highlighted some of the challenges in modelling O&G CH_4 inventories, it also revealed some insights on how to improve current inventories using data and knowledge that exists today. First, emission factors (whether by component or site) can be updated with existing empirical data collected by academics and industry as part of regulatory compliance. The Canadian federal government currently uses measurements from two studies (CAPP 2005, Clearstone Engineering 2014) to derive component-level emission factors, which have a combined sample size of <300 sites (less than 0.001% of the total population). New and existing measurement data can improve emission factor representativeness, and statistical analysis on these measurements can determine whether emission factors should be partitioned by other factors rather than component-type only (as was done in our analysis). Second, incorporating the contribution of super-emitters in inventories (via distribution fitting or a simple addition) will likely produce a more realistic uncertainty range. Even though the distributions included in our analysis were not statistically comparable to empirical distributions, we think that they provide better quantification of uncertainty ranges compared to current methods that do not incorporate the heavy-tail at all. It is worth

mentioning that such improvements align with IPCC guidelines, and therefore would be relatively straightforward to implement in future estimates.

Finally, whenever possible, emission inventories should be validated with empirical measurements, as this is ultimately the best way to reduce large uncertainties. Although it would be logistically challenging to perform measurement validation on a large (provincial, national) scale, it could be easily done using a small geographic subset which would still be of significant value. Additionally, new advancements in top-down measurement solutions (i.e. satellite, aircraft) will further remove barriers associated with model validation.

References

Alvarez, R. A., Zavala-Araiza, D., Lyon, D. R., Allen, D. T., Barkley, Z. R., Brandt, A. R., Davis, K. J., Herndon, S. C., Jacob, D. J., Karion, A., Kort, E. A., Lamb, B. K., Lauvaux, T., Maasakkers, J. D., Marchese, A. J., Omara, M., Pacala, S. W., Peischl, J., Robinson, A. L., Shepson, P. B., Sweeney, C., Townsend-Small, A., Wofsy, S. C., Hamburg, S. P., 2018. Assessment of methane emissions from the U.S. oil and gas supply chain. *Science* 361, 186-188.

Brandt, A. R., Heath, G. A., Cooley, D., 2016. Methane leaks from natural gas systems follow extreme distributions. *Environmental Science and Technology* 50, 22, 12512-12520. DOI: https://doi.org/10.1021/acs.est.6b04303

Canadian Association of Petroleum Producers (CAPP), 2005. A National Inventory of Greenhouse Gas (GHG), Criteria Air Contaminant (CAC) and Hydrogen Sulphide (H_2S) Emissions by the Upstream Oil and Gas Industry, Vols. 1–5. Retrieved from: https://www.capp.ca/wp-content/uploads/2019/11/A_National_Inventory_of_GHG_CAC_and_H2S_Emissions_Volume_1-86220.pdf

Clearstone Engineering Ltd., 2014. Technical Report on Canada's Upstream Oil and Gas

Industry. Vols. 1–4. Prepared for Environment Canada. Calgary (AB)

Chan, E., Worthy, D. E. J., Chan, D., Ishizawa, M., Moran, M. D., Delcloo, A., Vogel, F., 2020. Eight-Year Estimates of Methane Emissions from Oil and Gas Operations in Western Canada Are Nearly Twice Those Reported in Inventories. *Environmental Science and Technology* 54, 23, 14899-14909. DOI: https://doi.org/10.1021/acs.est.0c04117

Environment and Climate Change Canada (ECCC), 2021. National Inventory Report 1990–2019: Greenhouse Gas Sources and Sinks in Canada. Retrieved from: http://www.publications.gc.ca/site/eng/9.506002/publication.html

Intergovernmental Panel on Climate Change (IPCC), 2001. Chapter 6 of Good Practice Guidance and Uncertainty Management in National Greenhouse Gas Inventories: Quantifying Uncertainties in Practice. Retrieved from: https://www.ipcc-nggip.iges.or.jp/public/gp/english/6_Uncertainty.pdf (accessed on November 17, 2021).

Intergovernmental Panel on Climate Change (IPCC), 2010. Use of Models and Facility-Level Data in Greenhouse Gas Inventories, Report of the IPCC Expert Meeting on Use of Models and Measurements in GHG Inventories. Retrieved from: https://www.ipcc-nggip.iges.or.jp/meeting/pdfiles/1008_Model_and_Facility_Level_Data_Report.pdf (accessed on December 19, 2021).

Johnson, M., Tyner, D., Conley, S., Schwietzke, S. and Zavala-Araiza, D. 2017. Comparisons of Airborne Measurements and Inventory Estimates of Methane Emissions in the Alberta Upstream Oil and Gas Sector. *Environmental Science and Technology* 51(21): 13008–13017. DOI: https://doi.org/10.1021/acs.est.7b03525

MacKay, K., Lavoie, M., Bourlon, E., Atherton, E., O'Connell, E., Baillie, J., Fougère, C., Risk, D., 2021. Methane emissions from upstream oil and gas production in Canada are underestimated. *Scientific Reports*, 11, 8041. https://doi.org/10.1038/s41598-021-87610-3

Petrinex, Alberta Public Data. Public data archives. Retrieved from: https://www.petrinex.ca/PD/Pages/APD.aspx

R Core Team. A language and environment for statistical computing, R Foundation for Statistical Computing, Vienna, Austria, www.R-project.org/.

Robertson, A. M., Edie, R., Field, R. A., Lyon, D., McVay, R., Omara, M., Zavala-Araiza, D., Murphy, S. M., 2020. New Mexico Permian Basin Measured Well Pad Methane Emissions Are a Factor of 5–9 Times Higher Than U.S. EPA Estimates. *Environmental Science and Technology*, 54 (21), 13926-13934. DOI: 10.1021/acs.est.0c02927

United Nations Framework Convention on Climate Change (UNFCCC), 1992. Retrieved from: https://unfccc.int/resource/docs/convkp/conveng.pdf (accessed on December 10, 2021).

Zavala-Araiza, D., Lyon, D. R., Alvarez, R. A., Davis, K. J., Harriss, R., Herndon, S. C., Karion, A., Kort, E. A., Lamb, B. K., Lan, X., Marchese, A. J., Pacala, S. W., Robinson, A. L., Shepson, P. B., Sweeney, C., Talbot, R., Townsend-Small, A., Yacovitch, T. I., Zimmerle, D. J., Hamburg, S. P., 2015. Reconciling divergent estimates of oil and gas methane emissions. *Proceedings of the National Academy of Sciences*, 112(51): 15597–15602. DOI: https:// doi.org/10.1073/pnas.1522126112

Zhang, Y., Gautam, R., Pandey, S., Omara, M., Maasakkers, J. D., Sadavarte, P., Lyon, D., Nesser, H., Sulprizio, M. P., Varon, D. J., Zhang, R., Houweling, S., Zavala-Araiza, D., Alvarez, R. A., Lorente, A., Hamburg, S. P. Aben, I., Jacob, D. J., 2020. Quantifying methane emissions from the largest oil-producing basin in the United States from space. *Science Advances*, 6, 17, eaaz5120. DOI: 10.1126/sciadv.aaz5120

5. Aircraft-based measurements of methane emissions from Canada's offshore oil industry

5.1 Preface

This chapter has not been submitted to a journal at the time of writing. Due to significant challenges and uncertainties in the Gaussian approach for estimating emission rates in marine environments, further analysis is planned prior to submission for peer review, which will include a full mass balance analysis as noted in the future work section of this chapter. I led the writing, data collection, and analysis included in this chapter. My colleagues Lindi Coyle, Isaac Ketchum and supervisor David Risk assisted with campaign preparation and data collection. Colleagues Afshan Khaleghi and Evelise Bourlon helped with the analysis of data, and my supervisors David Risk and Lesley James provided valuable guidance and feedback throughout the analysis and writing of the manuscript. Everyone listed here will be listed as co-authors when a manuscript is submitted.

5.2 Abstract

Methane emissions from offshore oil and gas production are poorly understood and are rarely quantified using direct measurements. In this study, we collected the first independent measurements of methane emissions from Canada's offshore oil platforms, located 300-350 km off the coast of Newfoundland and Labrador. Aircraft-based measurements were used to estimate the offshore industry's contribution to Canada's CH_4 inventory, and to assess whether the platforms emissions are in line with current federally reported estimates. Our measurements revealed that Canada's offshore platforms emit an

average of 10,039 m^3 CH_4 day^{-1} (6.8 tonnes CH_4 day^{-1}), which is comparable to federal estimates reported in 2019. Production-weighted methane intensities calculated using measured emission rates and reported oil production show that Canadian offshore production is ranges from 1.3-6.1 kg CO_2e/bbl, making it among the least methane-intensive oil produced in all of Canada.

5.3 Introduction

As part of many new aggressive climate change targets and commitment to "net zero" greenhouse gas emissions by 2050, Canada has committed to significant reductions of methane (CH_4) emissions in coming years. CH_4 is a powerful greenhouse gas with the ability to trap heat 25 and 84 times better than carbon dioxide (CO_2) over 20 and 100-year timeframes, respectively (Myhre et al. 2013). The oil and gas (O&G) sector is Canada's largest emitter of CH_4, making up nearly half (44%) of the national total in 2019 (ECCC 2021), and newly enforced regulations are aiming to reduce this amount by 45%, by 2025 (ECCC 2018). While this reduction target includes the offshore sector, Canada's offshore oil production is thought to be the least CH_4 emissions-intensive oil produced in Canada (CAPP 2021). However, this is based on self-reported estimates that have not been independently validated using direct measurements of platform CH_4 emissions.

Compared to onshore production, research on emissions from offshore O&G production is scarce, likely in part due to the assumption that offshore platforms have low emissions because of increased safety protocols (e.g. 24 hour surveillance, no routine

venting, frequent leak surveys). Additionally, the remote nature of the facilities adds logistical challenges and increases the cost of measurement campaigns. In efforts to fill this gap, offshore O&G platforms in other parts of the world have recently been measured, like in the Gulf of Mexico and the North Sea, and these studies have found variable results. In some cases, offshore platforms are emitting more than expected (Gorchov Negron et al. 2020, Riddick et al. 2019), and in other cases measured emissions were more than an order of magnitude lower than reported estimates (Zavala-Araiza et al. 2021). For example, Gorchov Negron et al. (2020) found that offshore CH4 emissions in the U.S. Gulf of Mexico were 0.53 Tg/yr (2.9% loss rate) which is two times higher than the value reported in the EPA GHGI. In contrast, Zavala-Araiza et al. (2021)'s estimate for the Mexican offshore production in the Gulf of Mexico is 2800 kg/hr, which is ten times lower than the value reported in the Mexican national greenhouse gas inventory estimate. However, authors note that the Mexican GHG inventory uses a non-Mexican specific emission factors in their calculations, which could be the reason for the observed discrepancy (Zavala-Araiza et a. 2021). Similar work has yet to be done in Canada's offshore, where oil is produced via four production facilities located 300-350 km off the coast of Newfoundland and Labrador (NL). Considering these new findings, and Canada's commitment to reducing the carbon footprint of our O&G industry, in situ measurements of Canada's offshore CH_4 emissions is both important and necessary.

In this study, we collected the first independent direct measurements of CH_4 emissions from three of NL's offshore oil platforms: Hibernia, Hebron, and Sea Rose. Aircraft-based measurements and a Gaussian plume model were used to estimate the

offshore industry's contribution to Canada's CH_4 inventory, and to derive production-weighted emission intensities for each platform. Aircraft measurements were conducted during routine production and should be representative of typical emission levels. We compare our results to other platforms that have been the focus of similar work, and to Canadian onshore environments which are thought to have higher CH_4 intensity.

5.4 Study areas

5.4.1 Offshore production platforms

Newfoundland and Labrador's offshore industry comprises of four production platforms, all of which produce oil from the Jeanne d'Arc Basin, located 300-350 km southeast of St. John's (Figure 5.1) (C-NLOPB 2021a). The individual producing reservoirs within the basin that platforms currently produce from are the Hibernia, Ben Nevis-Avalon, and Jeanne d'Arc Formations (C-NLOPB 2021a). Current platforms producing oil offshore are named Hibernia, Hebron, Sea Rose, and Terra Nova (Figure 5.1). There are no pipelines that service NL's offshore, therefore all produced oil is transported to shore via transhipment vessels.

Hibernia (Figure 5.2), the oldest platform, is a Gravity Based Structure (GBS) that consists of a 224 m high platform that sits directly on the ocean floor. It has a production capacity of 230,000 barrels of crude oil per day (HMDC 2021). Hibernia has been producing oil since 1997, and produced 36.2 million barrels of oil (MMbbl) in 2021 (C-NLOPB 2022). The Hebron platform (Figure 5.2) similarly uses a GBS for oil production,

and has been producing oil since 2017 (C-NLOPB 2021a). In 2021, Hebron produced 50.6 MMbbl of oil (C-NLOPB 2022).

The two other platforms, Sea Rose (Figure 5.2) and Terra Nova, produce oil via a Floating, Production, Storage and Off-Loading vessel (FPSO). The Terra Nova FPSO is one of the largest FPSO's ever built, standing at 18 stories high and a storage capacity of 960,000 barrels of oil (Suncor Energy Inc. 2021). The Terra Nova FPSO was docked (for maintenance) during our 2021 measurement campaigns, and therefore was not included in this study. The Sea Rose FPSO began producing oil in 2005, and produced 7.3 MMbbl of oil in 2021 (C-NLOPB 2022). The Sea Rose has two satellite extensions, North Amethyst and South White Rose, which both produce back to the FPSO (Husky Energy 2020). Figure 5.3 shows monthly production history (MMbbl) from 1997-2021 for all producing fields (C-NLOPB 2022).

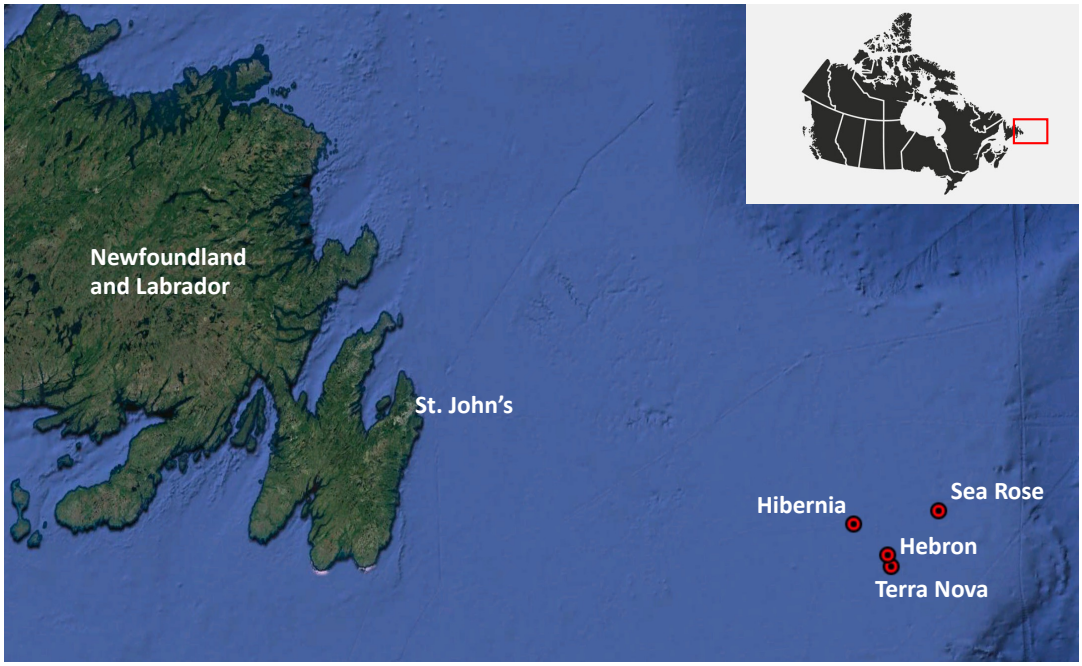

Figure 5.1. Locations of Canada's offshore production platforms. Note that Terra Nova was docked for maintenance at the time of measurements.

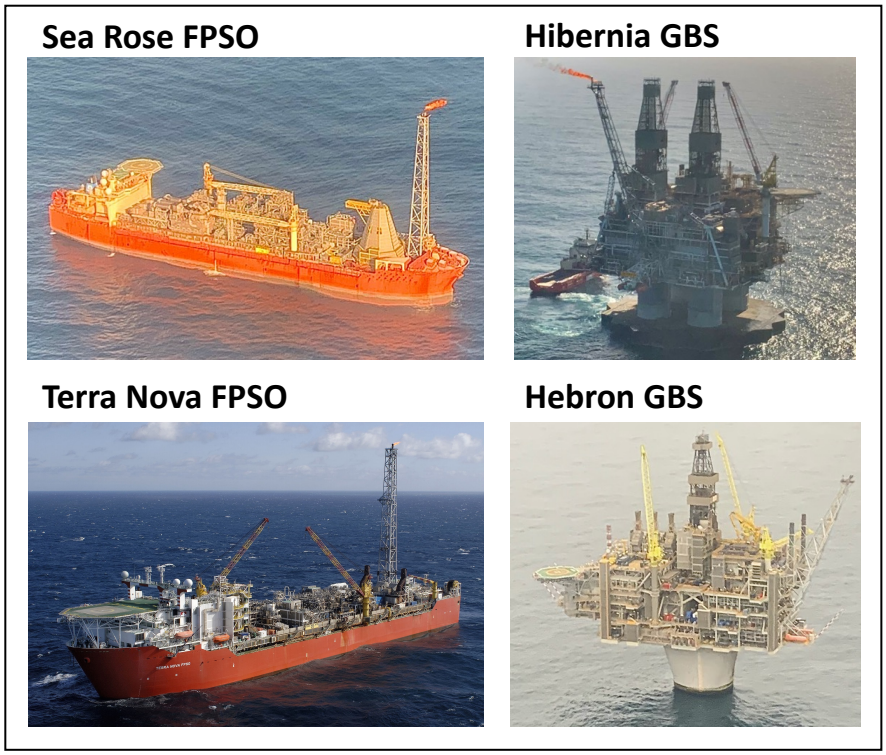

Figure 5.2. Photos of Canada's offshore production platforms. Note that Terra Nova was docked for maintenance at the time of measurements (Terra Nova image source: Suncor Energy).

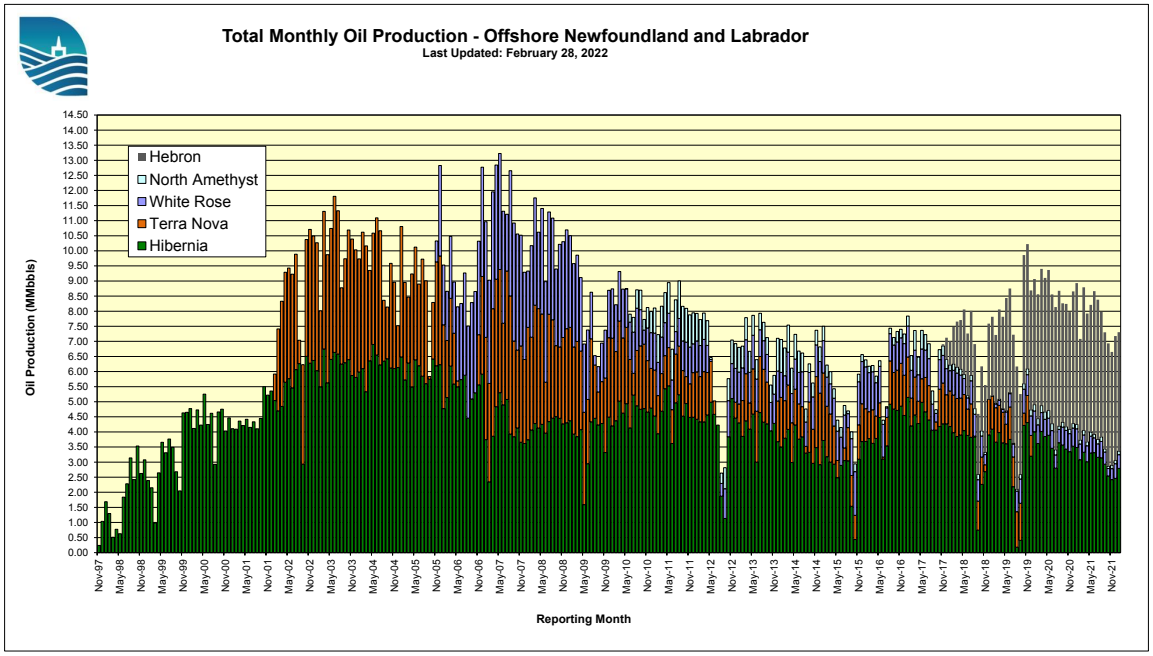

Figure 5.3. Monthly production history (November 1997 – 2021) for all producing fields. Note that the SeaRose FPSO produces from the White Rose and North Amethyst fields (C-NLOPB 2022).

5.4.2 Reported platform emissions and sources

NL's offshore oil production is the second largest source of CH_4 in the province (behind solid waste disposal) (ECCC 2021). CH_4 emissions for each platform are submitted annually to Canada's Greenhouse Gas Reporting Program (GHGRP), which at the time of writing, shows reported CH_4 emissions for all platforms up to 2019. Figure 5.4 shows reported emissions from 2004 to 2019 for each platform measured in this study, and Figure 5.5 shows the historical carbon intensity for each platform (calculated using reported emissions and production) (C-NLOPB 2022, Government of Canada 2021).

To date, gas that is produced offshore NL is not monetized or brought to market. Instead, all produced gas is either reinjected, used onsite as fuel, or flared (C-NLOPB 2021b). Figure 5.6 shows reported cumulative (up to 2021) gas production and gas disposition (Bscf) for NL's offshore production fields. Considering how produced gas is used offshore NL, there are three main sources of CH_4 emissions from offshore platforms: flaring, power generation, and fugitive equipment leaks. CH_4 emissions from flaring and power generation occur when there is inadequate combustion efficiency (i.e. not 100%), meaning that a portion of the gas is not combusted into CO_2, resulting in a release of CH_4. Fugitive leaks can occur from any compromised equipment (e.g. broken seal on valves) along the gas train.

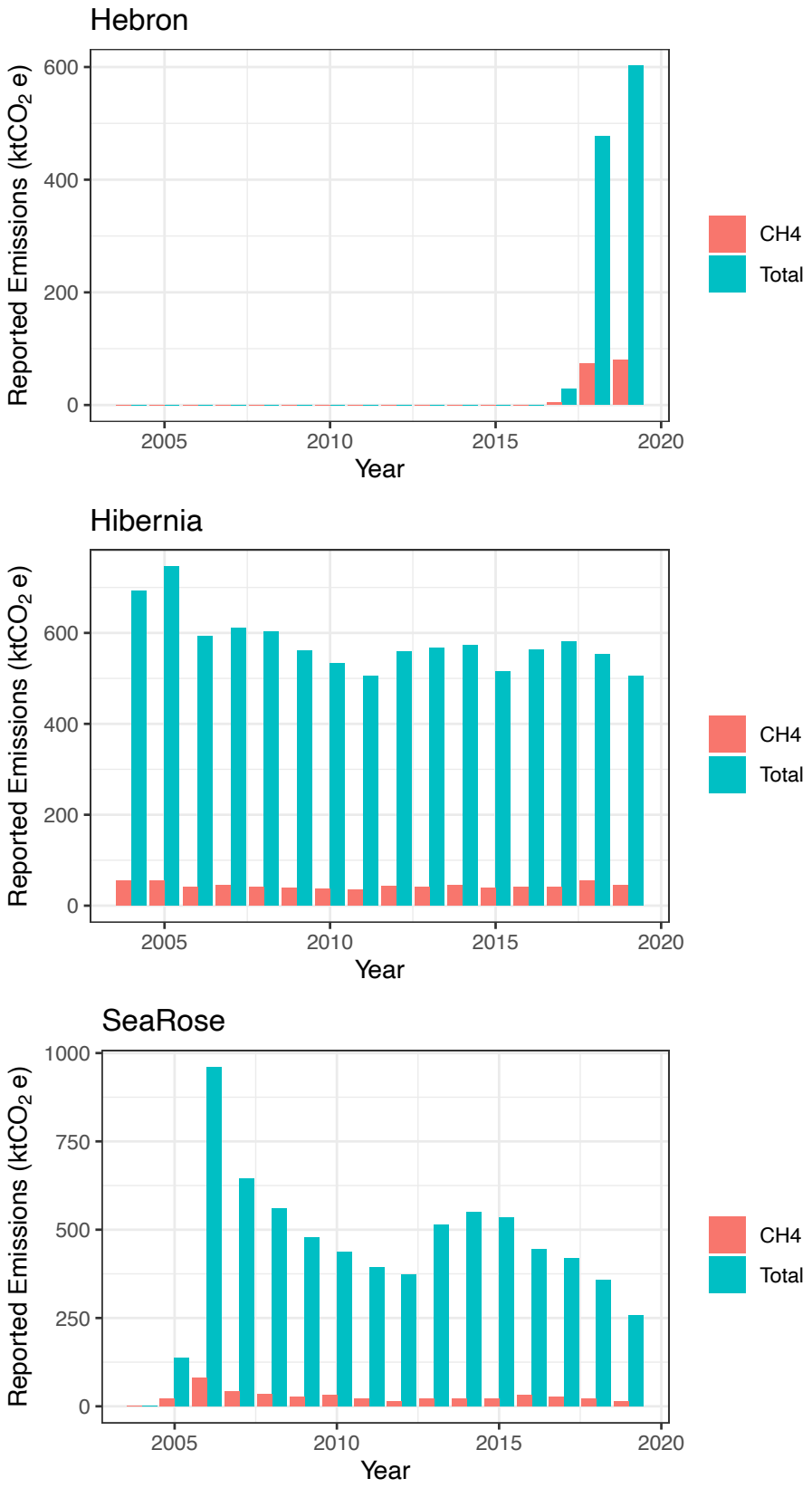
Hebron
Reported Emissions (ktCO2 e)
600
400
200
0
2005
2010
2015
2020
Year
CH4
Total
Hibernia
Reported Emissions (ktCO2 e)
600
400
200
0
2005
2010
2015
2020
Year
CH4
Total
SeaRose
Reported Emissions (ktCO2 e)
1000
750
500
250
0
2005
2010
2015
2020
Year
CH4
Total

Figure 5.4. Annual emissions for each platform reported to the GHGRP (2004-2019).

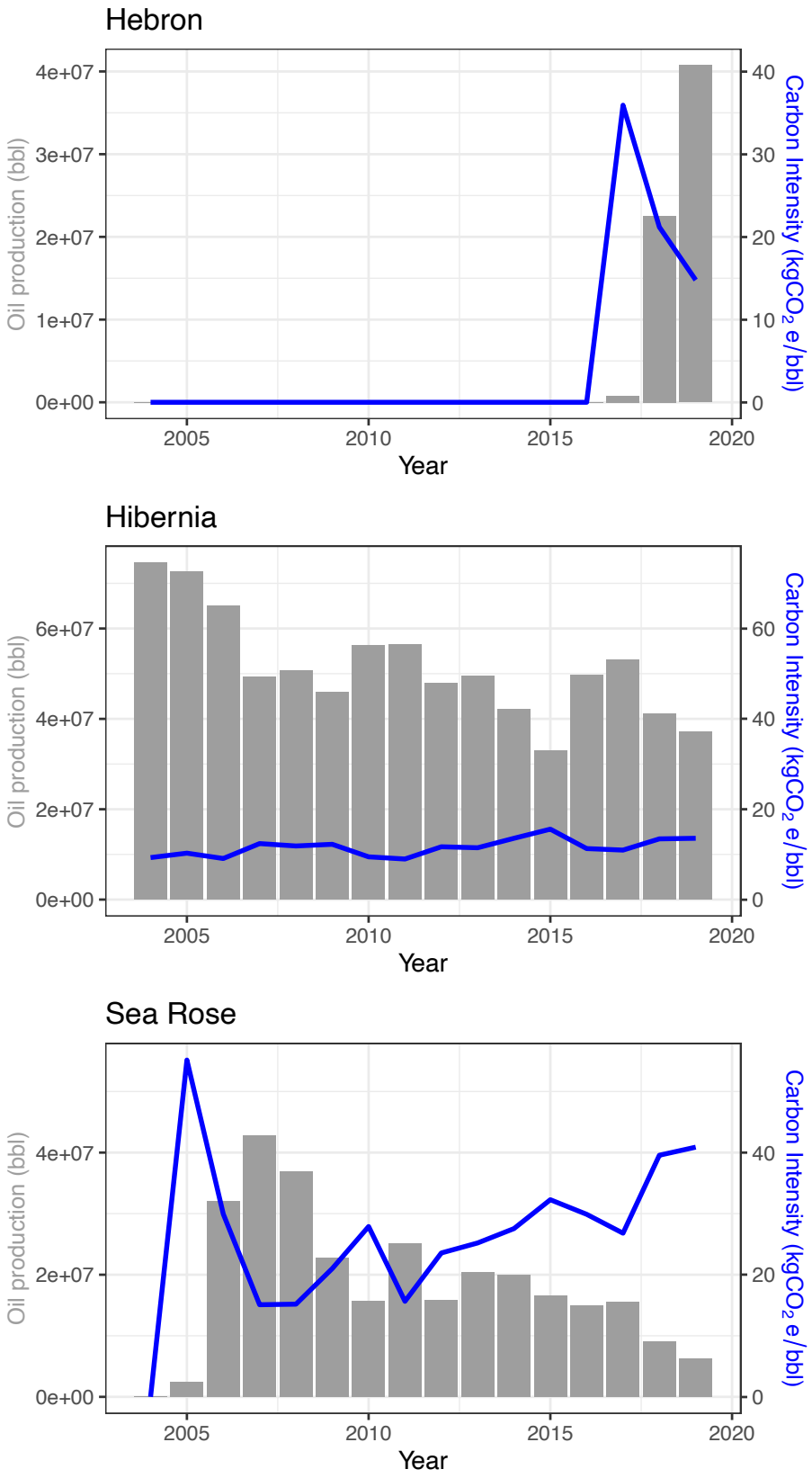
Hebron
Oil production (bbl)
4e+07
3e+07
2e+07
1e+07
0e+00
2005
2010
2015
2020
Year
Carbon Intensity (kgCO2 e/bbl)
40
30
20
10
0
Hibernia
Oil production (bbl)
6e+07
4e+07
2e+07
0e+00
2005
2010
2015
2020
Year
Carbon Intensity (kgCO2 e/bbl)
60
40
20
0
Sea Rose
Oil production (bbl)
4e+07
2e+07
0e+00
2005
2010
2015
2020
Year
Carbon Intensity (kgCO2 e/bbl)
40
20
0

Figure 5.5. Annual oil production and carbon intensities for each platform based on reported oil production and total GHG emissions reported to the GHGRP (2004-2019).

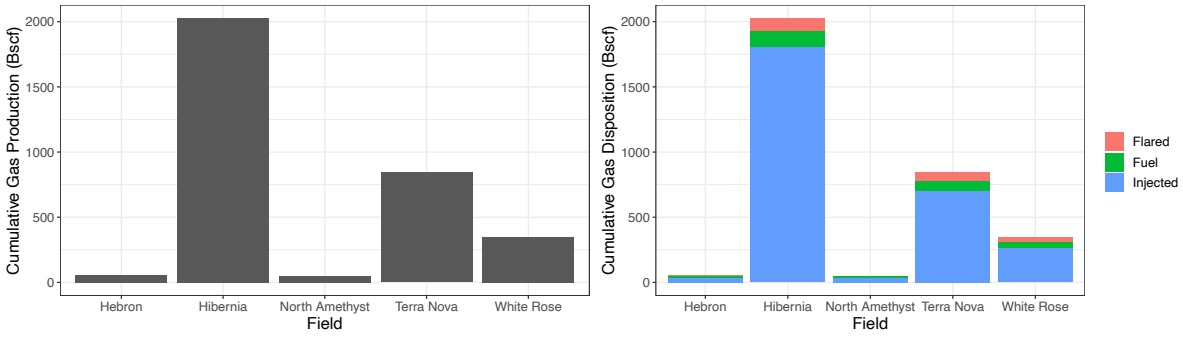

Figure 5.6. Cumulative gas production (up to 2021) and gas disposition for offshore production fields (C-NLOPB 2021b).

5.5 Methods

5.5.1 Overview

Our methods can be summarized into four main steps (Figure 5.7), which are as follows. 1) A twin-otter aircraft was outfitted with instrumentation to measure gas concentrations and meteorology continuously. 2) Measurement flights were completed, which involved orbiting the platform several times, and flying horizontal transects downwind of each platform at varying heights. 3) Raw timeseries data were processed and used in a Gaussian dispersion model to estimate CH_4 emission rates (m^3 day^{-1}) for each plume. 4) Per-plume emission rates were used to derive average emissions and production weighted emission intensities per platform. Additional details on each step are described in the subsections below. The general measurement approach described here has been demonstrated across multiple flight campaigns in both on (Baray et al. 2018, Johnson et

al. 2017) and offshore (France et al. 2021, Gorchov Negron et al. 2020) regions, though quantification approaches differ across studies.

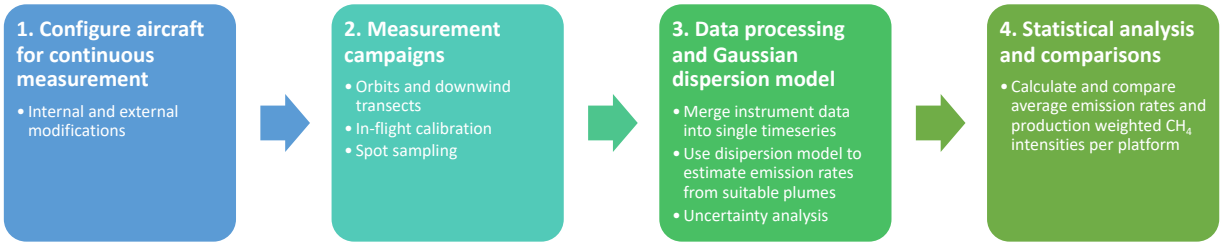

Figure 5.7. Overview of the study methods and workflow.

5.5.2 Aircraft instrumentation

A Twin Otter aircraft (Figure 5.8) was used to measure CH_4 emissions around offshore platforms. The Twin Otter was equipped with a Picarro 2210-i gas analyzer to measure continuous concentrations of CH_4, CO_2, and C_2H_6 (Picarro Inc.). The Picarro has a measurement frequency of 1.5 Hz and a precision of <0.1 ppb for CH_4. A CR1000x Campbell Scientific datalogger was used to log the 1.5 Hz Picarro data to a MicroSD. An AIMMS-30 measurement system (Aventech Research Inc.), consisting of an Air Data Probe (ADP), two GPS antennas, and a Central Processing Module (CPM), was also installed on the aircraft to measure aircraft position (latitude, longitude, elevation), temperature, pressure, relative humidity, wind speed, and three-dimensional wind direction. The GPS antennas were mounted on top of the wings, and the probe was mounted on the fuselage above the cockpit. GPS data meteorological data is logged by the CPM, which stores all data directly at 1 Hz frequency to an integrated USB FLASH memory drive. The AIMMS-30 system has a windspeed accuracy of 0.5 m/s, a temperature accuracy of 0.3 °C, a relative humidity accuracy of 2% and was calibrated

during a test flight. Raw wind data were manually checked and compared to local meteorological stations to ensure wind measurements were accurate and not impacted by flight maneuvers.

Two rear-facing air inlets were secured outside the co-pilot door (Figure 5.8). Two diaphragm pumps drew ambient air from the inlets through ¼ inch Synflex tubing, with one line connecting directly to the Picarro analyzer for continuous measurements, and the other connected to the bag sample system (described below) for spot sampling of plumes. During flights, time-series concentration data recorded by the Picarro is viewed in real-time using a laptop, which provided visual indications of when we were measuring CH_4 plumes.

Given the lengths of tubing that the air needs to travel through to the Picarro, and the Picarro's response time, there is lag in the recorded concentration time series that needs to be corrected in post-processing. The lag time for the aircraft setup was determined by performing a series of "breath tests", which involves breathing into the air inlets and measuring the time it takes for the Picarro to respond. The lag time for our set up was 49 and 56 sec, respectively for October and November campaigns, and these offsets were applied to data in post-processing. We note that the lag time for the instrument can vary from significant changes in altitude, however this was not an issue for our measurements as we flew steadily at lower altitudes.

Figure 5.8. Twin otter aircraft used for measurements. Locations of rear-facing inlets for atmospheric air sampling are shown on the right. The AIMMS-30 air data probe can (red) is visible on the left photo.

5.5.3 In-flight calibration

In-flight calibration of the Picarro gas analyzer was performed twice per flight using a gas cylinder filled with breathing grade air mounted to the back wall of the aircraft. During each calibration, the Picarro continuously measured air from the cylinder for five minutes to ensure equilibrium of measured values were reached. Negligible analyzer drift was observed across calibrations (see Appendix for summary statistics), as expected given the high precision of the Picarro and its well documented resistance to drift (Picarro Inc. 2022).

5.5.4 Sampling strategy

Two different sampling procedures were completed at each platform, as shown in Figure 5.9. The first procedure involved flying 6-10 stacked orbits around the platforms (~600 – 1000 m radius), starting at the lowest possible altitude (~150 m ASL), and increasing

altitude in between individual orbits by roughly 100 m. This procedure allowed us to capture the full profile of the plume. The second procedure involved flying 3-6 transects about 1.5 – 15 km downwind (perpendicular to prevailing wind direction) of the platform. For the downwind transects, we flew at various altitudes (in ~100 m increments), allowing us to capture vertical and horizontal profiles of the plume.

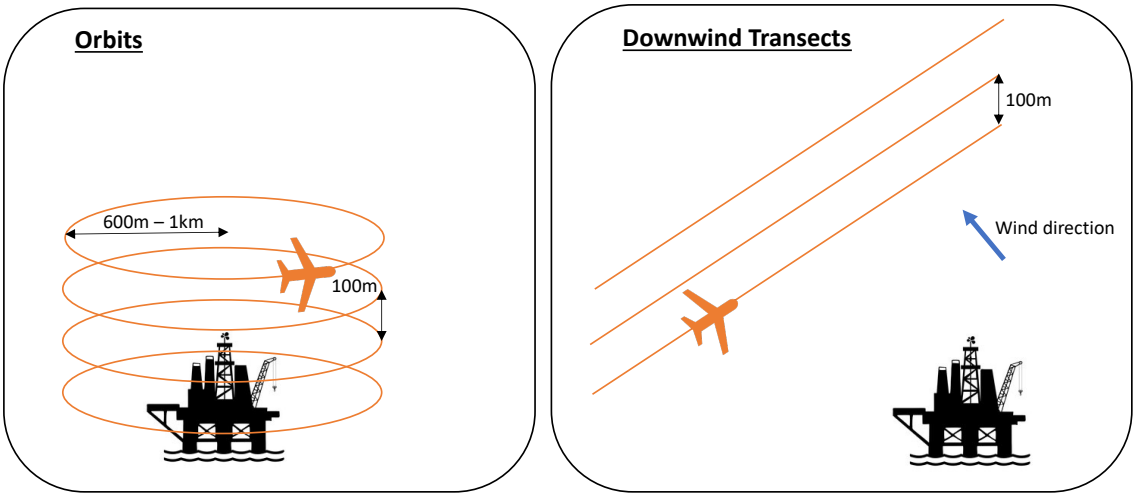

Figure 5.9. Cartoon schematic of the two sampling procedures followed during measurement campaigns.

5.5.5 Spot sampling of observed plumes

Periodic samples of air were collected during offshore flights for isotopic analysis of observed CH_4 plumes. Air samples were collected in 1L Tedlar bags during flights using a custom designed delay system, which was based on recommendations from France et al. (2021). To increase probability of successfully capturing observed plumes in bag samples, we created an artificial delay that was longer than response time of the Picarro

analyzer, since the Picarro's real-time data viewer was used to indicate when a plume was detected.

The custom-made delay system consisted of a 12V diaphragm pump that pulled air from the outside inlet at a rate of ~10 standard litres per minute (SLPM). This inlet was separate from the inlet to the Picarro analyzer. The pump then pushed air into a T-Splitter, where it split into two coils of tubing. One coil was about 80 m of 1/4 inch Synflex tubing, and the other was about 2 m of 1/8 inch ID Vinyl tubing. The lengths of tubing were calculated based on the flowrates of the pumps and the lag time from the Picarro and lengths of tubing. The 80 m Synflex tubing stores a timeseries of the air moving at a calculated speed. The 'resistance' (vinyl) tubing diverts some of the flow, slowing the rate of airflow going through the Synflex/Tedlar bag. However, considering the speed at which the aircraft is passing through the plume, we assumed the actual timeseries of the plume could be as little as eight seconds, and therefore we needed a mechanism to speed up the flow into the bag. This was achieved by attaching a manual valve to the end of the resistance tubing, which, when closed, quickly forced all the airflow through the Synflex tubing and into Tedlar bags. Prior to flights, the delay system was tested by breathing into the air inlets and collecting a bag sample using the procedure describe above and comparing bag sample concentration to the peak from the breath.

5.5.6 Emission rate estimates via Gaussian plume model

Following the measurement campaigns, data from individual instruments were processed and merged into consistent timeseries. We then manually selected plume measurements suitable for Gaussian dispersion. The Gaussian plume model has been previously used to estimate CH_4 emissions from onshore (e.g. O'Connell et al. 2019, Zavala-Araiza et al. 2018) and offshore (e.g. Riddick et al. 2019, Yacovitch et al. 2020) oil and gas facilities. The basis of Gaussian plume model is that the downwind mole fraction of a gas is a function of downwind distance from a point source, and is dependent on the source flux rate, horizontal wind speed (m/s), and the rate of dispersion (Riddick et al. 2019). The original equation, which solves for downwind concentration enhancement, can be rearranged to solve for the emission rate at the source:

$$Q = \frac{2\pi\sigma_y\sigma_z uC}{exp\left(-\frac{(h_m-h_s)^2}{2\sigma_z^2}\right)+exp\left(-\frac{(h_m+h_s)^2}{2\sigma_z^2}\right)} \quad (5.1)$$

where Q is the emission rate of the point source, u is the prevailing windspeed (m/s), C is the CH_4 concentration enhancement downwind (ppmv), h_m is the measurement height (m), h_s is the source height (m), and σ_y and σ_z are dispersion coefficients representing the horizonal and vertical distribution of the plume at the point of measurement. The model relies on assumption that the plume is dispersing according to a Gaussian distribution, and that the emission rate and wind speeds are constant at the time of measurement. An example calculation is shown in the Appendix.

Since C is the CH_4 concentration enhancement above ambient background, we had to calculate background concentrations of CH_4 to subtract from the raw CH_4

measurements. Background CH_4 was calculated using the average of 30 seconds of measurements from either side of the plume, as done in other offshore measurement studies such as France et al. (2021) and Gorchov Negron et al. (2020). We did this calculation separately for every observed plume, as background CH_4 can vary due to changes in atmospheric stability. The source height was estimated for each platform based on publicly available descriptions of the platform heights. σ_y and σ_z parameters were estimated using the Pasquill-Gifford stability class scheme and corresponding equations defined by Turner (1994).

5.5.7 Emission rate uncertainty

We identified three main sources of uncertainty in our emission rate estimates, related to estimated parameters used in the Gaussian plume model: 1) background concentration, 2), source height and 3) stability class. We used the standard deviation of every set of measurements used to calculate ambient background to estimate the magnitude of uncertainty related to our estimated background concentrations. Overall, we estimated that the uncertainty related to this parameter is less than ±10%, which is negligible compared to other uncertainties discussed below.

Since we do not know the exact source height of platform emissions (i.e. flare or platform deck), we calculated an emission rate for all plumes using both the deck height and the flare height for each platform, and included both results in our analysis. We took a similar approach to addressing uncertainty related to stability class, which was by far

the biggest source of uncertainty in this study. Through our analysis, we found that changes in stability class can result the emission rate to vary by an order of magnitude, which is especially significant because it was extremely hard to confidently select a stability class based on our empirical data alone. We tried several of the "standard" methods to estimate stability classes for our measurements, using measured windspeed, daytime insolation, wind direction, and vertical temperature gradients. We also tried the method used in Yacovitch et al. (2020), in which σ_y is calculated directly from measurements transecting the plume, and then σ_y and the downwind distance from the source are used to do a reverse look up of the Pasquill-Gifford stability class that is closest to the measured σ_y. For several of our measurements, each method indicated in a different stability class, therefore making it difficult to confidently select one for emission rate estimates. As a result, individual emission rates for each plume were calculated under a range of realistic stability classes (A – F), and the overall mean is used for subsequent analysis and comparisons. The upper and lower limits from all estimates (calculated using different source heights and stability classes) are used as the uncertainty range for each measured plume.

5.5.8 Methane intensity

We calculated CH_4 intensities in grams of carbon dioxide equivalent per megajoule (gCO_2e/MJ) and kilograms of carbon dioxide equivalent per barrel of oil ($kgCO_2e/bbl$) for each platform using our estimated emission rates and reported oil production (2021). Average emission rates for each platform were converted to CO_2e using a CH_4 density

678 g/m^3 (15ºC, 1 atm), and a global warming potential of 25. Although some studies recommend using a higher GWP for methane (e.g. using the 20-year timeframe), we chose to use the 100-year GWP for methane as it still remains the standard in Canadian and international inventories. Oil production was converted to megajoules using a conversion rate of 1 m^3 = 38,510 MJ (light crude) (Canada Energy Regulator 2016).

5.6 Results and Discussion

5.6.1 General

Flights occurred during two campaigns in the fall of 2021. The first campaign took place from October 6th – October 11th, 2021, and the second campaign ran from November 7th – November 10th, 2021. A total of nine offshore flights were conducted across both campaigns. Flights were constrained by weather, in that we only flew offshore on days with low-moderate wind speeds and clear skies. Due to the Twin Otter's maximum fuel range (~5 hours) and the ~1 hour transit to and from the platforms, only one platform was measured per flight. All platforms were measured three different times via stacked downwind transects and stacked orbits as described above, with each visit considered a unique measurement. Figure 5.10 shows the nine flight tracks completed during both campaigns. Table 5.1 is a summary of the flights, including the date, time, platform, and the number of individual transects that were completed during each flight.

A total of 41 downwind transects were completed across nine flights (Table 5.1). During downwind transects, 19 CH_4 plumes were detected on eight flights. Here, a plume is defined as persistent CH_4 enhancements (above background, measured across several

seconds) that are clearly distinguishable when viewing the timeseries concentration data. SR1 was the only flight where no clear CH_4 plumes were observed. However, through discussions with the operator, we learned that the Sea Rose platform was undergoing a planned shutdown at the time this flight occurred, which explains why no plumes were detected during the flight. That said, our measurements suggest that CH_4 emissions during this shutdown were minimal (if any at all), which is noteworthy as inactive facilities still have a potential to emit (via fugitive leaks).

Table 5.1: Summary of offshore flights.

Date (dd/mm/yyyy)	Local Time	Platform	Flight ID	Number of transects
06/10/2021	13:45 - 14:45	SeaRose	SR1	3
07/10/2021	10:00 - 11:00	Hibernia	HI2	5
07/10/2021	14:45 - 16:00	Hibernia	HI3	4
11/10/2021	12:55 - 13:45	Hebron	HE4	4
07/112021	9:20 - 10:20	SeaRose	SR5	5
08/11/2021	9:25 - 10:20	Hebron	HE6	6
08/11/2021	14:20 - 15:10	Hebron	HE7	5
10/11/2021	9:00 - 10:00	Hibernia	HI8	4
10/11/2021	13:15 - 14:05	SeaRose	SR9	5

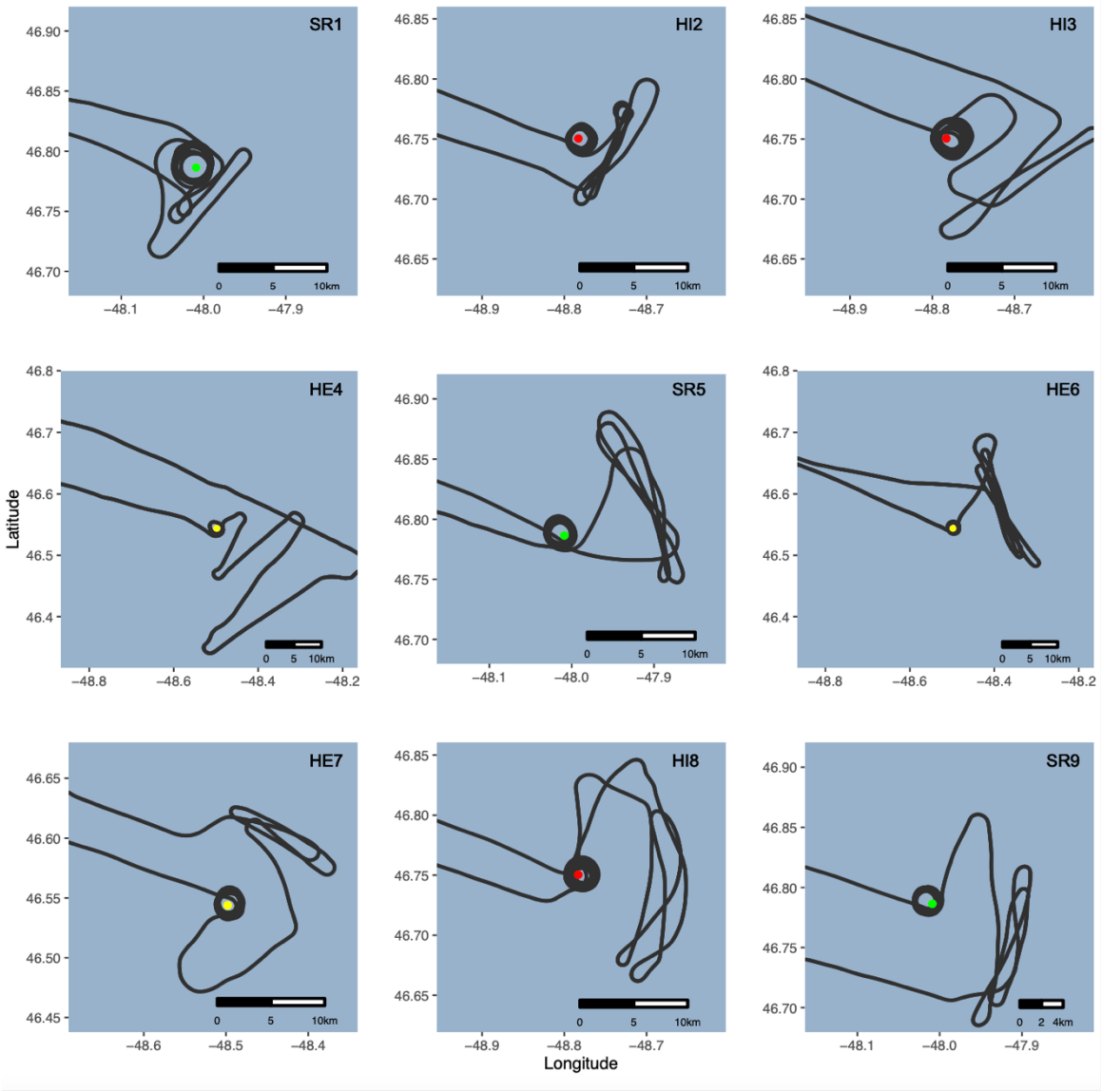

Figure 5.10. Flight tracks for all flights completed during two campaigns in October and November 2021. Offshore platforms are shown by colored dots (green = SeaRose, red = Hibernia, yellow = Hebron).

5.6.2 Complex boundary layer conditions

During some flights, the conditions of the marine boundary layer made measuring CH_4 plumes from the platforms challenging. Specifically, on the two flights completed on November 11th (HI8 and SR9), potential temperature increased steadily with height, suggesting that the boundary layer was partly stratified (France et al. 2021). Under these conditions, CH_4 varies linearly with height (example shown in Figure 5.11), and concentration enhancements from platform emissions become hard to differentiate from the variable background. Additionally, emissions can also become trapped in vertically thin layers, increasing the chances for plumes to be missed altogether (France et al. 2021). As a result, only one clear CH_4 plume was observed on SR9 (Figure 5.11, circled in red), and only two plumes were observed on HI8.

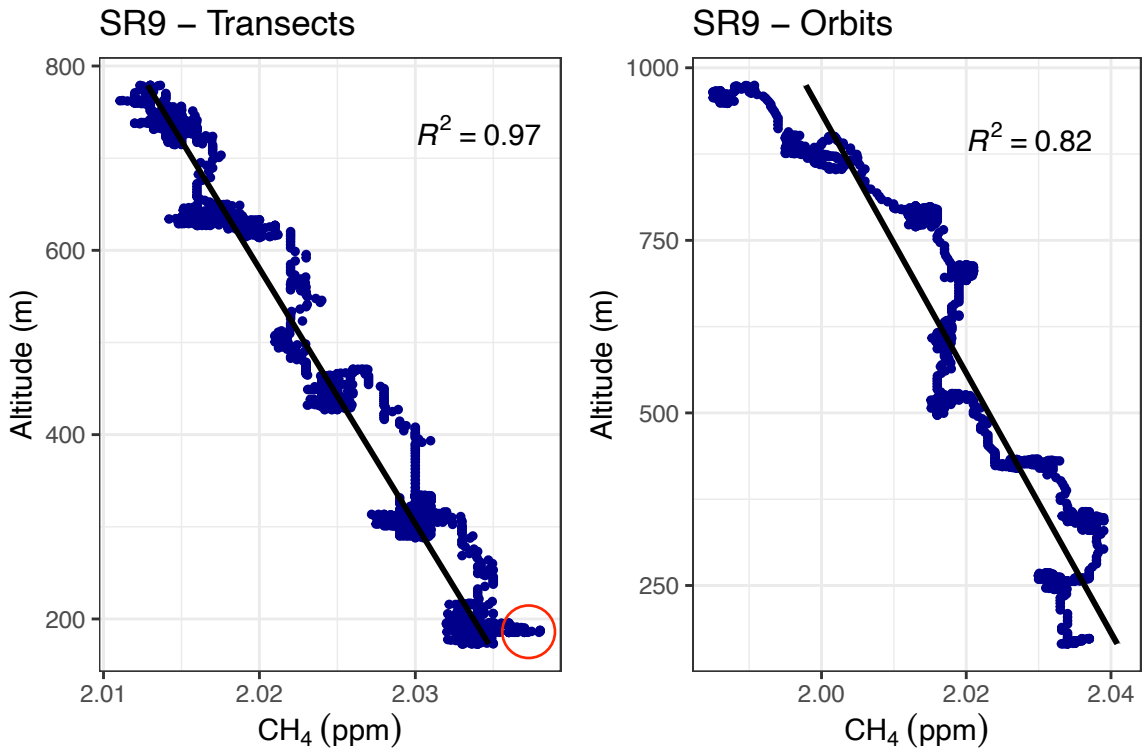

Figure 5.11. Measured CH_4 concentrations at differently altitudes flown during transects and orbits on Flight SR9 (November 11th). On this day the marine boundary layer was stratified, causing CH_4 to vary linearly with height. As a result, only one clear CH_4 plume (circled in red) was observed during a downwind transect at low altitude (187 m).

On days when boundary layer is well mixed, CH_4 stays relatively constant with altitude, and potential temperature also remains constant (neutral stratification of the boundary layer) (France et al. 2021). These conditions make it easier to identify plumes that meet the criteria for Gaussian dispersion emission rate estimates. Figure 5.12 shows the observed differences between a stratified (SR9) and well mixed (HE6) marine boundary layer. Here we can see that during flight SR9, CH_4 steadily decreases with height, making any potential emissions hard to differentiate from the background variability. In contrast, during flight HE6, CH_4 is relatively stable with height, and deviations from measured emissions are easily distinguishable from background.

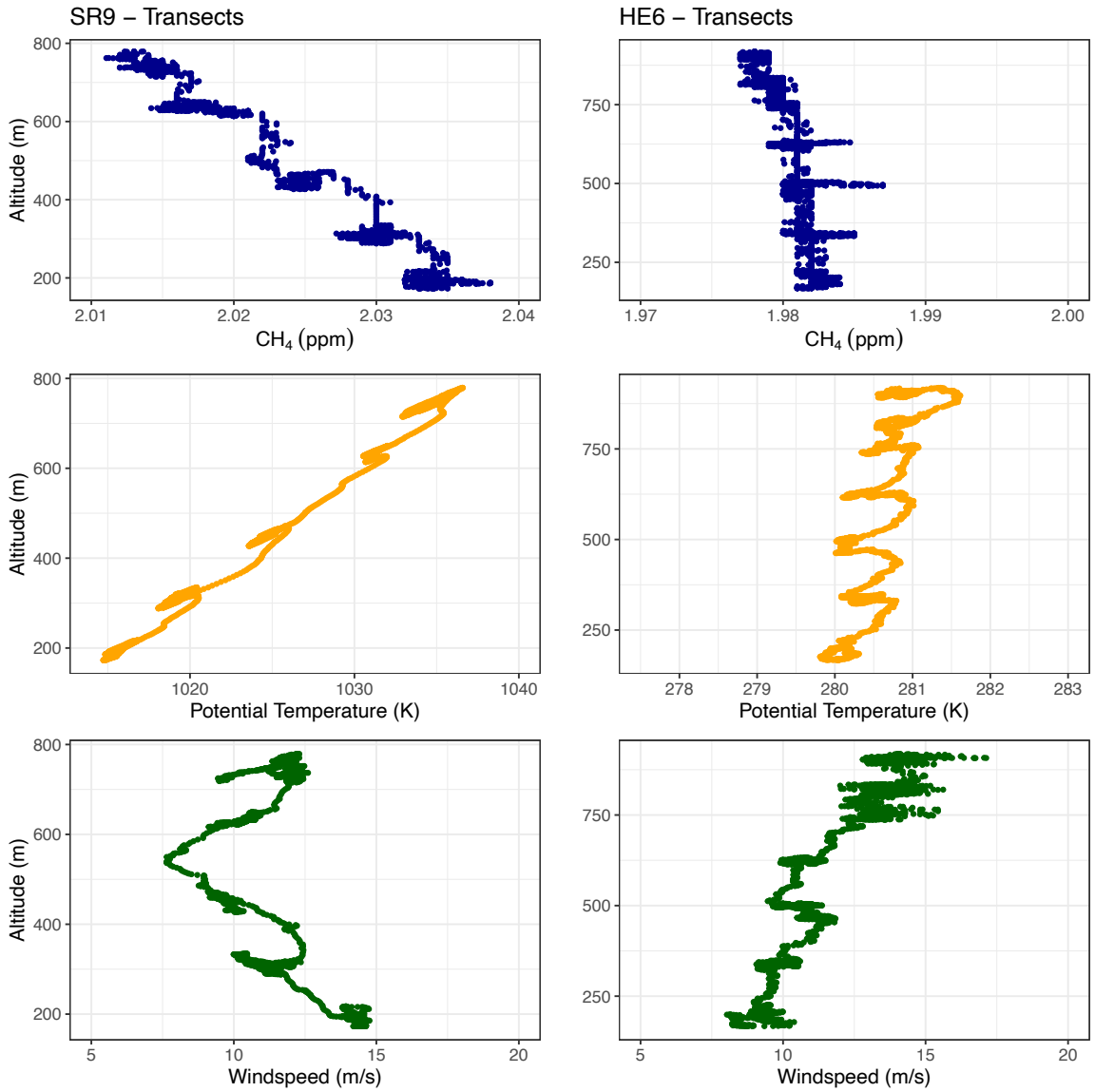

Figure 5.12. Measured variability of CH_4 concentrations, potential temperature, and windspeed at different flying altitudes for a stratified (SR9) and well mixed (HE6) boundary layer.

5.6.3 CH_4 emission rate estimates

After carefully observing measured meteorological conditions, time series concentrations of gases, and plume characteristics, 15 out of 19 plumes measured during downwind transects were identified as suitable for Gaussian dispersion estimates. Of those, ten were from Hebron, four were from Hibernia and one was from Sea Rose. Reasons why four plumes were determined as unsuitable for emission rate estimates are discussed below.

Figure 5.13 shows an example of an ideal plume measurement deemed appropriate for dispersion calculations. On this day (flight HE4), the boundary layer was well mixed, with consistent wind speeds and direction dispersing the plume in Gaussian form. We also flew transects at varying horizontal distances on this flight (instead of stacked transects as was done on all other flights) because the cloud ceiling was very low, preventing us from flying at higher altitudes during measurements. The plume was intercepted four times, allowing for four emission rates to be calculated (one per plume).

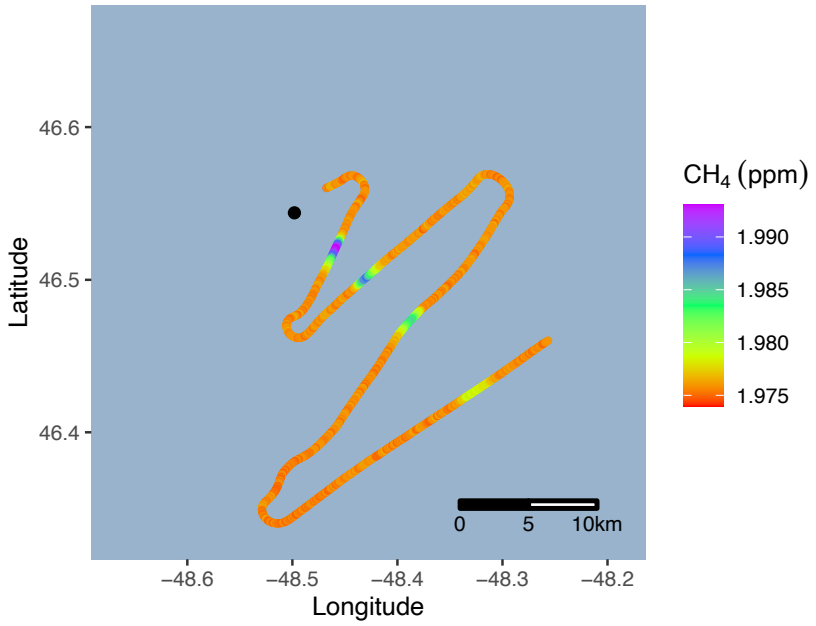

Figure 5.13. Map of downwind transect measurements for HE4. Colors of individual points represent measured CH_4 concentrations, with blue and purple colors showing the CH_4 enhancements from the emitting platform (black dot).

As mentioned, boundary layer conditions during flights HI8 and SR9 created challenges for identifying CH_4 plumes from those measurements. Four downwind transects were completed on HI8, but only two plumes observed (Figure 5.14). The second plume directly overlapped with elevation changes, and therefore we were unable to confirm whether the plume was coming from the platform. As a result, the plume was excluded, and only the first one was used for emission rate estimates (Figure 5.14).

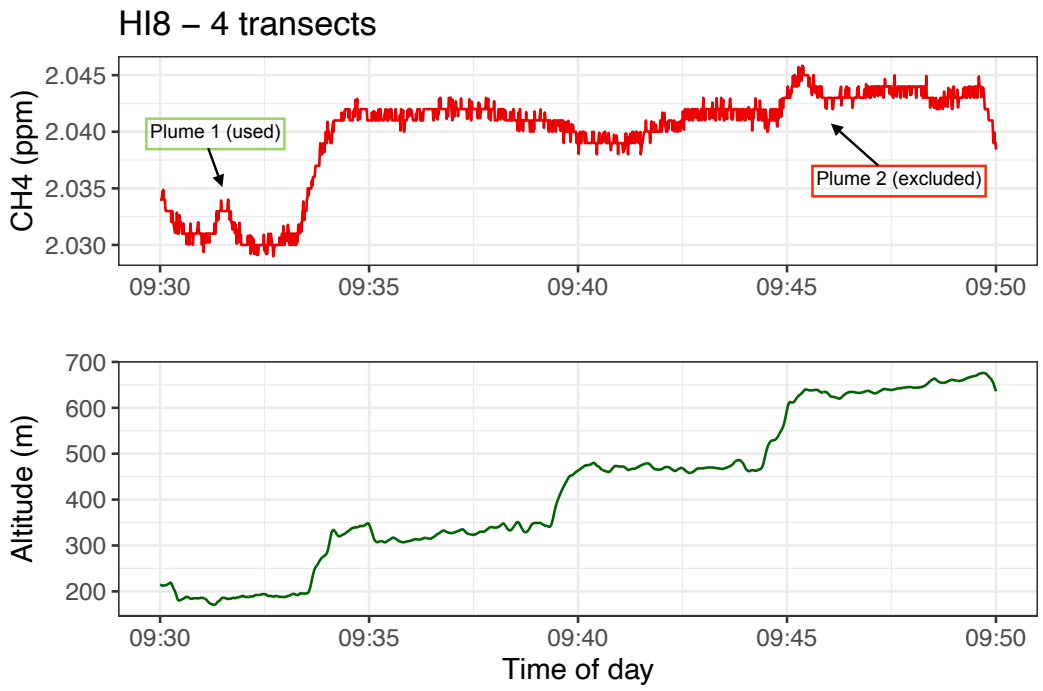

Figure 5.14. Timeseries of measured CH_4 concentrations and altitude for HI8 transects.

During SR5, two CH_4 plumes were observed, but both were deemed unsuitable for Gaussian dispersion emission rate calculations for the following reasons (Figure 5.15). First, both plume shapes did not align with the standard Gaussian curve, and one plume showed two distinct peaks. Second, both plumes were much wider than others that were measured during other flights (with elevated concentrations sustaining for a few minutes) (Figure 5.15). This was especially usual because the measured wind speeds were the highest on average out of all flights, so theoretically we would expect the plumes to be narrower. Third, both plumes overlapped with elevation changes.

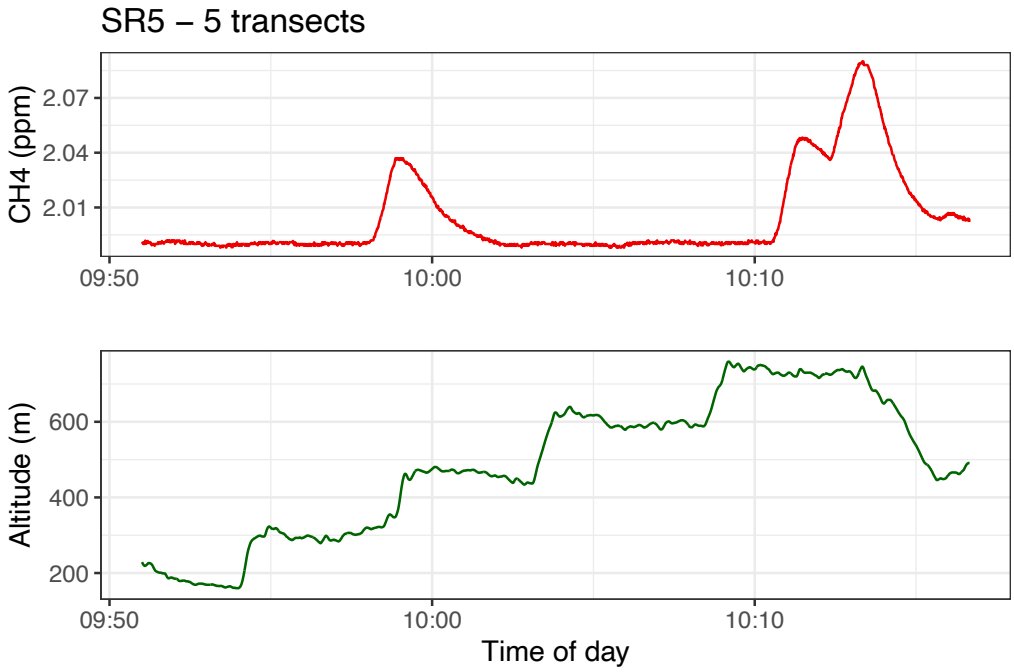

Figure 5.15. Timeseries of measured CH_4 concentrations and altitude for SR5 transects.

The last plume that we excluded was measured on flight HE7. During this flight, three plumes were observed, but like plumes measured on SR5, this plume was wider than expected, and overlapped with altitude changes (Figure 5.16). The two remaining plumes measured on this flight were included.

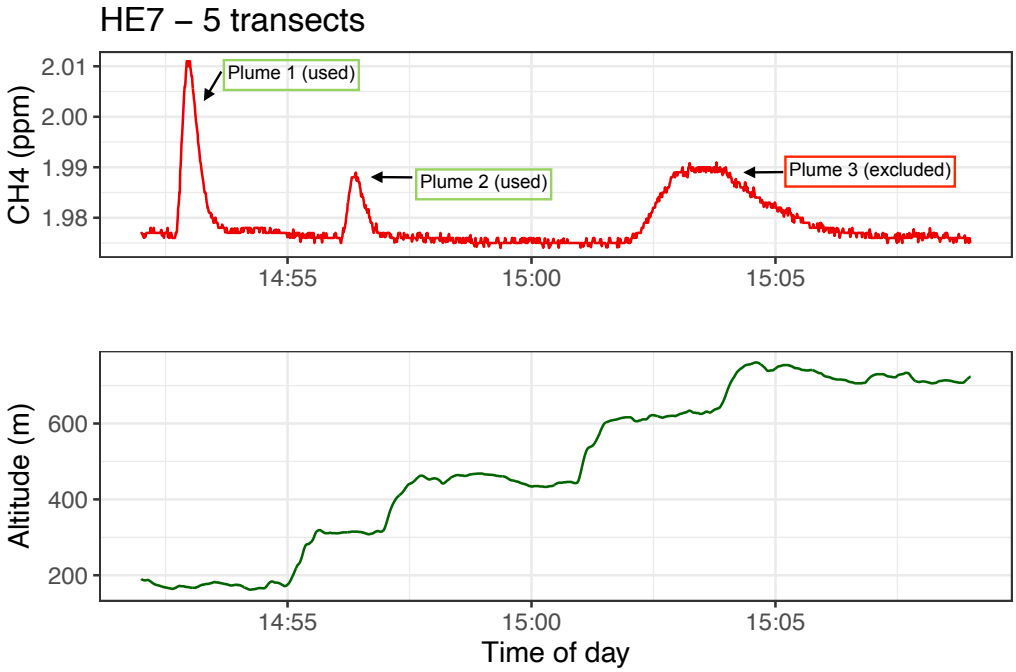

Figure 5.16. Timeseries of measured CH_4 concentrations and altitude for HE7 transects.

Figure 5.17 shows boxplots representing the estimated CH_4 emission rates for the 15 plumes. As previously mentioned, several emission rates were calculated for each plume, using different combinations of stability class and source height (platform base height and flare height), to incorporate the uncertainty related to these parameters. The black diamonds show overall mean for each plume. Average per plume emission rates ranged from 5195 m^3 day^{-1} (Hibernia) to 24,746 m^3 day^{-1} (Hebron). Except for HE7, individual plumes measured on the same flight show good agreement. The two plumes measured on HE7 showed a significant difference in CH_4 enhancement (0.036 ppm for 7.1 and 0.013 ppm for 7.2), which likely explains the differences in estimated emission rates.

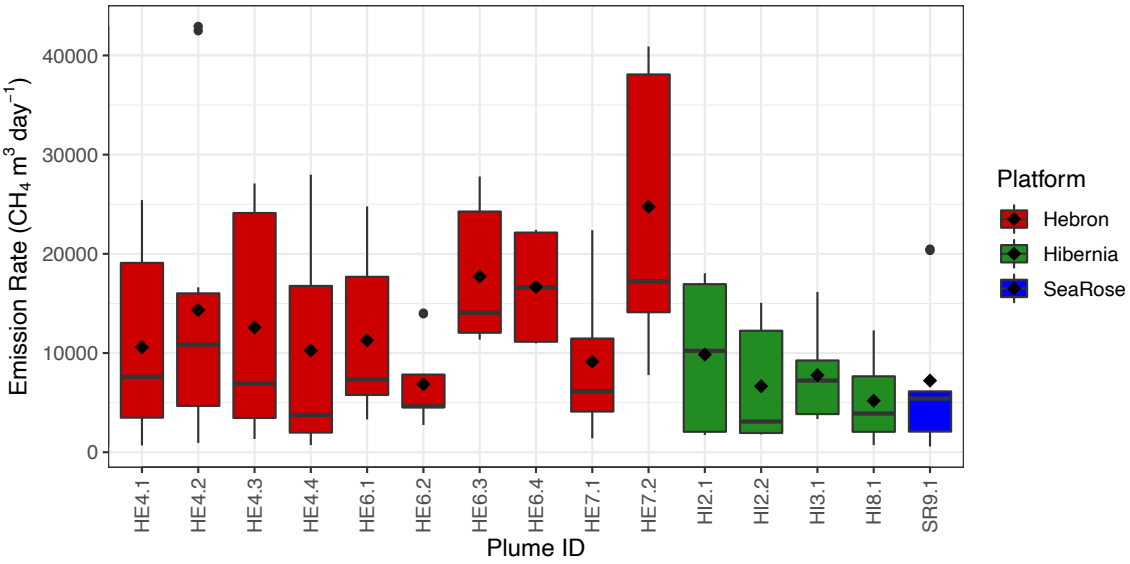

Figure 5.17. Estimated emission rates for 15 measured CH_4 plumes. Individual boxplots represent the range of emission rates under different source heights and atmospheric stability classes. The black diamond indicates the mean emission rate for each plume, and the black line is the median. Black dots outside the boxes are outliers.

5.6.4 Methane intensity

Our calculated CH_4 intensities for the three offshore platforms are listed in Table 5.2 below. It should be noted that these values are based on reported oil production for 2021 (C-NLOPB 2022), and assumes 365 days of production. Compared to onshore developments in Canada, offshore CH_4 intensities are low, and agree with previous estimates made by industry. MacKay et al. (2021) reported CH_4 intensities for six oil and gas regions in western Canada, which ranged from 0.17 gCO_2e/MJ in Peace River to 32

gCO_2e/MJ in Lloydminster. Out of all six regions included in the study, only the Peace River region ranked lower than the offshore platforms included in our analysis. Our estimated offshore CH_4 intensities are also well below other estimates for US-based production (Alvarez et al. 2018). That being said, Canadian offshore oil production should have a competitive edge in markets that are increasingly demanding lower carbon-intensive choices.

Table 5.2. CH_4 emission intensities for Canada's offshore production platforms. Values are based on reported oil production for 2021 (C-NLOPB 2022).

	Methane intensity	
	gCO_2e/MJ	**$kgCO_2e/bbl$**
Hibernia	0.21	1.27
Hebron	0.26	1.61
Sea Rose	1.00	6.13

5.6.5 Comparisons to reported estimates

Figure 5.18 shows flight averaged CH_4 emission rates, colored by platform. The mean emission rate per flight is the black diamond, and the red (Hebron), green (Hibernia), and blue (Sea Rose) dashed lines are the most recently available reported CH_4 emissions for each platform (2019). Total reported emissions were converted to daily emissions assuming 365 days of production in 2019, except for Sea Rose, in which we used 180 days of production, which was information provided to us from the operator. Overall, average emission rates for the Hebron, Hibernia, and Sea Rose platforms were 13,131 m^3

day^{-1}, 7242 m^3 day^{-1}, and 7221 m^3 day^{-1}, respectively. For all platforms, measured emission rates are comparable to most recent estimates reported in the GHGRP (Figure 5.17). Figure 5.19 shows the measured vs. reported emissions in tonnes of CH_4 per year (left), and kgCO_2e per bbl (right). Note that the difference in Sea Rose emissions shown here is expected due to the lower production in 2019 (180 days).

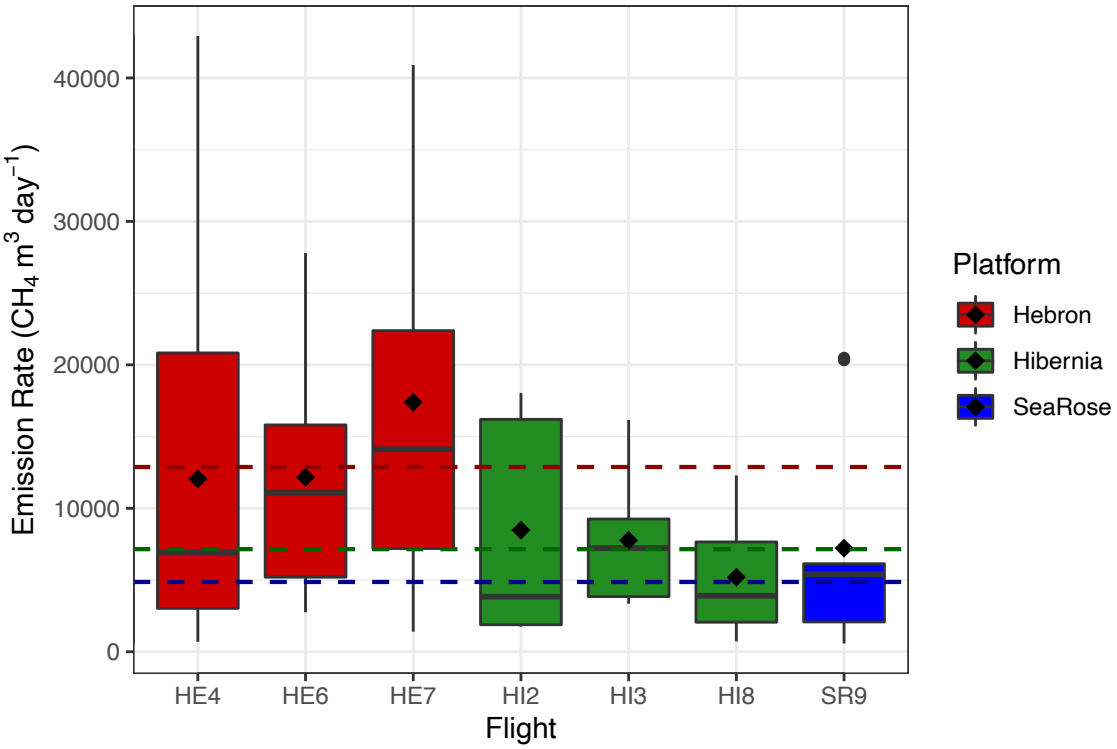

Figure 5.18. Flight averaged CH_4 emission rates derived from multiple plume transect measurements. Boxplots represent estimated ranges of emission rates under different source heights and atmospheric stability classes. The mean emission rate per flight is the black diamond, and the black solid line is the median. The red

(Hebron), green (Hibernia), and blue (Sea Rose) dashed lines are the most recently available reported CH_4 emissions for each platform (2019).

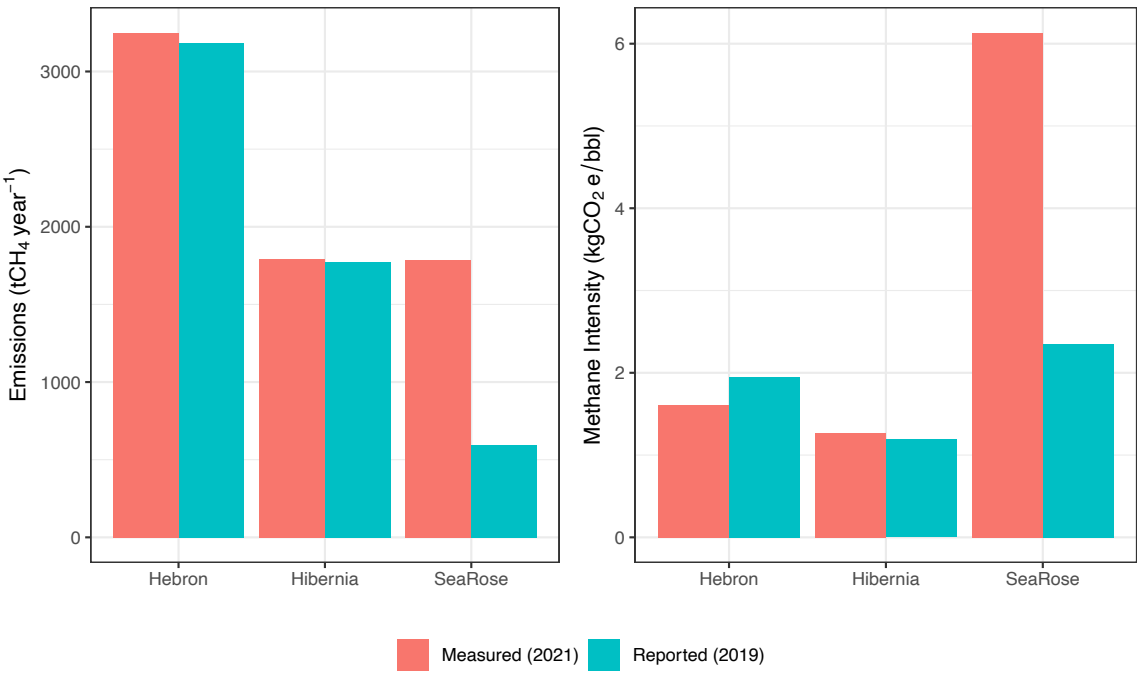

Figure 5.19. Comparison of reported vs. measured CH_4 emission rates (left) and CH_4 intensities (right) for each platform. Emission rates are overall averages derived from individual plume measurements.

5.6.6 Sources of observed emissions

Due to the nature of our measurement technique, it is difficult to attribute observed CH_4 emissions to exact sources on the platforms. However, through discussions with the operators and other offshore petroleum experts, we suspect that most of the observed emissions from the platforms are originating from the flare stacks, for reasons described below.

Since the platform's flare tips are constantly exposed to wind and weather, we expect that combustion efficiency is frequently compromised, resulting in greater potential for CH_4 emissions. Castiñeira and Edgar (2008) found that combustion efficiency drops to 90% when winds are 11 m/s, and similarly Johnson and Kostiuk (2002) saw turbulent conversion efficiencies at 87% for their experiments at 13 m/s windspeeds. The median wind speed for offshore NL is over 10 m/s for seven months of the year and over 12 m/s for three months of the year, and these values do not include wind gusts which reach much higher (C-Core 2017). Our measured wind speeds during plume transects used to estimate emissions ranged from 5-16 m/s, with over 75% of values measuring 10 m/s or higher. As well, aerial measurements of Mexico's offshore sector and ship-based measurements of offshore platforms off the coast of Southeast Asia also found flaring to be a major contributor to observed CH_4 emissions (Zavala-Araiza et al. 2021, Nara et al. 2014). A recent study by Plant et al. (2022) also found that onshore flares across the U.S. are only destroying 91.1% of CH_4.

Lastly, we believe that emissions from power generation and fugitive leaks are minimal. While the volume of gas used for power generation is about 3-4 times more than the volume of gas that is flared, the combustion efficiency is much higher as combustion occurs inside boilers/turbines as opposed to at the flare tip that is exposed to wind and weather. As well, leak detection and repair (LDAR) surveys are done twice a year, which should result in low fugitive emissions.

5.6.7 Comparisons to other offshore platforms

Figure 5.20 shows a comparison of our overall average platform CH_4 emission rate (i.e. mean emissions from all three platforms) to other platforms recently measured in other parts of the world. In general, our estimates are within similar range to those estimated for other platforms, although two studies that measured platforms in the North Sea show notably lower emissions per platform for this region. Yacovitch et al. (2020) and Gorchov Negron et al. (2020) both estimate CH_4 emissions from platforms in the US Gulf of Mexico, and found order of magnitude differences in average emissions, although Gorchov Negron et al. (2020) noted that when they exclude platforms with disproportionately high emissions, their estimates agree well with ship-based observations by Yacovitch et al. (2020).

Platform-level emissions may vary due to several factors such as production and platform complexity and design (Gorchov Negron et al. 2020). Unfortunately, for the studies shown in Figure 5.20, much of this information is lacking, therefore it is difficult to determine if any of these factors are contributing to observed platform-level differences in emissions across these studies.

While we lack platform-level production data for all studies in Figure 5.20, we have some indication that differences in oil and gas production may explain some of the observed differences in emissions from these platforms and production regions. It seems that areas where oil production is dominant (e.g. Canada and Malay Peninsula), CH_4

emissions are higher than areas with significant gas production. For instance, the platforms in the North Sea produce about 0.01% of the oil produced by Canada's offshore platforms, but more than seven times more gas (UK Oil and Gas Authority 2021). Moreover, the Malay Peninsula is dominated by oil production and has similar daily production rates as Canada's offshore (U.S. Energy Information Administration 2021). It is possible that this is because when oil production is the priority, there may be less incentive to conserve produced gas. Similar conclusions have also been noted for Canada's onshore production (MacKay et al. 2021), and both Gorchov Negron et al. (2020) and Riddick et al. (2019) found a negative relationship between CH_4 emissions and natural gas production for the offshore sectors in the Gulf of Mexico and the North Sea.

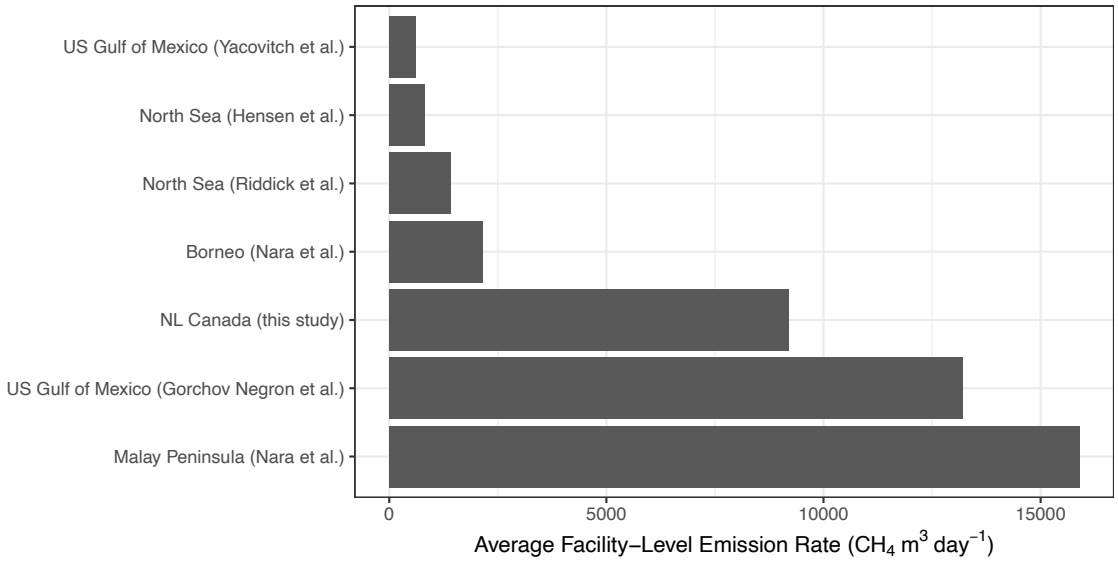

Figure 5.20: Comparison of facility-level CH_4 emission rates to other offshore production facilities measured in other recent studies. For this study, individual (i.e.

per flight, per plume) emission rates were averaged to get a facility average for each platform.

In addition to average platform emissions, some offshore studies estimate an overall loss rate for their study regions, that is the total CH_4 emitted divided by the natural gas produced. Assuming constant CH_4 emissions and using reported gas production for 2021 (C-NLOPB 2022), we calculate a cumulative loss rate of 0.23% for NL's offshore platforms. This is comparable to the 0.19% estimated for the North Sea (Riddick et al. 2019), but notably lower than the 2.9% estimated for the US Gulf of Mexico (Gorchov Negron et al. 2020).

5.7 Future work

Further analysis of the measurements is planned to better refine platform emission rates. First, the orbit measurements which were mostly excluded from this analysis, will be used to estimate emission rates using Environment and Climate Change Canada's Top Down Emission Rate Retrieval (TERRA) algorithm. This method will likely produce more accurate emission rates than the ones presented in this study, although emission rates estimated from both methods should show good agreement. Second, we will analyze bag sample measurements of observed plumes, and use them to create keeling plots to better understand the isotopic signature of platform emissions. Finally, we will be acquiring platform activity data (i.e. assumed emissions and sources) from operators to compare

with our observed results, which will help us better understand the primary sources of observed emissions and potentially identify mitigation strategies.

5.8 Summary

In conclusion, this study demonstrates the feasibility of aircraft-based measurements for CH_4 emissions monitoring for Canada's offshore industry, but also highlights the shortcomings of using a Gaussian dispersion model to estimate emission rates from offshore platforms. Overall, CH_4 emissions from Canada's offshore platforms are in line with federally reported estimates and are comparable to emissions from other offshore oil platforms in other parts of the world. We estimate 2021 annual CH_4 emissions from Hibernia, Hebron, and SeaRose are 6873 tonnes, which is not significantly higher than the combined reported value of 5549 tonnes in 2019. Production weighted CH_4 intensities ranged from 1.3-6.1 $kgCO_2e/bbl$ which means that oil produced offshore of NL among the least CH_4-intensive oil produced in Canada and the US.

We suspect that flaring is the primary source of CH_4 emissions from NL's offshore platforms, given the harsh wind and weather conditions that are common in the offshore region. Better and improved flare recovery systems including better flare monitoring and control, maintenance to remove black soot, and ensuring more uniform combustion (heat transfer) can reduce back burning and improve combustion efficiency.

Another important conclusion from our study echoes findings from an aircraft-based study in the North Sea (France et al. 2021), which is that the conditions of the marine boundary layer can have a significant impact on the success of measuring CH_4 plumes, and subsequently estimating emission rates via dispersion modelling. It is possible that such conditions were more prevalent during the time of year that our campaigns took place (mid to late fall). Conducting campaigns at a different time of year could yield better meteorological conditions, or at the very least, would allow for more replicate flights.

In closing, this research is important for achieving Canada's greenhouse gas reductions under the Pan Canadian Framework on Clean Growth and Climate Change. The technical knowledge generated from this study can be used by both industry and regulators to increase inventory certainty, and to inform future regulatory design as we move towards our net zero goals.

References

Alvarez, R. A., Zavala-Araiza, D., Lyon, D. R., Allen, D. T., Barkley, Z. R., Brandt, A. R., Davis, K. J., Herndon, S. C., Jacob, D. J., Karion, A., Kort, E. A., Lamb, B. K., Lauvaux, T., Maasakkers, J. D., Marchese, A. J., Omara, M., Pacala, S. W., Peischl, J., Robinson, A. L., Shepson, P. B., Sweeney, C., Townsend-Small, A., Wofsy, S. C., Hamburg, S. P., 2018. Assessment of methane emissions from the U.S. oil and gas supply chain. *Science* 361, 186-188. DOI: 10.1126/science.aar7204

Baray, S., Darlington, A., Gordon, M., Hayden, K. L., Leithead, A., Li, S.-M., Liu, P. S. K., Mittermeier, R. L., Moussa, S. G., O'Brien, J., Staebler, R., Wolde, M., Worthy, D., and McLaren, R., 2018. Quantification of methane sources in the Athabasca Oil Sands Region of Alberta by aircraft mass balance. *Atmospheric Chemistry and Physics* 18, 7361–7378, DOI: https://doi.org/10.5194/acp-18- 7361-2018

Canadian Association of Petroleum Producers (CAPP), 2021. Canada's Natural Gas and Oil Emissions: Ongoing Reductions, Demonstrable Improvement. Retrieved from: https://www.capp.ca/wp-content/uploads/2021/07/Canadas-Natural-Gas-and-Oil-Emissions-Ongoing-Reductions-Demonstrable-Improvement-394473-1.pdf

C-CORE, 2017. Metocean Climate Study Offshore Newfoundland & Labrador. Prepared for Nalcor Energy Oil and Gas. Retrieved from: https://oilconl.com/wp-content/uploads/2018/01/NALCOR-MetOcean-Vol.-2-Final-2017.pdf (accessed on July 13, 2022).

Canada Energy Regulator, 2016. Energy conversion tables. Retrieved from: https://apps.cer-rec.gc.ca/Conversion/conversion-tables.aspx#s1ss1 (accessed on December 21, 2021).

Canada-Newfoundland & Labrador Offshore Petroleum Board (C-NLOPB), 2021a. Offshore Activities. Retrieved from: https://www.cnlopb.ca/offshore/ (accessed on November 2, 2021)

Canada-Newfoundland & Labrador Offshore Petroleum Board (C-NLOPB), 2021b. Annual Reports. Retrieved from: https://www.cnlopb.ca/information/annualreports/ (accessed on July 14, 2022)

Canada-Newfoundland & Labrador Offshore Petroleum Board (C-NLOPB), 2022. Resource Management Statistics. Retrieved from: https://www.cnlopb.ca/information/statistics/#rm (accessed on March 24, 2022)

Castiñeira, D., & Edgar, T. F. (2008). Computational Fluid Dynamics for Simulation of Wind-Tunnel Experiments on Flare Combustion Systems. Energy & Fuels, 22(3), 1698–1706. https://doi.org/10.1021/ef700545j

Environment and Climate Change Canada (ECCC), 2018. Technical Backgrounder: Federal methane regulations for the upstream oil and gas sector. Retrieved from: https://www.canada.ca/en/environment-climate-change/news/2018/04/federal-methane- regulations-for-the-upstream-oil-and-gas-sector.html

Environment and Climate Change Canada (ECCC), 2021. National Inventory Report 1990–2019: Greenhouse Gas Sources and Sinks in Canada. Retrieved from: http://www.publications.gc.ca/site/eng/9.506002/publication.html

France, J.L., Bateson, P., Dominutti, P., Allen, G., Andrews, S., Bauguitte, S., Coleman, M., Lachlan-Cope, T., Fisher, R.E., Huang, L., Jones, A.E., Lee, J., Lowry, D., Pitt, J., Purvis, R., Pyle, J., Shaw, J., Warwick, N., Weiss, A., Wilde, S., Witherstone, J., Young, S., 2021. Facility level measurement of offshore oil and gas installations from a medium-sized airborne platform: method development for quantification and source

identification of methane emissions. *Atmospheric Measurement Techniques*, 14, 71–88. DOI: https://doi.org/10.5194/amt-14-71-2021

Gorchov Negron, A. M., Kort, E. A., Conley, S. A., Smith, M., 2020. Airborne Assessment of Methane Emissions from Offshore Platforms in the U.S. Gulf of Mexico, *Environmental Science and Technology,* 54, 5112-5120. DOI: https://dx.doi.org/10.1021/acs.est.0c00179

Government of Canada, 2021. Greenhouse Gas Reporting Program data search. Retrieved from: https://climate-change.canada.ca/facility-emissions/ (accessed on November 30, 2021)

Hensen, A. Velzeboer, I. Frumau, K. F. A., van den Bulk, W. C. M., van Dinther, D., 2019. Methane Emission Measurements of Offshore Oil and Gas Platforms; TNO Report R10895: The Netherlands, Petten. Retrieved from: https://repository.tno.nl/islandora/object/uuid%3Aa9c705b9-ec88-4316-827f-f9d7ffbd05c2 (accessed on December 20, 2021)

Hibernia Management and Development Company Ltd. (HMDC), 2021. About Hibernia. Retrieved from: https://www.hibernia.ca/ (accessed on November 2, 2021).

Husky Energy, 2020. Project Overview. Retrieved from: https://husky.force.com/wwrp/s/ (accessed on November 2, 2021).

Johnson, M., Tyner, D., Conley, S., Schwietzke, S. and Zavala-Araiza, D. 2017. Comparisons of Airborne Measurements and Inventory Estimates of Methane Emissions in the Alberta Upstream Oil and Gas Sector. *Environmental Science and Technology* 51(21): 13008–13017. DOI: https://doi.org/10.1021/acs.est.7b03525

Johnson, M. R., & Kostiuk, L. W. (2002). A parametric model for the efficiency of a flare in crosswind. Proceedings of the Combustion Institute, 29(2), 1943–1950. https://doi.org/10.1016/S1540-7489(02)80236-X

MacKay, K., Lavoie, M., Bourlon, E., Atherton, E., O'Connell, E., Baillie, J., Fougère, C., Risk, D., 2021. Methane emissions from upstream oil and gas production in Canada are underestimated. *Scientific Reports*, 11, 8041. https://doi.org/10.1038/s41598-021-87610-3

Myhre, G., Shindell, D., Breìon, F.-M., Collins, W., Fuglestvedt, J., Huang, J., Koch, D., Lamarque, J.-F., Lee, D., Mendoza, B., Nakajima, T., Robock, A., Stephens, G., Takemura, T., and Zhang, H., 2013. Anthropogenic and Natural Radiative Forcing, in: Climate Change 2013: The Physical Science Basis. Contribution of Working Group I to the Fifth Assessment Report of the Inter- governmental Panel on Climate Change, edited by: Stocker, T. F., Qin, D., Plattner, G.-K., Tignor, M., Allen, S. K., Boschung,

J., Nauels, A., Xia, Y., Bex, V., and Midgley, P. M., Cambridge University Press, Cambridge, United Kingdom and New York, NY, USA.

Nara, H. Tanimoto, H. Tohjima, Y. Mukai, H. Nojiri, Y. Machida, T., 2014. Emissions of methane from offshore oil and gas platforms in Southeast Asia. *Scientific Reports*, 4, 65053. DOI: https://doi.org/10.1038/srep06503

O'Connell, E., Risk, D., Atherton, E., Bourlon, E., Fougère, C., Baillie, J., Lowry, D., Johnson, J., 2019. Methane emissions from contrasting production regions within Alberta, Canada: Implications under incoming federal methane regulations. *Elementa Science of the Anthropocene* 7. DOI:10.1525/elementa.341.

Picarro Inc. G2210-I Analyzer Datasheet. Retrived from: https://www.picarro.com/support/library/documents/g2210i_analyzer_datasheet (accessed on March 24, 2022)

Plant, G., Kort, E. A., Brandt, A. R., Chen, Y., Fordice, G., Gorchov Negron, A. M., Schwietzke, S., Smith, M., Zavala-Araiza, D., 2022. Inefficient and unlit natural gas flares both emit large quantities of methane. *Science* 377, 6614, 1566-1571. DOI: https://www.science.org/doi/10.1126/science.abq0385

Riddick, S. N., Mauzerall, D. L., Celia, M., Harris, N. R. P., Allen, G., Pitt, J., Staunton-Sykes, J., Forster, G. L., Kang, M., Lowry, D., Nisbet, E. G., Manning, A. J., 2019. Methane emissions from oil and gas platforms in the North Sea, *Atmospheric Chemistry and Physics* 19, 9787-9796. DOI: https://doi.org/10.5194/acp-19-9787-2019

Suncor Energy Inc., 2021. Terra Nova. Retrieved from: https://www.suncor.com/en-ca/what-we-do/exploration-and-production/east-coast-canada/terra-nova (accessed on November 2, 2021).

Turner, B. D., 1994. Workbook of Atmospheric Dispersion Estimates: an introduction to dispersion Modeling. 2nd edition, CRC Press, Inc. Boca Raton, Florida.

UK Oil and Gas Authority, 2021. Production and expenditure projections. Retrieved from: https://www.ogauthority.co.uk/data-centre/data-downloads-and-publications/production-projections/ (accessed on December 29, 2021)

U.S. Energy Information Administration, 2021. Country Analysis Executive Summary: Malaysia. Retrieved from: https://www.eia.gov/international/content/analysis/countries_long/Malaysia/malaysia.pdf (accessed on December 29, 2021)

Yacovitch, T. I., Daube, C., Herndon, S. C., 2020. Methane emissions from Offshore Oil

and Gas Platforms in the Gulf of Mexico, *Environmental Science and Technology* 54, 6, 3530-3538. DOI: https://doi.org/10.1021/acs.est.9b07148

Zavala-Araiza, D., Herndon, S. C., Roscioli, J. R., Yacovitch, T. I., Johnson, M. R., Tyner, D. R., Omara, M., Knighton, B., 2018. Methane emissions from oil and gas production sites in Alberta, Canada. *Elementa Science of the Anthropocene* 6(1): 27. DOI: https://doi.org/10.1525/ elementa.284

Zavala-Araiza, D., Omara, M., Gautam, R., Smith, M. L., Pandey, S., Aben, I., Almanza-Veloz, V., Conley, S., Houweling, S., Kort, E. A., Maasakkers, J. D., Molina, L. T., Pusuluri, A., Scarpelli, T., Schwietzke, S., Shen, L., Zavala, M., Hamburg, S., 2021. A tale of two regions: methane emissions from oil and gas production in offshore/onshore Mexico, *Environmental Research Letters* 16, 024019. DOI: https://doi.org/10.1088/1748-9326/abceeb

6. Conclusions and Recommendations for Future Work

6.1 Conclusions

In conclusion, recent methane (CH_4) emissions measurements from oil and gas (O&G) facilities yield important insights for emissions patterns across the Canadian O&G sector. Analysis of measurements from onshore O&G sites in western Canada in Chapter 2 showed that emissions vary geographically, which we believe is due to variable extraction techniques, region-specific regulation, and fluid types. On average, oil-producing sites emit more CH_4 than gas producing sites, since CH_4 is a by-product of oil production, and at many sites, installing equipment to capture CH_4 is not economically favorable. The heavy-oil region of Lloydminster, which straddles the Alberta-Saskatchewan border, was the highest emitting area in all of Canada, on absolute and intensity-based scales. Fortunately, new regulations should address some of these prominent emission sources (especially vented emissions) that were observed in Lloydminster.

While Chapter 2 showed that average site-level emissions vary by production region, our analysis in Chapter 3 revealed a common trend across the entire onshore Canadian O&G sector: CH_4 emissions follow extremely skewed distributions, with 10% of sites contributing to over 50% of emissions. These rare "super-emitters" represent a low hanging fruit for reduction efforts and should thus be a primary focus of regulatory monitoring programs, as well as future technology development.

In addition to examining emission patterns and distributions, site-level measurements collected in Alberta were used in a Monte Carlo model to derive a measurement-based CH_4 inventory for the provincial upstream O&G sector. Our measurement-based inventory for Alberta was about 1.5 times higher than the federally reported estimate for the same year, which was in line with other studies of specific areas in Canada and the US. On the other hand, measurements of CH_4 emissions from Canada's offshore platforms (Chapter 5) show that offshore CH_4 emissions are in line with federally reported estimates.

When comparing measured emissions from offshore platforms to onshore sites, offshore platforms have much higher (about an order of magnitude) absolute emission rates. However, this is expected, as offshore platforms have substantially higher production than typical onshore O&G sites. From an efficiency standpoint, that is when emissions are normalized by production, offshore production outperforms onshore production. For context, combined oil production for the three active offshore platforms is

roughly 10% of oil production for the entire province of Alberta, however, our estimated CH_4 inventory for Alberta is about 200 times higher than our estimate for Canada's offshore. In other words, there is a 200-fold increase in emissions for only a 10-fold increase in production.

Compared to absolute emissions, production-weighted emission intensities are much more variable across regions, with three orders of magnitude differences between the highest and lowest intensities. Our analysis revealed that older, low producing regions like Medicine Hat (Alberta) have high intensities, which has both environmental and economic implications that should be considered as we move towards a low-carbon future. In contrast, Montney (British Columbia) and Peace River (Alberta) regions showed very low emission intensities. Emission intensities were also low for offshore oil production, which endorses previous claims made by industry. Therefore, O&G produced in these areas should have a competitive edge in markets that are increasingly demanding lower carbon-intensive choices.

Chapter 4 revealed interesting insights on modelled CH_4 emission inventories. Arguably the most important finding from this analysis was that the extremely skewed nature of O&G CH_4 emission distributions are an important factor that needs to be considered in inventory models. When the heavy-tail (or super emitters) are not factored in to emissions distributions, the resulting inventory will be underestimated. Our analysis also revealed that the uncertainty for O&G CH_4 inventories is likely much wider than current estimates, and that using the simplified error propagation method to calculate

uncertainty will not capture the asymmetrical uncertainty limits caused by super emitters. Based on our results, we recommend that new measurements (that are being collected by academic and industry as a result from new reporting requirements) should be used to inform future inventory estimates, to improve overall uncertainty and to ensure annual reductions are accurately estimated.

In closing, both the data and conclusions presented in this thesis can and should accelerate reductions of O&G CH_4 emissions in Canada. Humanity is at a race against time to avoid unreversible climate change, and so it is imperative that we must continue our efforts in understanding the most efficient ways to address this global issue.

6.2 Contributions

The research presented in this thesis significantly advances current knowledge on O&G CH_4 emissions in Canada and provides key insights for achieving Canada's GHG reductions under the Pan-Canadian Framework on Clean Growth and Climate Change. Major contributions include:

1. A regionally-nuanced estimate of Canadian upstream O&G CH_4 emissions, including production-weighted emission intensity estimates by development, which is an important metric used by companies and investors with Environmental, Social, and Governance (ESG) standards. These new measurement-based estimates fill important knowledge gaps for onshore emission patterns and magnitudes.

2. A publicly available CH_4 emissions measurement database for Canada, containing more than 20,000 component-level, and 9500 site-level measurements that were not previously accessible. These data can be used for future research, and are extremely useful for producers, regulators, and technology companies working on CH_4 measurement and mitigation.
3. Development of a measurement-based CH_4 inventory model and framework that will help increase inventory certainty and inform regulatory design. Since the current regulations were developed at a time when emissions were not well understood, it is possible that they are more burdensome and costly for industry than what is necessary for compliance. Optimizing regulatory frameworks will remove potential barriers for compliance and could even result in some producers aiming beyond compliance, especially if the economics of doing so are favourable. Additionally, improving regulation efficiency also promotes better relationships and collaboration among producers and regulators (provincial and federal), which is important since achieving our goals will not be possible without a collaborative effort across all parties working on this timely issue.
4. The first-ever direct measurements of CH_4 emissions from Canada's offshore oil and gas industry, which provide novel insights on CH_4 emission levels from different production platforms.

O&G related CH_4 emissions are not specific to Canada – they are a global issue. The IPCC has stated that reducing global CH_4 emissions will play a critical role in keeping global temperatures below 2°C. Furthermore, improved CH_4 inventory models

may also be extensible to other pollutant inventories, in Canada and abroad, since these inventories are constructed using similar methods (and thus have common limitations that are addressed in this thesis).

6.3 Recommendations for future work

As with any research topic, there is always room for further investigation. With respect to the research presented in this thesis, the following is a list of recommendations for future work. First, the scope of this thesis excludes emissions from inactive (i.e. abandoned) sites, mainly because there are limited data on CH_4 emissions from abandoned sites in Canada. Future research should focus on collecting new measurements from inactive infrastructure and incorporating them into future inventory estimates. Emissions from abandoned wells were only recently (as of 2021) included in Canada's national inventory, and while this is a good first step, the estimate is likely underestimating actual emissions. Williams et al. (2020) states that emission inventories for inactive sites likely have the largest uncertainties out of all sources included in national reporting. Not only are emission levels not well understood, but the actual number of abandoned wells is also unclear, further increasing the inventory uncertainty. The site count uncertainty is not unique to abandoned wells either. In fact, when we compared active site counts across different databases (e.g. AER's ST37 and IHS wells and facilities), the numbers of active infrastructure is not consistent. Although this discrepancy was not addressed in this thesis, future work should consider it, especially for inventory modeling. Site count uncertainty could be resolved using similar methods that we used to address emission factor

uncertainty, which was by fitting data to a distribution of values rather than using a single value.

Second, future work should continue to build upon the public data resource that was created from this research, and we encourage anyone who is collecting emission measurements to contribute to the public data repository described in Chapter 3. Compared to Alberta, emissions data for other oil and gas producing provinces (Saskatchewan, British Columbia, Manitoba) is limited. Although Alberta is the biggest oil and gas producing province, emissions reductions from all provinces is necessary to meet our national reduction goals. As well, through this work we have seen that emissions vary across geographies, therefore more measurements in understudied regions could reveal new patterns specific to those areas. Greater spatial coverages will also further reduce inventory uncertainty. Increased accessibility to measurement data not only improves our understanding of emission patterns, but it also helps technology innovators because it helps paint an accurate picture of the detection needs and is also essential for advanced data analysis such as artificial intelligence (AI) and machine learning.

Third, additional analysis of the new offshore measurements collected as part of this thesis has already begun, which includes a full mass balance analysis using the orbit measurement data. This analysis will address the short-comings of the Gaussian approach presented in Chapter 5. The Top Down Emission Rate Retrieval Algorithm (TERRA) will be used, which was developed by scientists at Environment and Climate Change Canada and has been successfully used to measure emission rates from Canadian oil sands

facilities. This mass balance method has better accuracy compared to the standard Gaussian plume model used in this thesis, although emission rates estimated from both methods should show good agreement. Additionally, bag sample measurements of observed plumes will be analyzed to better understand the isotopic signature of platform emissions. Finally, we will be acquiring platform activity data (i.e. assumed emissions and sources) from operators to compare with our observed results, which will help us better understand the primary sources of observed emissions and potentially identify mitigation strategies.

7. Appendix

7.1 Summary of in-flight calibration for Chapter 5

Table 7.1. Mean and standard deviation of CH_4 concentration (ppmv) measured by the Picarro analyzer during in-flight calibrations (~5 min) conducted during offshore flights.

Calibration gas	Flight ID	Date and time of calibration	Mean CH_4 conc. (ppmv)	SD CH_4 conc. (ppmv)
CAL1	SR1	06/10/2021 13:07:48 – 13:12:08	1.970	0.0005
CAL1	SR1	06/10/2021 14:37 – 14:43	1.971	0.0005
CAL1	HI2	07/10/2021 09:31 – 09:36	1.970	0.0004
CAL1	HI2	07/10/2021 11:05 – 11:10	1.971	0.0004
CAL1	HI3	07/10/2021 14:35 – 14:41	1.971	0.0005
CAL1	HI3	07/10/2021 15:48 – 15:53	1.971	0.0005

CAL1	HE4	11/10/2021 12:08 – 12:14	1.969	0.0005
CAL1	HE4	11/10/2021 13:54 – 14:00	1.971	0.0004
CAL2	SR5	07/11/2021 08:42 – 08:50	1.973	0.0005
CAL2	HE6	08/11/2021 08:53 – 09:01	1.973	0.0007
CAL2	HE6	08/11/2021 10:30 – 10:36	1.974	0.0004
CAL2	HE7	08/11/2021 13:31 – 13:39	1.973	0.0005
CAL2	HE7	08/11/2021 15:16 – 15:22	1.974	0.0005
CAL2	HI8	10/11/2021 08:28 – 08:36	1.973	0.0004
CAL2	HI8	10/11/2021 10:07 – 10:13	1.973	0.0005
CAL2	SR9	10/11/2021 13:06 – 13:11	1.973	0.0005
CAL2	SR9	10/11/2021 14:09 – 14:15	1.973	0.0005

7.2 Gaussian dispersion sample calculation (Chapter 5, equation 5.1)

The following is an example calculation of how CH_4 emission rates are calculated from raw timeseries data collected from the offshore measurement campaign. Note that all data processing and emission rate calculations are complete in R programming software, which is advantageous as it automates several steps, which allows the user to efficiently calculate emission rates for every plume under a range of scenarios. Using R also reduces the probability of manual error in the calculations.

The example below uses empirical data from plume 4.1 and calculates estimated emissions from the Hebron platform using equation 5.1. For this example, we use the

flare height as the source height (h_m) and Pasquill stability class "C" to define the dispersion coefficients (σ_y and σ_z). As mentioned in Chapter 5, we estimated emissions (using the same process below) under a range of stability class (A-F) and source height combinations (base, flare), and used the overall mean emission rate for subsequent analysis. In order words, the Gaussian dispersion equation (equation 5.1) was used to calculate multiple emission rates for every measured plume that met the required criteria. Flight averaged emissions and uncertainties were then calculated using all individual plume emission rate estimates calculated for each flight.

Step 1: Define parameters for Gaussian equation using empirical data.

Table 7.2. Input parameters for equation 5.1, based on empirical data from plume 4.1.

Input parameter	Description	Calculation method	Value for transect 4.1
C	CH_4 concentration enhancement downwind (ppmv)	Empirically derived using measured peak concentration and subtracting the measured background concentrations (60 sec average from crosswind measurements)	0.018
h_m	Measurement height (m)	Empirically derived using measured altitude at time of plume measurement	197.9
h_s	Emission source height (m)	Estimated based on publicly available information	178 (flare)
σ_y and σ_z	Dispersion coefficients	Estimated based on empirical data (wind speed, width of plume, and distance to source) and Pasquill-Gifford stability class scheme	Stability class C σ_y = 358.88

			σ_z= 215.69
u	prevailing wind speed (m/s)	Empirically derived using measured windspeed at time of plume measurement	15.88

Step 2: Solve for Q (ppmv/sec) using the defined parameters.

$$Q = \frac{2\pi\sigma_y\sigma_z uC}{exp\left(-\frac{(h_m - h_s)^2}{2\sigma_z^2}\right) + exp\left(-\frac{(h_m + h_s)^2}{2\sigma_z^2}\right)}$$

$$Q = \frac{2\pi(358.88)(215.69)(15.88)(0.018)}{exp\left(-\frac{(197.9 - 178)^2}{2(215.69)^2}\right) + exp\left(-\frac{(197.9 + 178)^2}{2(215.69)^2}\right)}$$

$$Q = 113798.45\ ppmv/sec$$

Step 3: Convert Q (ppmv/sec) to m^3/day using ideal gas law (pv=nrt, n=mass$_{CH4emitted}$/M) and CH_4 density at 15℃ and 1 atm.

Constants:
R = 8.31447
M_{CH4} = 16.04 g/mol
p = 101325 Pa
T = 288.15 K
D_{CH4} = 678 g/m^3
1 μg = 10^6 g
1 day = 86400 seconds

$$Q_{\frac{\mu g}{m^3}/sec} = \frac{Q_{ppm/sec}}{\left[\frac{1}{M} \times R \times T \times \frac{1}{p}\right]}$$

$$Q_{\frac{\mu g}{m^3}/sec} = \frac{Q_{ppm/sec}}{\left[\frac{1}{16.04} \times 8.31447 \times 288.15 \times \frac{1}{101325}\right]}$$

$$Q_{\frac{\mu g}{m^3}/sec} = \frac{113798.45}{[0.001474]}$$

$$Q_{\frac{\mu g}{m^3}/sec} = 77413911.6$$

$$Q_{\frac{m^3}{day}} = Q_{\frac{\mu g}{m^3}/sec} \times \frac{1g}{10^6 \mu g} \times \frac{1}{678 g/m^3} \times 86400 \frac{sec}{day}$$

$$Q_{\frac{m^3}{day}} = 77413911.6 \times \frac{1g}{10^6 \mu g} \times \frac{1}{678 g/m^3} \times 86400 \frac{sec}{day}$$

$$Q_{\frac{m^3}{day}} = 9685.14$$